

## The Degree of Standardisation in the An Sôn Ceramic Assemblage

### Introduction: Methodology for the study of standardisation

The level of standardisation within an assemblage of pottery is used as an indirect measure of organisation of production and the skill of potters (Costin 1991). However, the assumption that a higher degree of organisation of craft production and skill may be inferred from a higher level of standardisation in an assemblage is only plausible when the individual pottery forms are intended to be homogeneous. Sometimes uniqueness is required for elite wares, for example, and a measure of group standardisation is not appropriate for such vessels (Costin and Hagstrum 1995). Therefore, while this chapter presents a study of standardisation in the An Sôn assemblage, the actual levels of variability and homogeneity within certain classes of ceramics may be related to a number of different cultural/social and technological factors. This study focuses on complete rim forms that belong to the more frequently observed classes shown in Figure 5.1.

Homogeneity in the thickness of the body wall of a vessel is often attributed to the skill of a potter (see Costin and Hagstrum 1995), but additional variables were measured from the rim forms in this analysis. These variables differ according to each form, as shown in Figure 7.1. The measured dimensional variables were generally diameter at the rim, thickness of the rim, thickness of the body, angle of the rim, and length of the rim for restricted vessels. Not all variables are always present on each measured rim sherd. Additional measurements were taken for the class D vessels to account for variation in the wave or serrated shape of the rims. The most common method of analysis of standardisation is the coefficient of variation (CV) (Roux 2003a; Eerkens and Bettinger 2001; Foias and Bishop 1997; Costin and Hagstrum 1995; Blackman *et al.* 1993; Longacre *et al.* 1988). The method for the CV calculation was presented in Chapter 3, and is applied in this chapter in addition to the previously applied statistical analyses, principal components analysis (PCA), hierarchical cluster analysis and canonical variate analysis (CVA).

A more thorough examination of standardisation for the A2a, B1a, C1b, and D1a forms follows. These forms were frequently observed at An Sôn and characterise the ceramic assemblage of the site. They were included in the fabric analysis (Chapter 6, Part II), and a more comprehensive presentation of the variability and consistency in morphology, decorations (where relevant), and fabrics is provided for these rim forms. This includes variability over time within these form groups. While there has been research into whether ceramic fabrics correlate with standardisation, and it has been suggested that ceramic fabrics cannot inform about production organisation (Arnold 2000), the use of a combination of morphological and fabric variables may support interpretations regarding manufacture and organisation. To guarantee that only those vessels that can be accurately assigned to each vessel form were included in this analysis, sherds that represented at least one third of the profile of the vessel were chosen, i.e. those that show the shape of the

rim, shoulder and at least part of the body. While this limited the sample size, it ensured that only comparable vessels were analysed for standardisation. When archaeologists unintentionally combine two or more groups of ceramics and analyse these groups as one category, the variability within the ceramic category increases, and affects the results of standardisation (Eerkens and Bettinger 2001).

The applied statistical methods, PCA, hierarchical cluster analysis and CVA, were previously described in Chapter 3 and used in Chapter 6, Part II. The PCA and hierarchical average-linkage cluster analysis provide two exploratory multivariate statistics of the dimensional and fabric compositional data. The CVA provides similar results as PCA and cluster analysis but with *a priori* groups added, such as the form and provenance of the ceramic samples. The PCA and CVA applied untransformed values for dimensional data and log ratio transformed values for compositional data from the SEM-EDX clay matrix analyses. The PCAs and CVAs are presented with plots and the hierarchical cluster analyses with dendrograms. The addition of CV calculations provides values that indicate the levels of variation with lower values reflecting a more homogeneous sample, and higher values a more variable sample. Together, these methods provide a holistic picture of variation versus homogeneity in the dimensional, decorative and fabric variables within rim form groups at An Sơn.

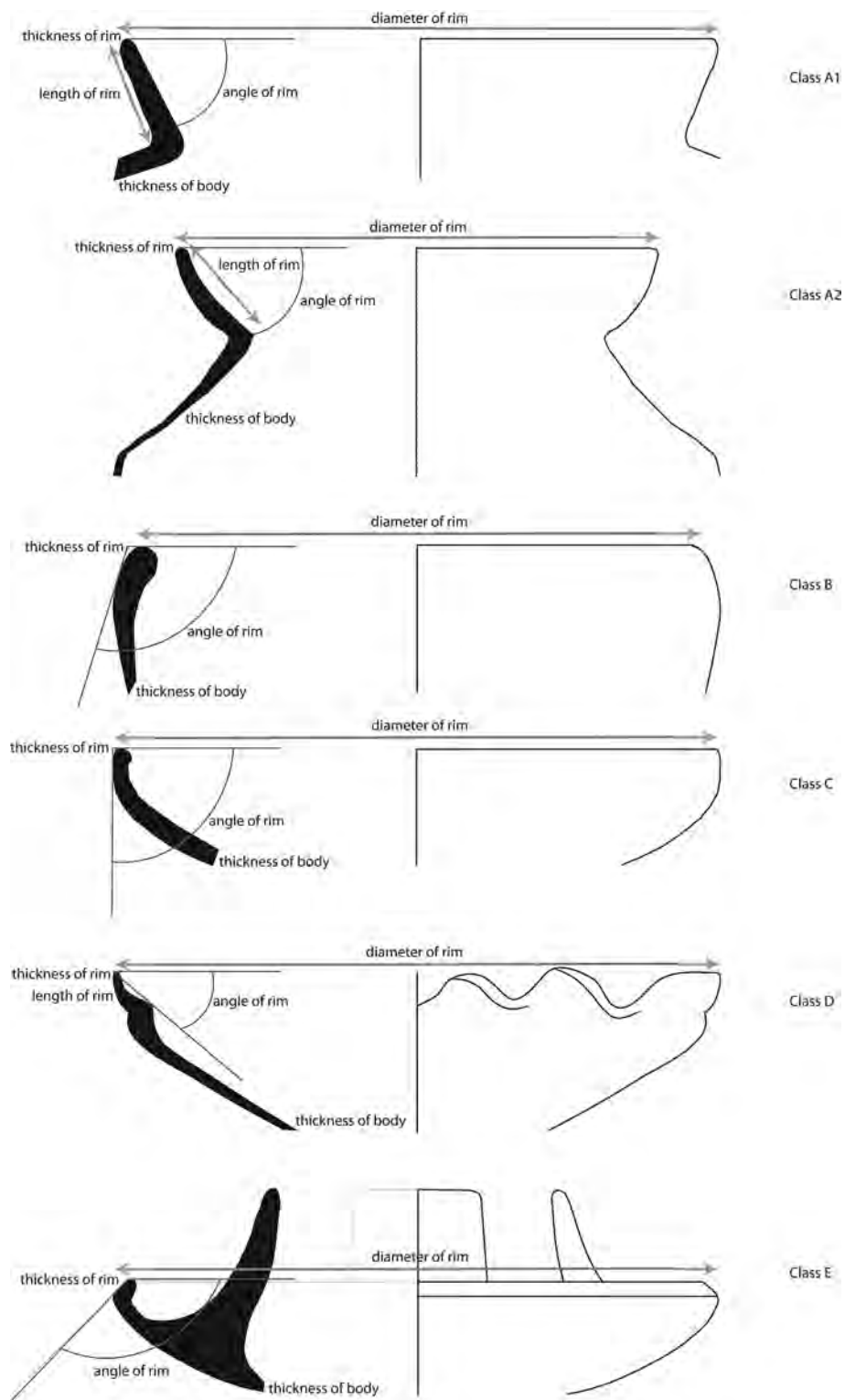


Figure 7.1. The measured dimensional variables used in the study of standardisation for each vessel class. Not to scale.

Source: C. Sarjeant.

## Standardisation of morphology

### *Class A1*

Class A1 vessels have straight everted rims (Figure 5.1). The study of dimensional variables in this class concentrated on restricted vessels only. The measured variables were angle of the rim, diameter of the rim, length of the rim, thickness of the body, and thickness of the rim (Figure 7.1). The four statistical methods previously described (PCA, cluster analysis, CVA and CV) were applied to understand the variability and homogeneity in the morphology of the A1 class ceramics (see Chapter 3 and this chapter).

### *Principal components analysis*

The greatest variability in the following PCA plot (Figure 7.2) is a result of the angle of the rim and the diameter (Table 7.1). Generally, the PCA plot shows the majority of the samples form a main cluster, inclusive of all the A1 forms, with some samples from each rim form dispersed from this main cluster (Figure 7.2). The clusters are clarified in the following hierarchical cluster analysis (Figure 7.3, Table 7.2).

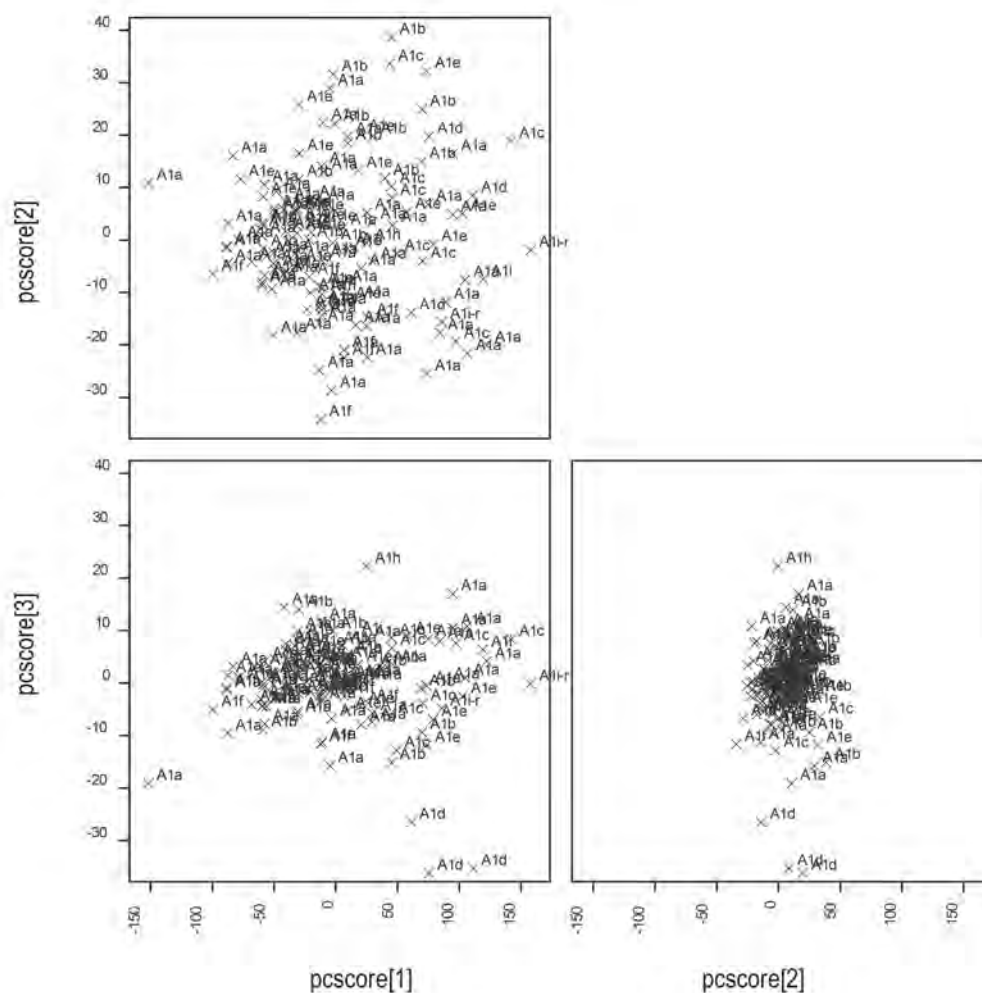


Figure 7.2. PCA plot of class A1 dimensional variables with rim forms labelled. First three dimensions. Refer to Figure 5.1 for rim form images.

Source: C. Sarjeant.

Table 7.1. PCA loadings for Figure 7.2 of class A1 dimensional variables. First three dimensions. The bold values indicate the variables that presented the greatest variability in the PCA.

Variables	PC 1 (92.28%)	PC 2 (5.53%)	PC 3 (1.99%)
Angle of rim (degrees)	<b>-0.04527</b>	<b>0.74554</b>	<b>0.66462</b>
Diameter (mm)	<b>0.97831</b>	<b>-0.10100</b>	0.17995
Length of rim (mm)	0.20096	0.65673	<b>-0.72469</b>
Thickness of body (mm)	0.01494	0.05053	-0.02657
Thickness of rim(mm)	<b>0.01559</b>	<b>-0.01139</b>	<b>0.00473</b>

Source: Compiled by C. Sarjeant.

#### *Hierarchical cluster analysis*

The dendrogram was cut at 0.925 (Figure 7.3) to divide the class A1 assemblage into clusters or groups. The numbers of samples within each form in these groups are shown in Table 7.2 The dendrogram indicates that specific groups can be identified for A1d (group 4), A1f (group 1), A1g (group 3) and A1i (group 5), suggesting these forms were relatively standardised in dimensional measurements. The other forms were more variable and the samples clustered in multiple groups.

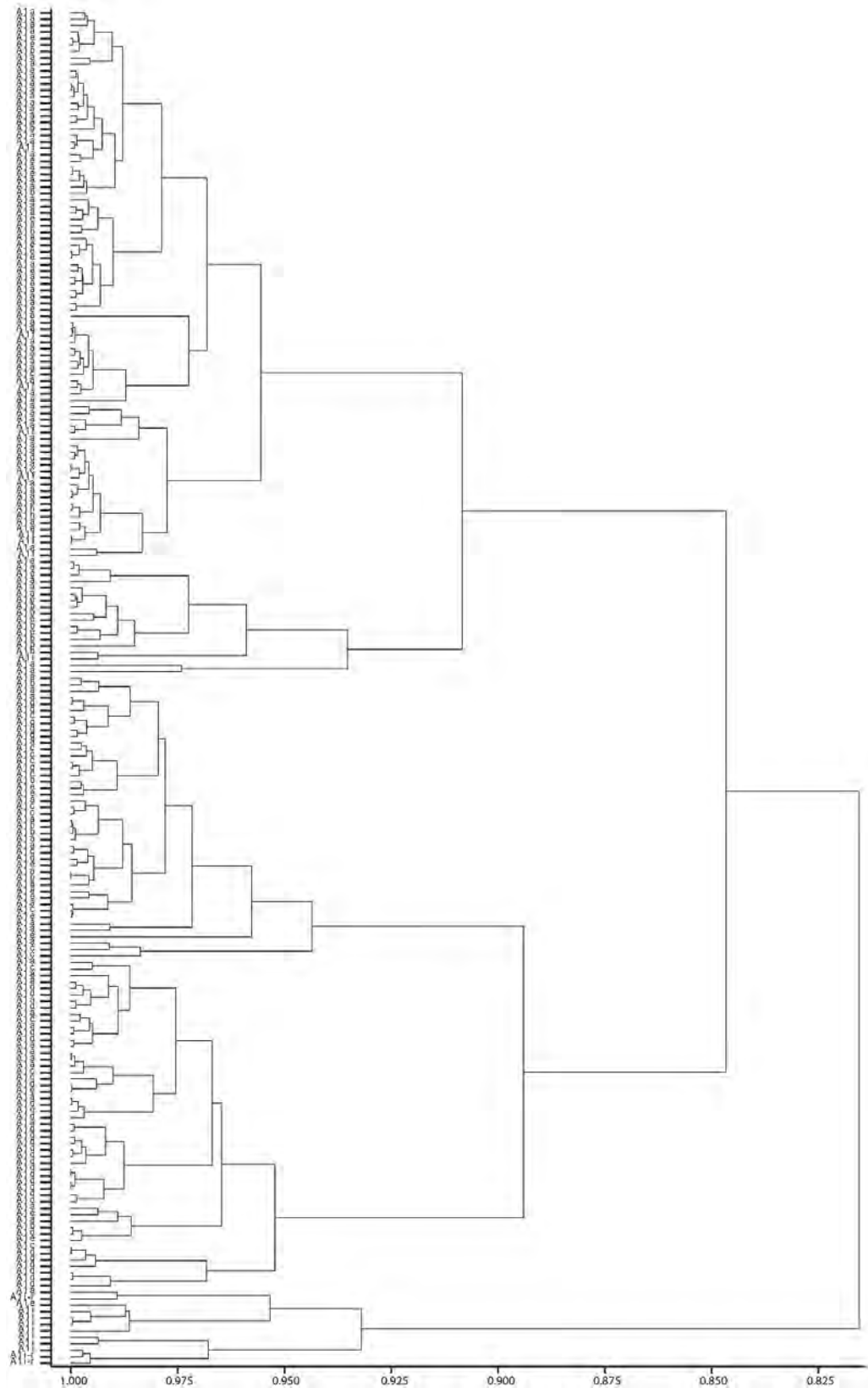


Figure 7.3. Dendrogram of average-linkage hierarchical cluster analysis of class A1 dimensional variables with rim forms labelled. Refer to Figure 5.1 for rim form images.

Source: C. Sarjeant.

Table 7.2. Number of samples in the hierarchical cluster analysis dendrogram groupings by rim form in Figure 7.3 of class A1 dimensional variables when cut at 0.925. Refer to Figure 5.1 for rim form images.

Group (cut at 0.925)	A1a	A1b	A1c	A1d	A1e	A1f	A1g	A1h	A1i	A1i-r
1	58	4	2	1	10	8	0	2	0	0
2	6	5	0	0	5	0	0	1	1	0
3	15	5	11	1	6	0	6	0	0	0
4	13	1	5	27	5	0	0	0	0	0
5	1	0	0	0	1	0	0	0	7	3

Source: Compiled by C. Sarjeant.

### *Canonical variate analysis*

The analysed vessel forms group quite close together in the CVA, although there were a few forms that plotted separately from the main cluster, especially A1d, A1i and its variant A1i-r. The variability within the main cluster is most marked within the A1b and A1c rim forms. The most standardised vessel form in this CVA was A1i-r, although very few examples of this form were included in this analysis. The other forms were variable (Figure 7.4, Table 7.3).

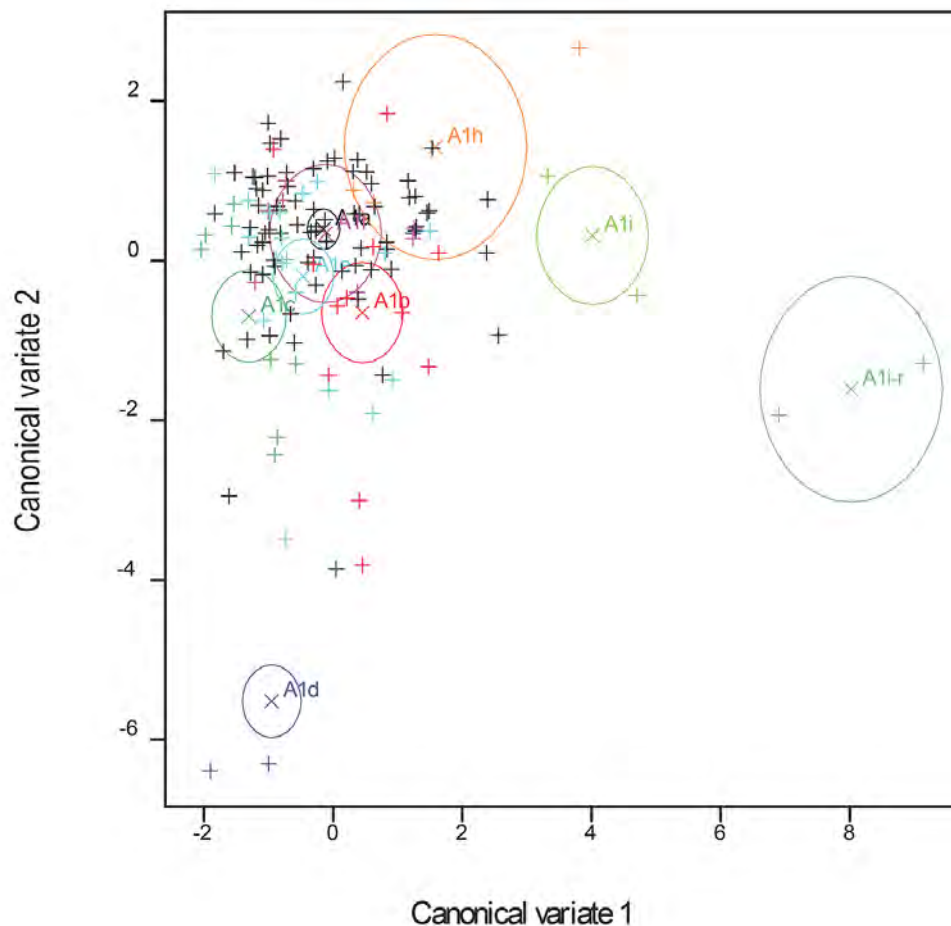


Figure 7.4. CVA plot of class A1 dimensional variables with 95% confidence circles and rim forms labelled. First two dimensions. Refer to Figure 5.1 for rim form images.

Source: C. Sarjeant.

Table 7.3. CVA loadings for Figure 7.4 of class A1 dimensional variables. First three dimensions.

Variables	1 (42.27%)	2 (31.86%)	3 (14.21%)
Angle of rim (degrees)	0.77347	-0.01225	0.01082
Diameter (mm)	0.01240	0.06493	0.09896
Length of rim (mm)	-0.05754	0.01652	-0.12303
Thickness of rim (mm)	0.00043	0.01533	0.00995
Thickness of body (mm)	-0.01712	-0.12133	0.00521

Source: Compiled by C. Sarjeant.

### *Coefficient of variation*

Many of the A1 forms had the lowest CV values for the angle of the rim and the highest CV values for the thickness of the body. The coefficient of variation analysis indicated that rim forms A1d, A1g, A1h and A1i-r have low CV values for the majority of the measured variables. The remaining rim forms had mid to high CV values for the majority of the measured variables. This suggests that deliberate standardised manufacturing methods were unlikely to have been practiced in the production of rim forms A1a, A1b, A1c, A1e, A1f and A1i, but standardised practices may have applied to A1d, A1g, A1h and A1i-r for some of the measured variables (Figure 7.5, Figure 7.6).

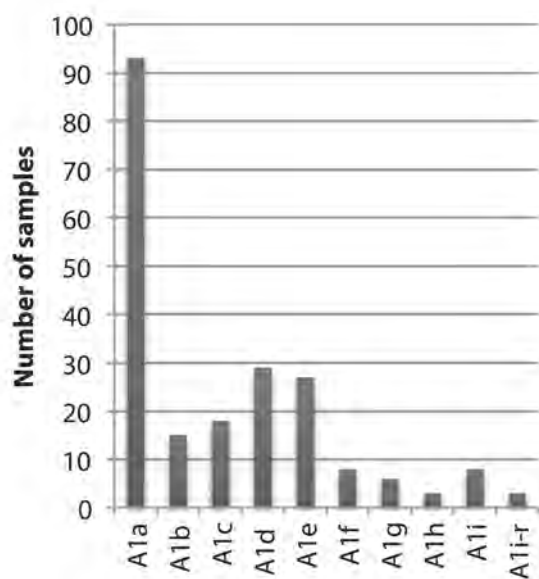


Figure 7.5. Number of class A1 samples of each rim form in the study of standardisation. Refer to Figure 5.1 for rim form images.

Source: C. Sarjeant.



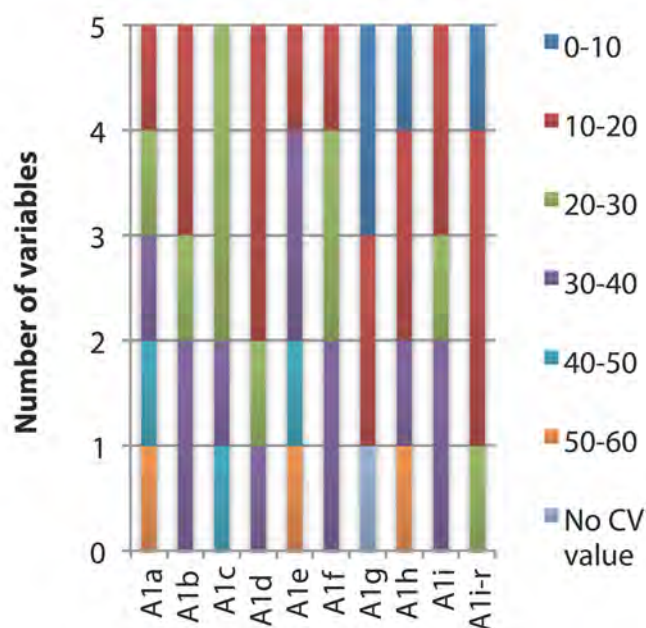


Figure 7.6. Number of variables with CV values 0–60% for each rim form in the class A1 sample. 0–10% CV represents the lowest CV values, i.e. a higher level of standardisation, and 50–60% CV represents the highest CV values, i.e. a lower level of standardisation. Refer to Figure 5.1 for rim form images.

Source: C. Sarjeant.

#### *Summary of class A1 standardisation analysis*

When the above statistical procedures are considered alongside each other, it is clear that the A1 class encompasses a wide variety of forms, which includes ten rim forms, each with additional variations. It was expected that the standardisation study of the class A1 dimensional variables would show this variability. Some forms, however, displayed more homogeneity than others. More common forms that appear throughout the sequence, such as A1a, were the most variable. In contrast, forms A1d, A1g and A1i (and A1i-r) displayed more homogeneity in all of the statistical results.

#### *Class A2*

Class A2 forms are similar to A1 in that they are restricted vessels with everted rims, however the rim is curved and internally concave in shape (Figure 5.1). Decorative panels were frequently identified on the shoulder of these forms, usually a band of roulette stamping within two incised lines. The measured variables were angle of the rim, diameter of the rim, length of the rim, thickness of the body, and thickness of the rim (Figure 7.1). Once again, the four previously described statistical methods (PCA, cluster analysis, CVA and CV) were applied to understand the variability and homogeneity in the morphology of the A2 class ceramics.

#### *Principal components analysis*

The greatest variability in the following PCA plot (Figure 7.7) is a result of the diameter and thickness of the body (Table 7.4). Most of the class A2 samples cluster close together in the plot, but some A2a and A2b sherds were major outliers (Figure 7.7). The clusters are clarified in the following hierarchical cluster analysis (Figure 7.8, Table 7.5).

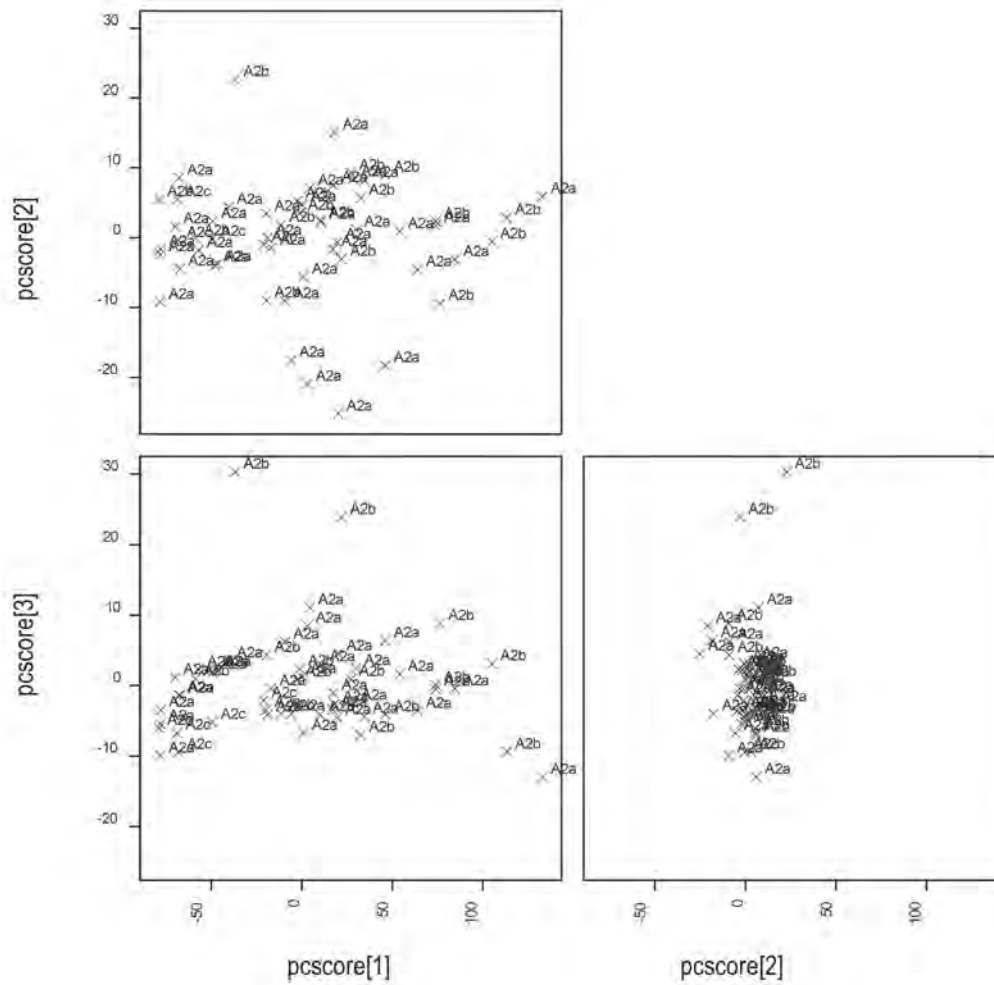


Fig 7.7. PCA plot of class A2 dimensional variables with rim forms labelled. First three dimensions. Refer to Figure 5.1 for rim form images.

Source: C. Sarjeant.

Table 7.4. PCA loadings for Figure 7.7 of class A2 dimensional variables. First three dimensions. The bold values indicate the variables that presented the greatest variability in the PCA.

Variables	PC 1 (95.71%)	PC 2 (2.31%)	PC 3 (1.77%)
Angle of rim (degrees)	0.04187	<b>0.68288</b>	<b>0.72720</b>
Diameter (mm)	<b>0.98803</b>	0.07919	<b>-0.13199</b>
Length of rim (mm)	0.14727	<b>-0.72578</b>	0.66951
Thickness of body (mm)	<b>0.00169</b>	-0.02473	0.02322
Thickness of rim (mm)	0.01878	0.00504	0.07056

Source: Compiled by C. Sarjeant.

#### *Hierarchical cluster analysis*

The dendrogram was cut at 0.925 (Figure 7.8) to divide the class A2 assemblage into groups. The numbers of samples within each form in these groups are shown in Table 7.5. While there are distinct concentrations of certain rim forms in some of the groups, such as form A2a in groups 4 and 5, there is a high degree of overlap in the measured dimensional variables of the three A2 forms. This suggests that the A2 forms are very similar in morphology except for the shape of the lip, which is their main distinguishing factor.

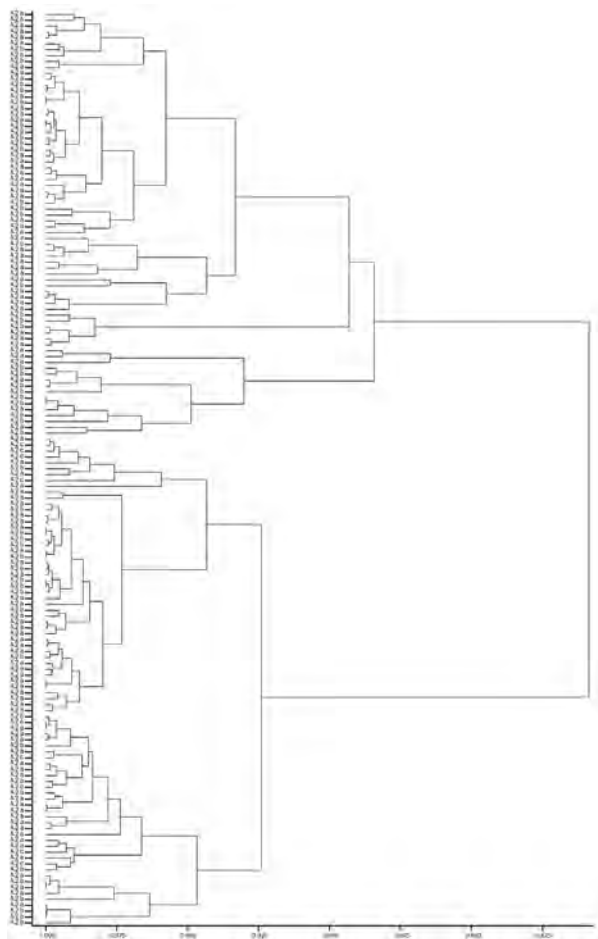


Figure 7.8. Dendrogram of average-linkage hierarchical cluster analysis of class A2 dimensional variables with rim forms labelled. Refer to Figure 5.1 for rim form images.

Source: C. Sarjeant.

Table 7.5. Number of samples in the hierarchical cluster analysis dendrogram groupings by rim form in Figure 7.8 of class A2 dimensional variables when cut at 0.925. Refer to Figure 5.1 for rim form images.

Group (cut at 0.925)	A2a	A2b	A2c
1	37	13	1
2	3	3	0
3	6	9	0
4	31	12	4
5	23	7	6

Source: Compiled by C. Sarjeant.

#### *Canonical variate analysis*

The CVA displays variability and shows that there is considerable overlap between the three A2 vessel forms. This suggests that different A2 forms have a similar morphology to each other, but also that there is no significant standardisation within each form (Figure 7.9, Table 7.6).

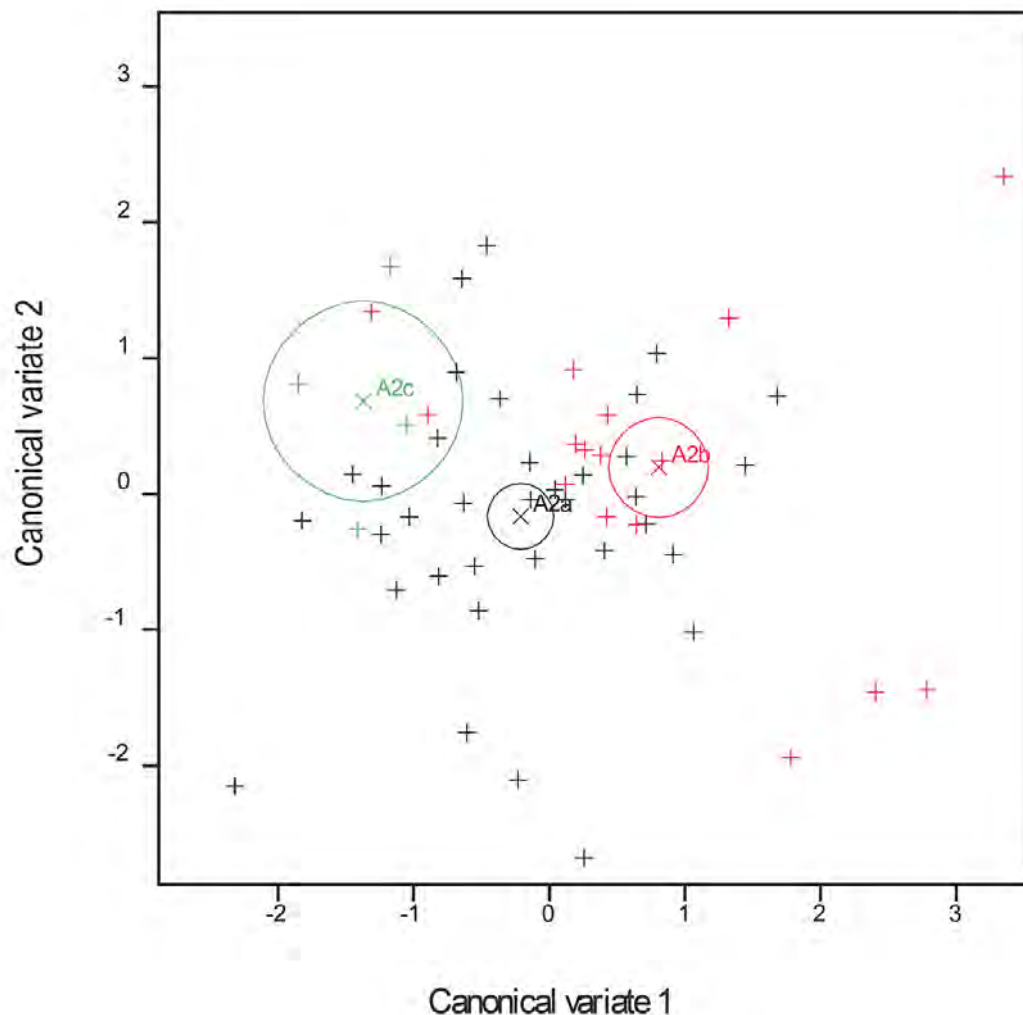


Figure 7.9. CVA plot of class A2 dimensional variables with 95% confidence circles and rim forms labelled. First two dimensions. Refer to Figure 5.1 for rim form images.

Source: C. Sarjeant.

Table 7.6. CVA loadings for Figure 7.9 of class A2 dimensional variables. First two dimensions.

Variables	1 (84.99%)	2 (15.01%)
Angle of rim (degrees)	0.2321	-0.0098
Diameter (mm)	0.0834	0.0415
Length of rim (mm)	0.2077	0.3734
Thickness of rim (mm)	0.0031	0.0051
Thickness of body (mm)	0.0123	-0.0984

Source: Compiled by C. Sarjeant.

#### *Coefficient of variation*

Within the class A2 assemblage, low CV values were calculated for angle of rim and diameter, while higher CV values were calculated for the length of the rim, thickness of body and thickness of rim. There were very few low CV values overall, except within the A2c rim forms, of which fewer samples were analysed (Figure 7.10, Figure 7.11).

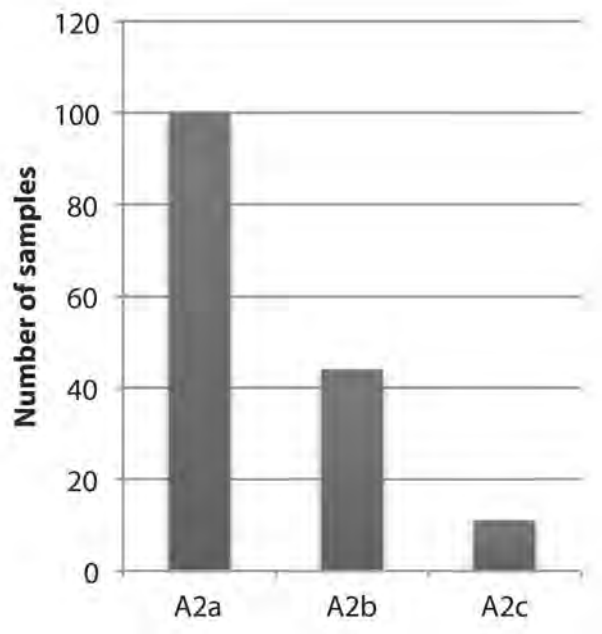


Figure 7.10. Number of class A2 samples of each rim form in the study of standardisation. Refer to Figure 5.1 for rim form images.

Source: C. Sarjeant.

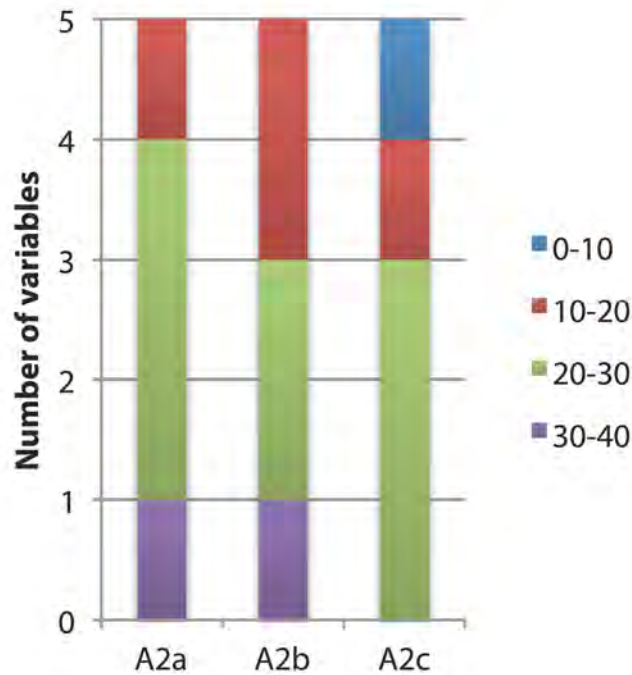


Figure 7.11. Number of variables with CV values 0–40% for each rim form in the class A2 sample. 0–10% CV represents the lowest CV values, i.e. a higher level of standardisation, and 30–40% CV represents the highest CV values, i.e. a lower level of standardisation. Refer to Figure 5.1 for rim form images.

Source: C. Sarjeant.

#### *Summary of class A2 standardisation analysis*

Generally, the class A2 forms exhibited a great deal of variability in all of the statistical procedures. However, there was greater homogeneity within the A2c rim form group in terms of the dimensional variables. The close study of form A2a may indicate whether this is an accurate assessment, especially when combining morphological, decorative and fabric variables.

#### *Class B*

The class B ceramics are simple restricted forms, typically bowl shaped with an inverted rim (Figure 5.1). The measured variables were angle of the rim, diameter of the rim, thickness of the body, and thickness of the rim (Figure 7.1). Once again, four previously described statistical methods (PCA, cluster analysis, CVA and CV) were applied to understand the variability and homogeneity in the morphology of the B class ceramics.

#### *Principal components analysis*

The greatest variability in the following PCA plot (Figure 7.12) is a result of the diameter and thickness of the rim (Table 7.7). The PCA plot shows that generally the samples cluster together, with some B2a samples grouping separately, and a few B1a, B1b and B3a outliers (Figure 7.12). These clusters are clarified by the following hierarchical cluster analysis (Figure 7.13, Table 7.8).

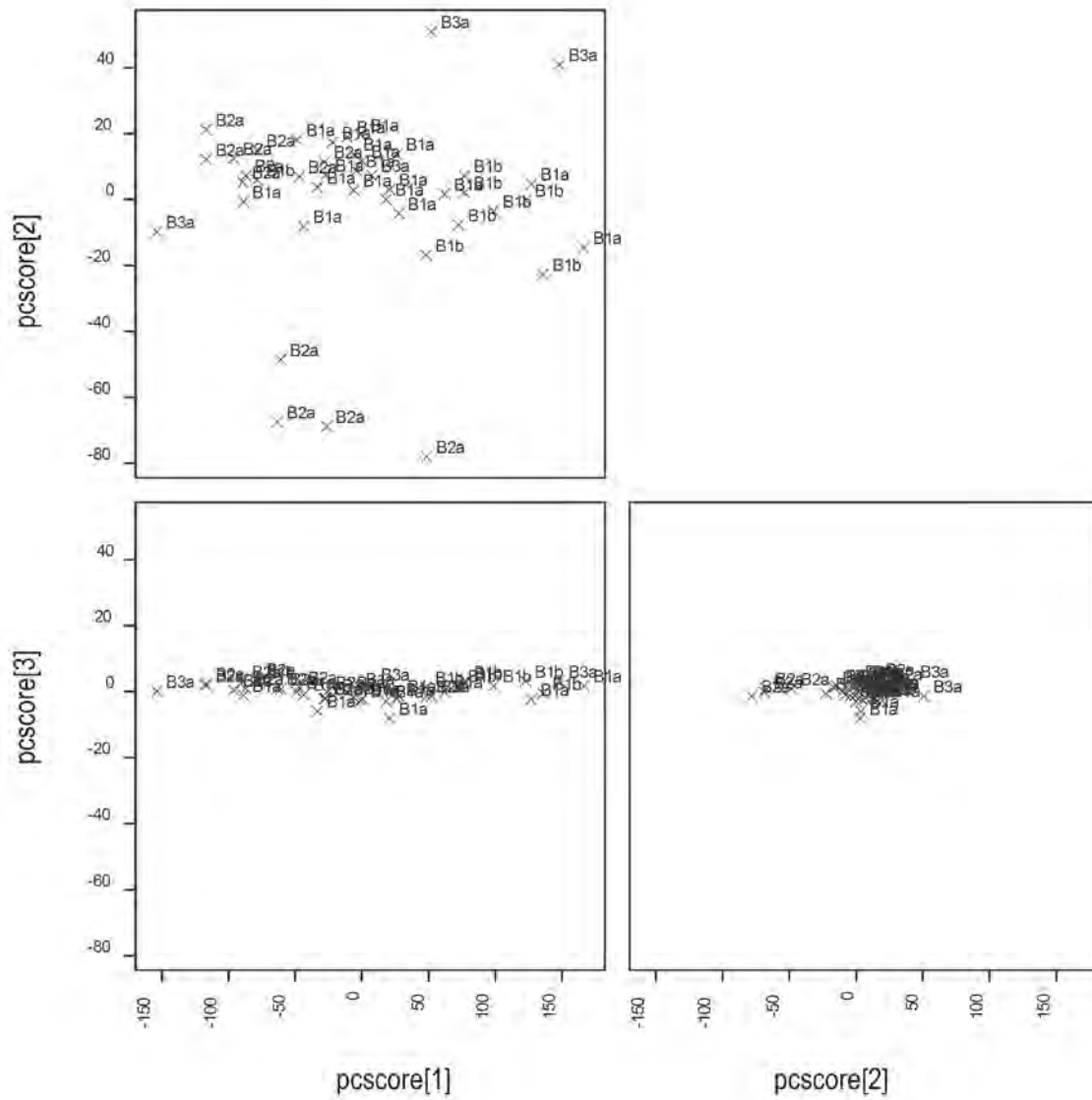


Figure 7.12. PCA plot of class B dimensional variables with rim forms labelled. First three dimensions. Refer to Figure 5.1 for rim form images.

Source: C. Sarjeant.

Table 7.7. PCA loadings for Figure 7.12 of class B dimensional variables. First three dimensions. The bold values indicate the variables that presented the greatest variability in the PCA.

Variables	PC 1 (90.36%)	PC 2 (9.52%)	PC 3 (0.09%)
Angle of rim (degrees)	0.03079	<b>0.99924</b>	<b>0.01524</b>
Diameter (mm)	<b>0.99951</b>	<b>-0.03074</b>	0.00297
Thickness of body (mm)	0.00608	-0.01145	-0.39022
Thickness of rim (mm)	<b>0.00116</b>	0.02129	<b>-0.92059</b>

Source: Compiled by C. Sarjeant.

### *Hierarchical cluster analysis*

The dendrogram was cut at 0.90 (Figure 7.13) to divide the class B assemblage into groups. The number of samples within each form in these groups is shown in Table 7.8. The cluster analysis indicated homogeneity within form B1a, with the majority of the samples in group 1, likewise for form B1b in group 3 and form B2a in group 1. Form B3a displayed less homogeneity and the samples were spread over a number of groups in the cluster analysis.

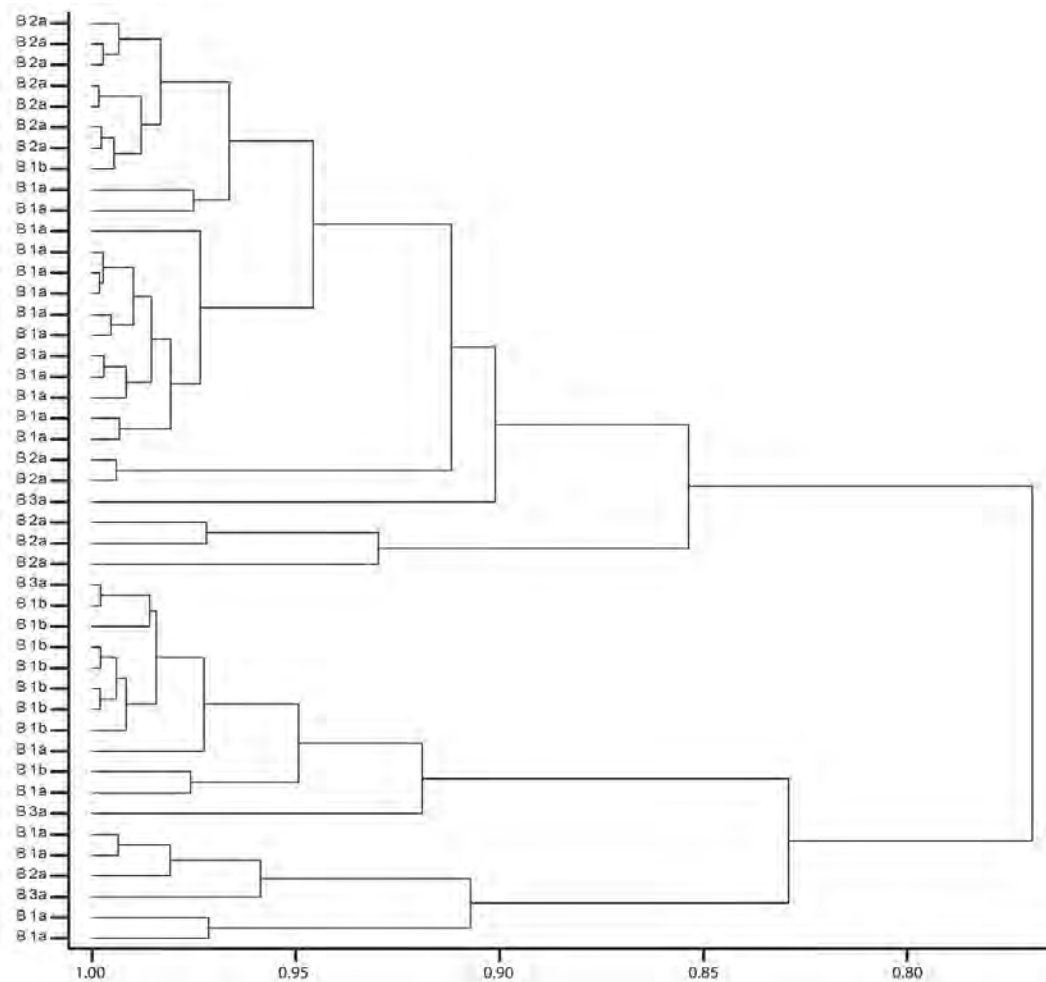


Figure 7.13. Dendrogram of average-linkage hierarchical cluster analysis of class B dimensional variables with rim forms labelled. Refer to Figure 5.1 for rim form images.

Source: C. Sarjeant.



Table 7.8. Number of sherds in the hierarchical cluster analysis dendrogram groupings by rim form in Figure 7.13 of class B dimensional variables, when cut at 0.90. Refer to Figure 5.1 for rim form images.

Group (cut at 0.90)	B1a	B1b	B2a	B3a
1	13	1	9	1
2	0	0	3	0
3	2	8	0	2
4	4	0	1	1

Source: Compiled by C. Sarjeant.

#### *Canonical variate analysis*

Rim form B1b appears to be the least variable in morphological dimensions, when compared to other class B rim forms in the CVA. The few sampled B3a rim form sherds are particularly variable (Figure 7.14, Table 7.9).

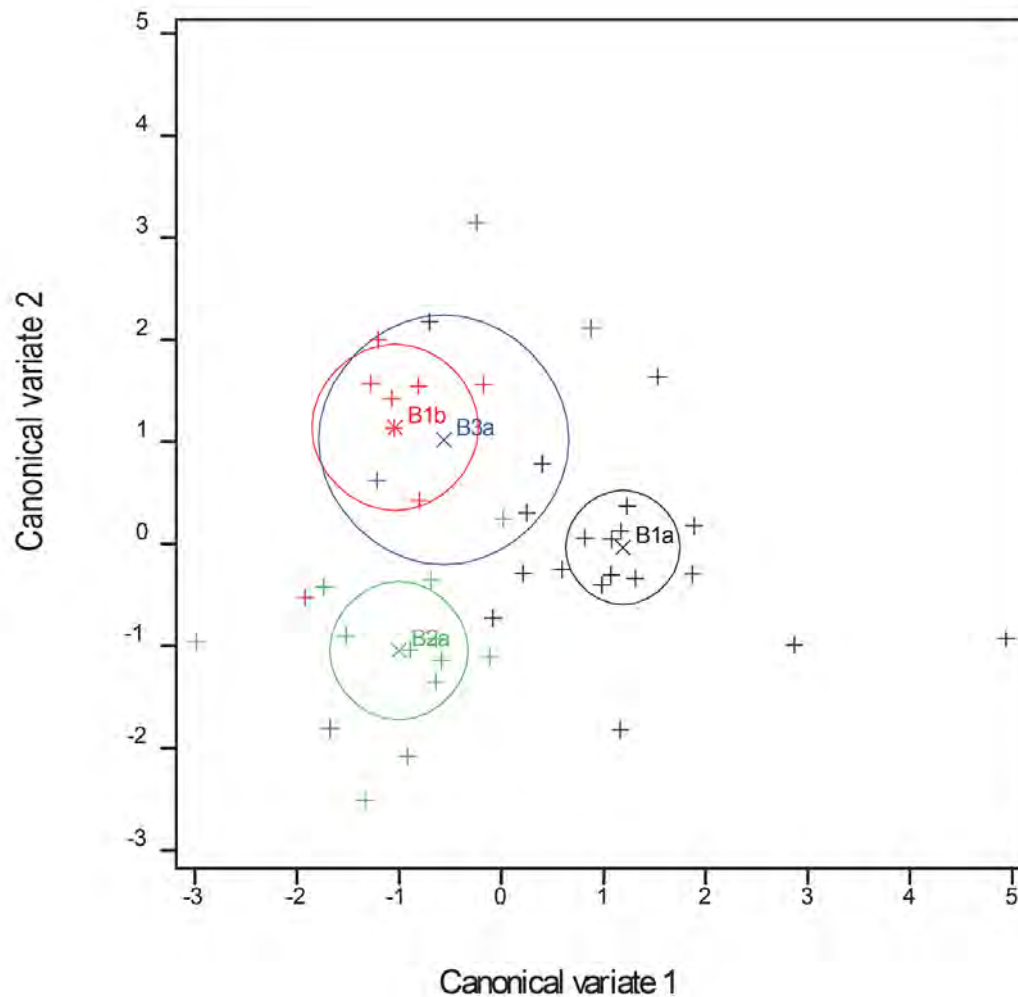


Figure 7.14. CVA plot of class B dimensional variables with 95% confidence circles and rim forms labelled. First two dimensions. Refer to Figure 5.1 for rim form images.

Source: C. Sarjeant.

Table 7.9. CVA loadings for Figure 7.14 of class B dimensional variables. First three dimensions.

Variables	1 (55.18%)	2 (34.66%)	3 (8.23%)
Angle of rim (degrees)	-0.0832	-0.6550	-0.2888
Diameter (mm)	0.0864	0.0067	0.0097
Thickness of rim (mm)	-0.0010	-0.0015	0.0034
Thickness of body (mm)	0.4151	0.9116	-0.3910

Source: Compiled by C. Sarjeant.

### *Coefficient of variation*

Low CV values were most frequently calculated for the angle of the rim, while higher CV values were calculated for diameter and thickness of the body. Low CV values were rare for class B, except for two variables in rim form B1b, the angle and thickness of the rim (Figure 7.15, Figure 7.16).

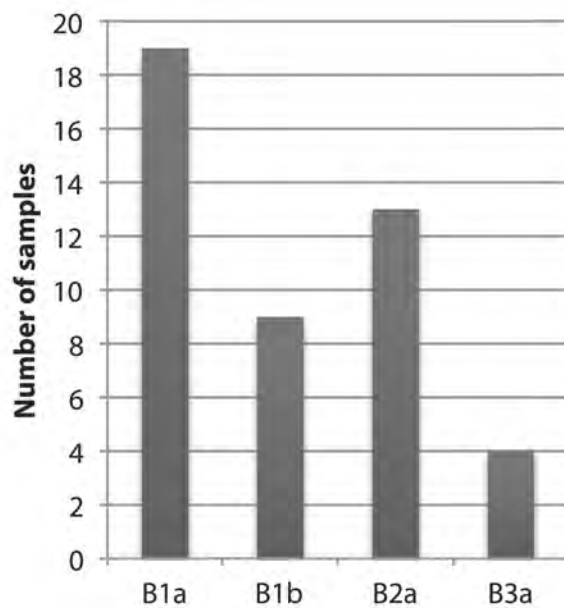


Figure 7.15. Number of class B samples of each rim form in the study of standardisation. Refer to Figure 5.1 for rim form images.

Source: C. Sarjeant.

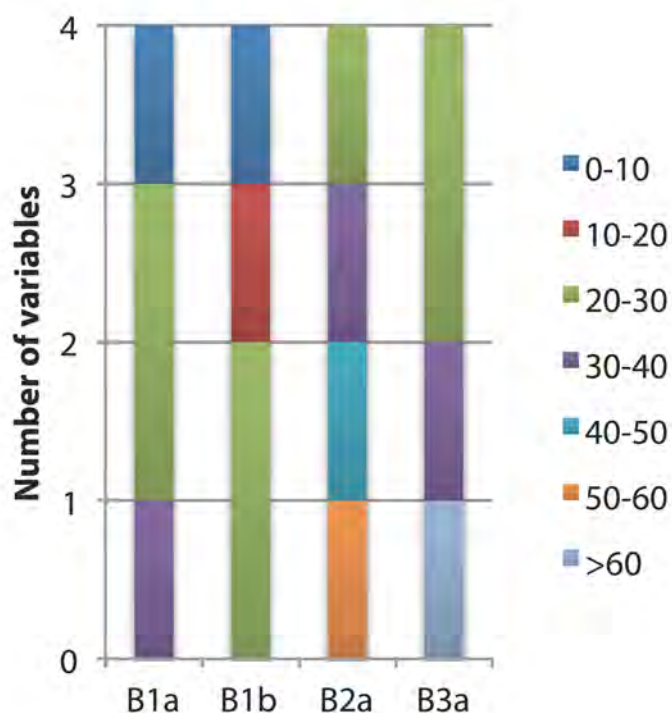


Figure 7.16. Number of variables with CV values 0–>60% for each rim form in the class B sample. 0–10% CV represents the lowest CV values, i.e. a higher level of standardisation, and 50–60% CV represents the highest CV values, i.e. a lower level of standardisation. Refer to Figure 5.1 for rim form images.

Source: C. Sarjeant.

#### *Summary of class B standardisation analysis*

There was some homogeneity within forms B1a, B1b and B2a in all of the statistical procedures, except for the PCA and CV values, which displayed variability within the form B2a samples. None of the statistical methods indicated homogeneity in the form B3a samples. In terms of the CV values for dimensional variables, only form B1a and B1b exhibited evidence of standardisation.

#### *Class C*

Class C consists of simple, unrestricted vessels. These forms differ to class B in that they are commonly dish rather than bowl-shaped (Figure 5.1). Class C vessels incorporate a great deal of morphological variation, particularly in the lip shape of the C1 forms. The measured variables were angle of the rim, diameter of the rim, thickness of the body, and thickness of the rim (Figure 7.1). Once again, the four previously described statistical methods (PCA, cluster analysis, CVA and CV) were applied to understand the variability and homogeneity in the morphology of the C class ceramics.

#### *Principal components analysis*

The greatest variability in the following PCA plot (Figure 7.17) is a result of the angle of the rim and diameter (Table 7.10). Generally, the PCA plot shows that the samples cluster together. There is some separation between forms C1a, C2b and C3a, whereby the different forms tend to cluster together, exhibiting some degree of standardisation within each form (Figure 7.17). The clusters are clarified in the following hierarchical cluster analysis (Figure 7.18, Table 7.11).

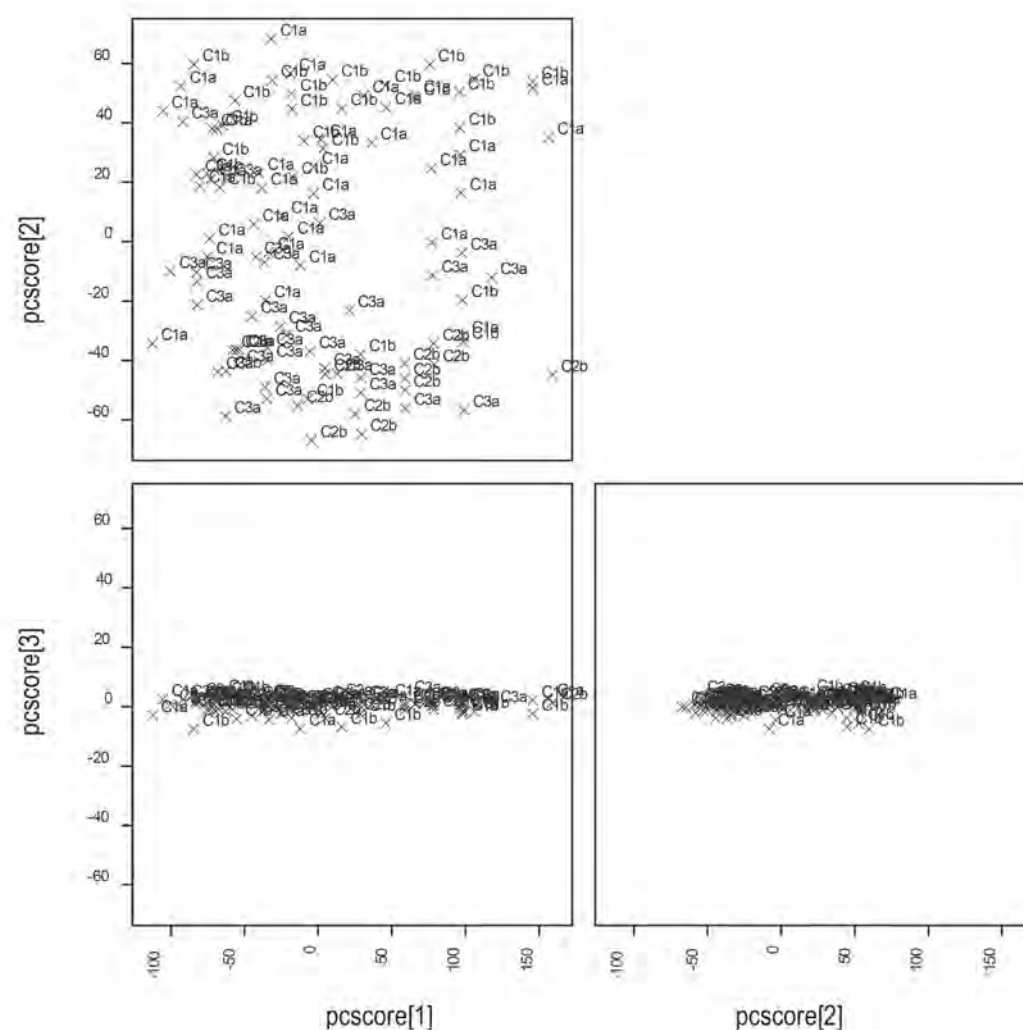


Figure 7.17. PCA plot of class C dimensional variables with rim forms labelled. First three dimensions. Refer to Figure 5.1 for rim form images.

Source: C. Sarjeant.

Table 7.10. PCA loadings for Figure 7.17 of class C dimensional variables. First three dimensions. The bold values indicate the variables that presented the greatest variability in the PCA.

Variables	PC 1 (74.77%)	PC 2 (25.10%)	PC 3 (0.08%)
Angle of rim (degrees)	<b>-0.03096</b>	<b>0.99934</b>	<b>0.01591</b>
Diameter (mm)	<b>0.99946</b>	0.03075	0.01031
Thickness of body (mm)	0.00670	0.01482	-0.26426
Thickness of rim (mm)	0.00834	<b>0.01275</b>	<b>-0.96427</b>

Source: Compiled by C. Sarjeant.

#### *Hierarchical cluster analysis*

The dendrogram was cut at 0.90 (Figure 7.18) to divide the class C assemblage into groups. The number of samples within each form in these groups is shown in Table 7.11. The cluster analysis indicated there was considerable dimensional overlap between forms C1a and C1b. Form C2a samples cluster together, albeit separately from forms C1a and C1b, in group 7 in the dendrogram. Form C2b is more variable, and the form C3a samples cluster with the majority of the class C samples in groups 1, 2 and 3.

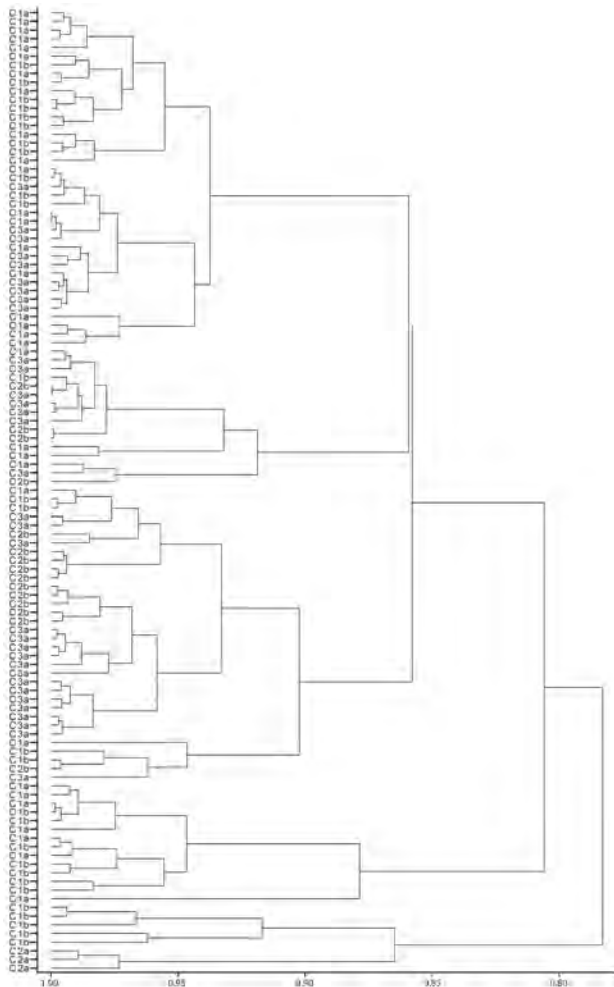


Figure 7.18. Dendrogram of average-linkage hierarchical cluster analysis of class C dimensional variables with rim forms labelled. Refer to Figure 5.1 for rim form images.

Source: C. Sarjeant.

Table 7.11. Number of samples in the hierarchical cluster analysis dendrogram groupings by rim form in Figure 7.18 of class C dimensional variables when cut at 0.90. Refer to Figure 5.1 for rim form images.

Group (cut at 0.90)	C1a	C1b	C2a	C2b	C3a
1	19	11	0	0	9
2	4	2	0	3	7
3	2	4	0	11	17
4	6	7	0	0	0
5	1	0	0	0	0
6	0	5	0	0	0
7	0	0	3	0	0

Source: Compiled by C. Sarjeant.

### *Canonical variate analysis*

The number of C2a rim forms was too few to be included in the analysis, and only forms C1a, C1b, C2b and C3a were applied to the CVA. The CVA indicated a high amount of variability within these class C forms in terms of morphological measurements (Figure 7.19, Table 7.12).

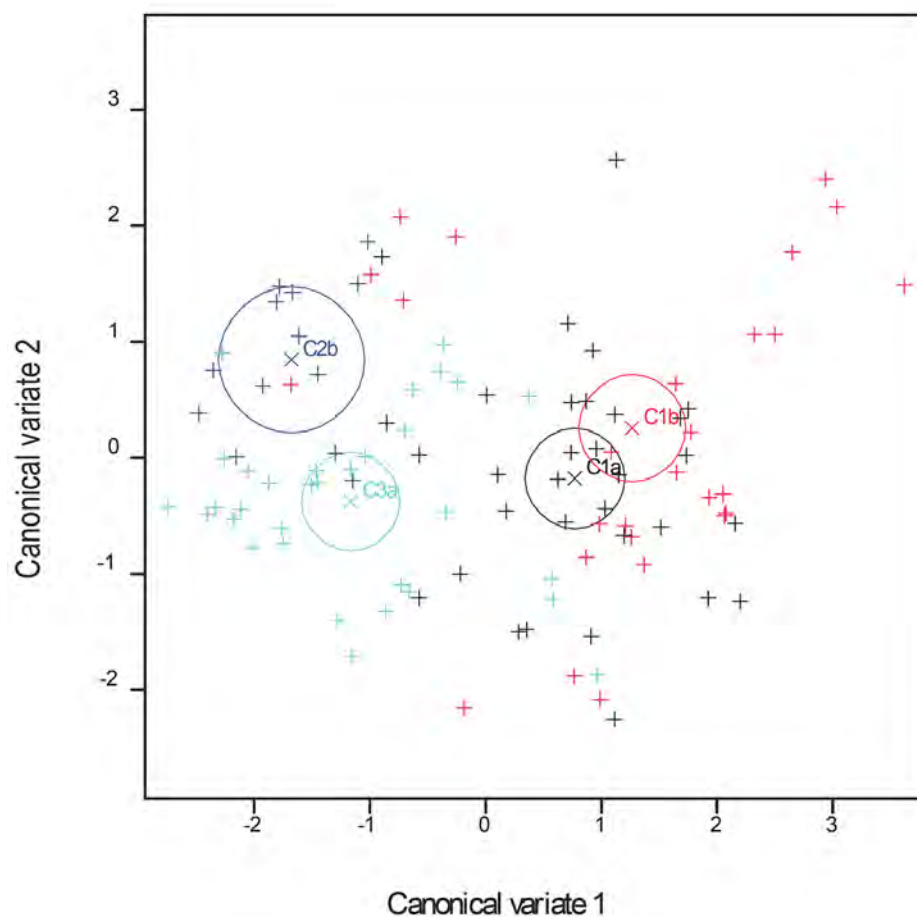


Figure 7.19. CVA plot of class C dimensional variables with 95% confidence circles and rim forms labelled. First two dimensions. Refer to Figure 5.1 for rim form images.

Source: C. Sarjeant.

Table 7.12. CVA loadings for Figure 7.19 of class C dimensional variables. First three dimensions.

Variables	1 (89.33%)	2 (10.44%)	3 (0.23%)
Angle of rim (degrees)	0.1788	0.3555	-0.2855
Diameter (mm)	0.0343	-0.0119	0.0028
Thickness of rim (mm)	0.0000	0.0060	0.0116
Thickness of body (mm)	0.0763	0.0396	0.2123

Source: Compiled by C. Sarjeant.

### *Coefficient of variation*

No specific variables contributed to a presence of low or high CV values for the class C samples. This is because many of the variables resulted in relatively mid-range CV values, indicating a low level of control in standardising the production of these forms. The only form to exhibit low variability was C2a, however very few samples of this form were included in the study. The angle of the rim and thickness of the rim variables had low CV values within the form C2a sample (Figure 7.20, Figure 7.21).

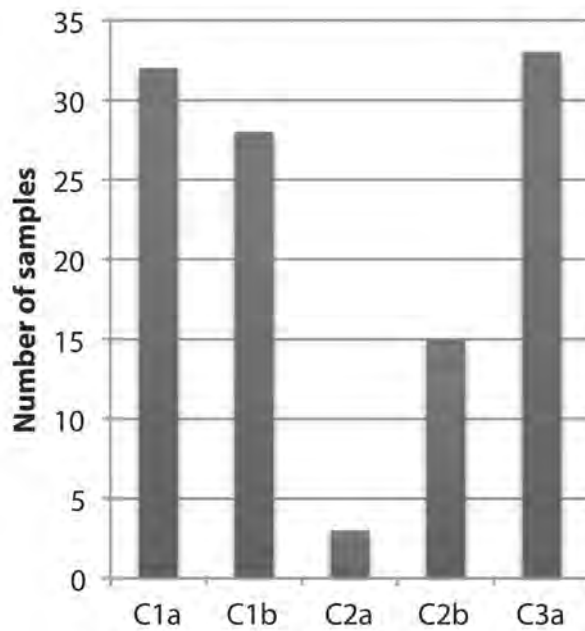


Figure 7.20. Number of class C samples of each rim form in the study of standardisation. Refer to Figure 5.1 for rim form images.

Source: C. Sarjeant.

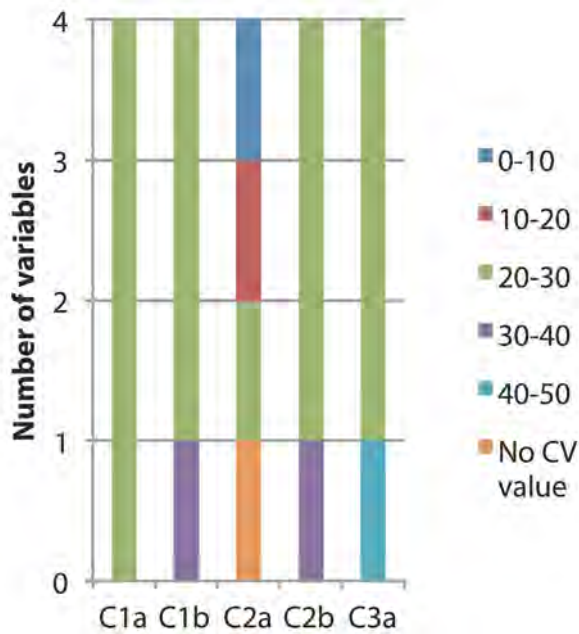


Figure 7.21. Number of variables with CV values 0–50% for each rim form in the class C sample. 0–10% CV represents the lowest CV values, i.e. a higher level of standardisation, and 40–50% CV represents the highest CV values, i.e. a lower level of standardisation. Refer to Figure 5.1 for rim form images.

Source: C. Sarjeant.

#### *Summary of class C standardisation analysis*

The high degree of variability within all of the class C forms is clear from all of the statistical procedures. The only form that presents less variability is C3a, but this is most likely a result of the small sample size.

#### *Class D*

Class D vessels are unique to An Sơn and there are very few known comparative examples elsewhere in Southeast Asia. The class D1 forms are wavy rimmed, unrestricted bowl-shaped vessels and the class D2 forms are serrated rimmed, unrestricted conical-shaped vessels (Figure 5.1). The measured variables include angle of the rim to the internal ridge, diameter of the rim, length of the rim to the internal ridge, height of a single wave, width of a single wave, thickness of the body, and thickness of the rim (Figure 7.1). Once again, PCA, cluster analysis, CVA and CV, statistical methods were applied to understand the variability and homogeneity in the morphology of the D class ceramics, these being.

#### *Principal components analysis*

The greatest variability in the following PCA plot (Figure 7.22) is a result of the angle, diameter and length of the rim (Table 7.13). Generally, the PCA plot shows that there is a distinct group of form D1a rims that cluster separately from the other D1a and D1b samples, while the form D2a samples cluster separately (Figure 7.22). The clusters are clarified in the following hierarchical cluster analysis (Figure 7.23, Table 7.14).



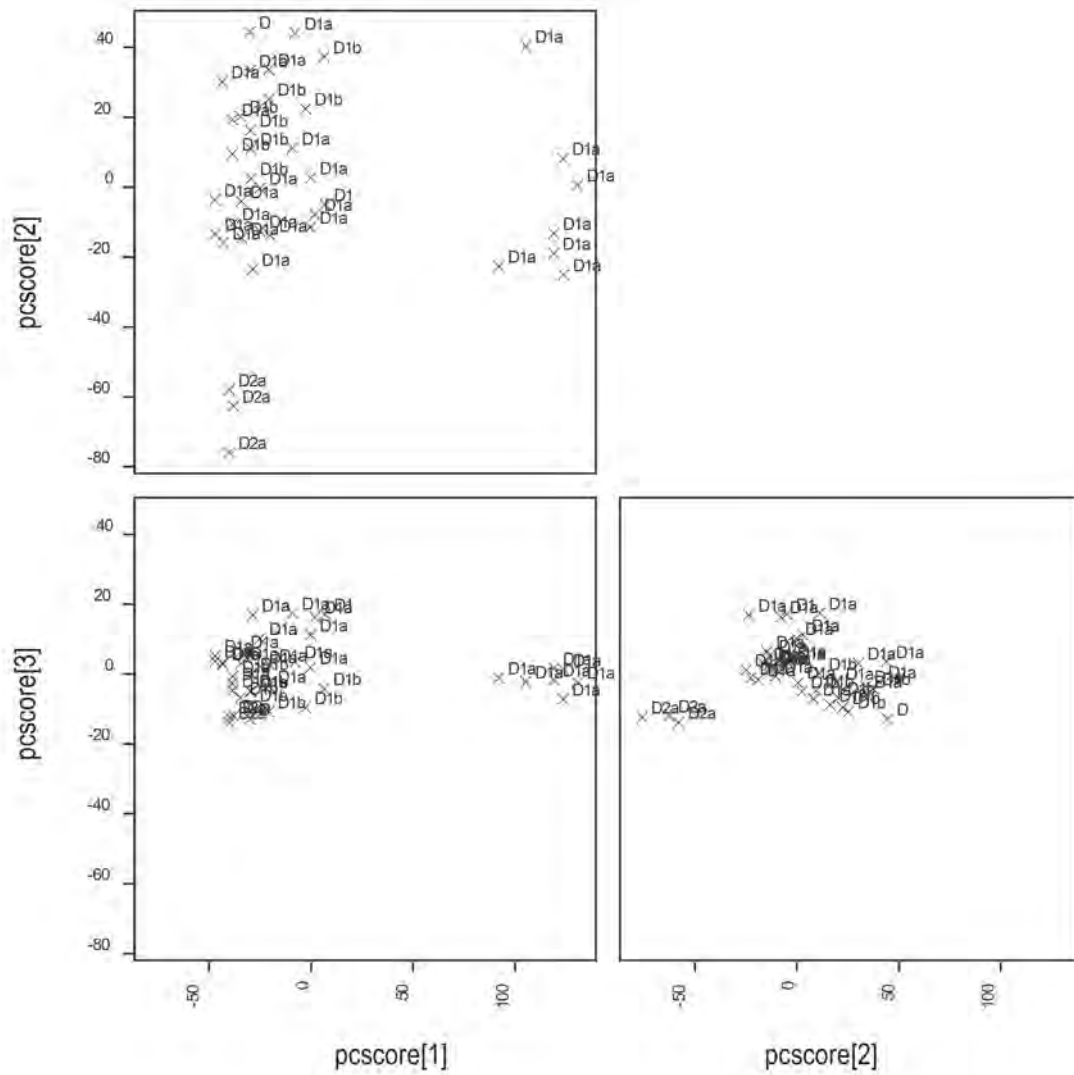


Figure 7.22. PCA plot of class D dimensional variables with rim forms labelled. First three dimensions. Refer to Figure 5.1 for rim form images.

Source: C. Sarjeant.

Table 7.13. PCA loadings for Figure 7.22 of class D dimensional variables. First three dimensions. The bold values indicate the variables that presented the greatest variability in the PCA.

Variables	PC 1 (79.14%)	PC 2 (8.67%)	PC 3 (1.71%)
Angle of rim to internal ridge (degrees)	<b>0.99950</b>	0.00919	-0.02119
Diameter (mm)	<b>-0.01197</b>	<b>0.99492</b>	<b>-0.07478</b>
Length of rim to internal ridge (mm)	<b>-0.01100</b>	<b>-0.04286</b>	0.27507
Height of single wave (mm)	-0.00085	0.03239	0.40203
Width of single wave (mm)	0.02707	0.08388	<b>0.86719</b>
Thickness of body (mm)	-0.00157	0.00722	0.00364
Thickness of rim (mm)	0.00264	0.00873	0.06812

Source: Compiled by C. Sarjeant.

### *Hierarchical cluster analysis*

The dendrogram was cut at 0.90 (Figure 7.23) to divide the class D assemblage into groups. The number of samples within each form in these groups is shown in Table 7.14. The cluster analysis revealed distinct groups for the class D samples based on the dimensional variables. However, there is substantial overlap between forms D1a and D1b in group 2. The D2a samples were also distinct, with the majority in group 6. The single D2a sample in group 4 and the class D variant in group 5 were outliers.

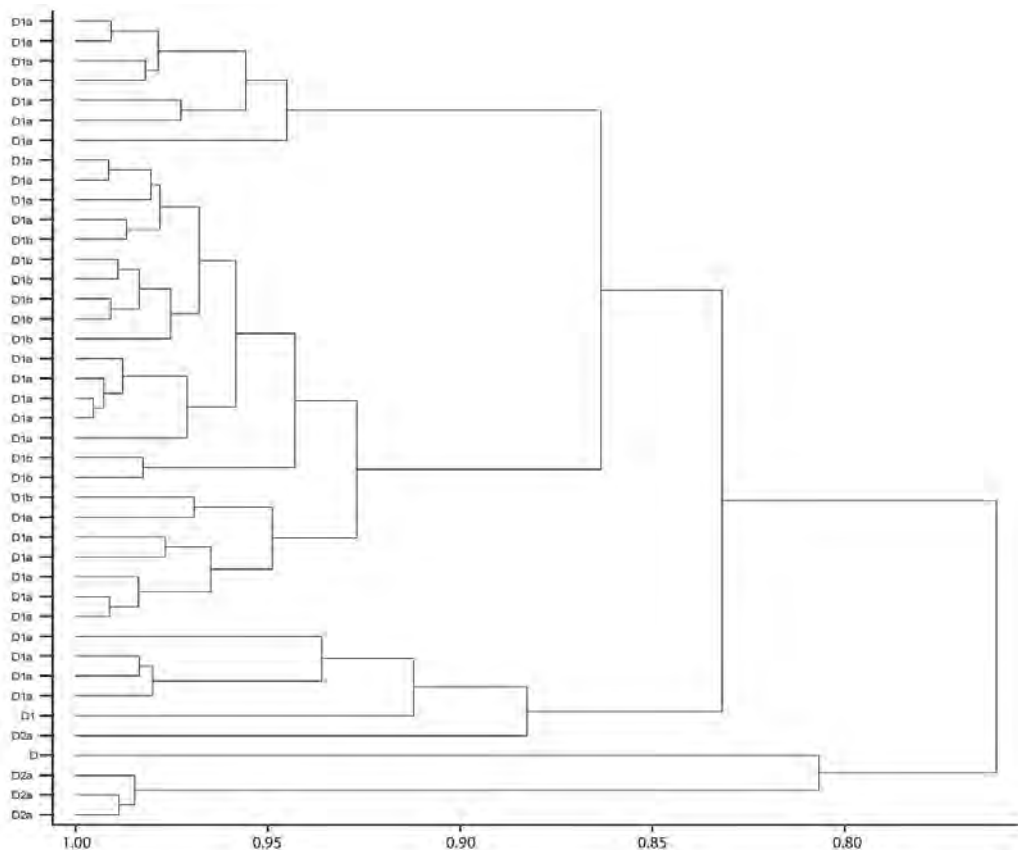


Figure 7.23. Dendrogram of average-linkage hierarchical cluster analysis of class D dimensional variables with rim forms labelled. Refer to Figure 5.1 for rim form images.

Source: C. Sarjeant.

Table 7.14. Number of sherds in the hierarchical cluster analysis dendrogram groupings by rim form in Figure 7.23 of class D dimensional variables when cut at 0.90. Refer to Figure 5.1 for rim form images.

Group (cut at 0.90)	D1a	D1b	D2a
1	7	0	0
2	15	9	0
3	5 (D1: n=1)	0	0
4	0	0	1
5	1 (D: n=1)	0	0
6	0	0	3

Source: Compiled by C. Sarjeant.

#### *Canonical variate analysis*

The CVA indicates quite a low level of variation, with form D2a separate from the D1 forms. Generally, the D1a and D1b sherds cluster together, suggesting limited morphological variability within these forms (Figure 7.24, Table 7.15).

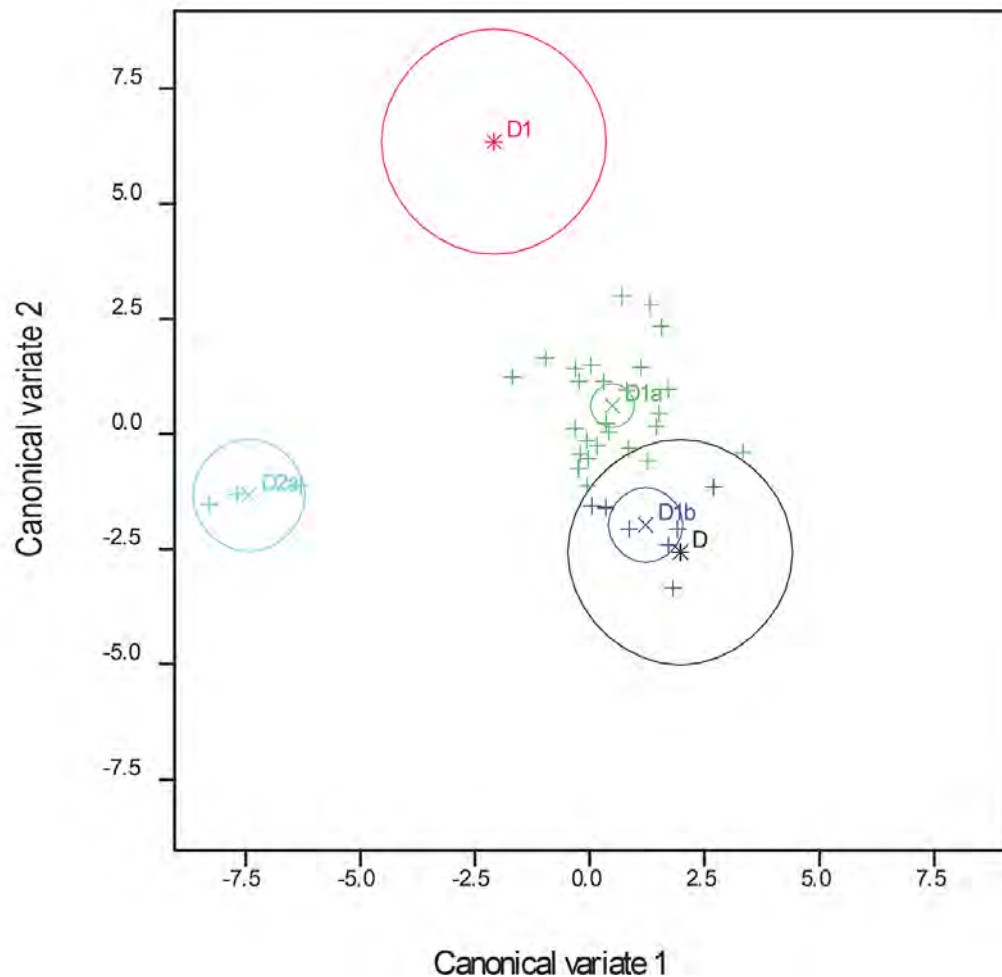


Figure 7.24. CVA plot of class D dimensional variables with 95% confidence circles and rim forms labelled. First two dimensions. Refer to Figure 5.1 for rim form images.

Source: C. Sarjeant.

Table 7.15. CVA loadings for Figure 7.24 of class D dimensional variables. First three dimensions.

Variables	1 (61.82%)	2 (30.09%)	3 (6.22%)
Angle of rim to internal ridge (degrees)	0.1043	0.0927	0.0525
Diameter (mm)	0.0011	0.0100	0.0034
Length of rim to internal ridge (mm)	0.0448	-0.0180	-0.0112
Height of single wave (mm)	0.0649	0.2726	-0.2680
Width of single wave (mm)	-0.2188	0.0914	0.1767
Thickness of rim (mm)	0.0625	0.4490	0.2988
Thickness of body (mm)	0.5207	-0.6457	0.6448

Source: Compiled by C. Sarjeant.

### *Coefficient of variation*

CV values were lower for the diameter and the length of the rim to the internal ridge. The D1 vessels had high CV values calculated for the angle of the rim to the internal ridge, and the D2a vessels had high CV values calculated for the variables of height and width of single wave (see Figure 7.1 for measured variables). Rim form D2a had a greater number of variables with low CV values than that of rim form D1 (Figure 7.25, Figure 7.26).

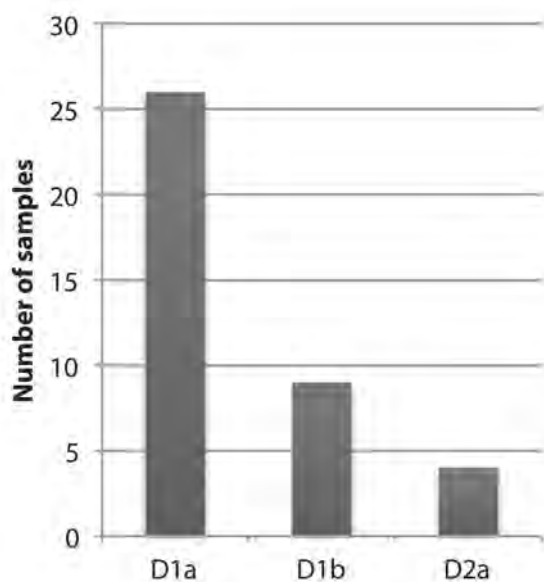


Figure 7.25. Number of class D samples of each rim form in the study of standardisation. Refer to Figure 5.1 for rim form images.

Source: C. Sarjeant.

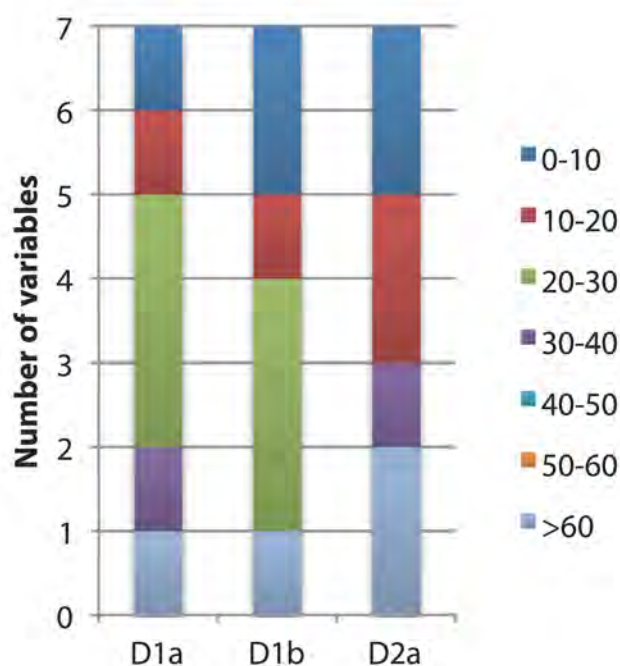


Figure 7.26. Number of variables with CV values 0–>60% for each rim form in the class D sample. 0–10% CV represents the lowest CV values, i.e. a higher level of standardisation, and 50–60% CV represents the highest CV values, i.e. a lower level of standardisation. Refer to Figure 5.1 for rim form images.

Source: C. Sarjeant.

#### *Summary of class D standardisation analysis*

The statistical procedures indicated that there was some degree of standardisation in each of the class D forms, particularly form D2a. The D1a and D1b forms were similar in their dimensional variables, but the PCA also displayed two separate groups for D1. This may be clarified further by the following study of standardisation in the D1a form.

#### *Class E*

Class E vessels are ceramic stoves, known as *cà ràng* in Vietnamese. They are similar in rim shape to the C1 forms except that the body incorporates three square or rounded-shaped projections, which support another pottery vessel during cooking (Figure 5.1). The measured variables include angle of the rim, diameter of the rim, thickness of the body, and thickness of the rim (Figure 7.1). The number of class E samples included in the standardisation study was minimal and only one analysis was possible, the CV calculation.

*Coefficient of variation*

There were too few class E sherds in the sample to suggest any kind of standardisation. However, one variable, thickness of the body, had a very low CV value (Table 7.16).

Table 7.16. Number of variables with CV values 0–60% for each rim form in the class E sample. 0–10% CV represents the lowest CV values, i.e. a higher level of standardisation, and 50–60% CV represents the highest CV values, i.e. a lower level of standardisation.

	CV (%)	0–10	10–20	20–30	30–40	40–50	50–60
E1a (n = 5)		1	0	1	0	0	1

Source: Compiled by C. Sarjeant.

**Standardisation of morphology, decoration and fabric**

Several rim forms were studied more closely in order to combine dimensional variables with decorative and fabric variables. Distinct forms that occurred in high proportions in the An Son assemblage were selected for this study. The clay matrix compositional data also presented groups (Chapter 6, Part II) that contribute to the following analyses. The included forms are A2a, B1a, C1b and D1a, and considers the variability and standardisation of these forms within each context, either layer/square or burial.

*Form A2a*

Form A2a is an everted, restricted vessel, commonly appearing with a decorative panel on the shoulder (Figure 5.1). The dimensional, decorative and fabric variables of this form were assessed statistically. The measured variables include angle of the rim, diameter of the rim, length of the rim, thickness of the body, and, thickness of the rim (Figure 7.1). The four previously described statistical methods (PCA, cluster analysis, CVA and CV) were applied to understand the variability and homogeneity in the morphology of the A2a form ceramics. The decorative data were assessed with CV calculations, and the clay matrix compositional data with PCA.

*Standardisation of morphology***Principal components analysis**

The greatest variability in the following PCA plot (Figure 7.27) is a result of the form's diameter and thickness of the body (Table 7.17). Generally, the PCA plot shows that there is one main cluster, with some outliers from Trench 1 layers 2 and 8. There are no groups associated with any particular layer, but the samples from Trench 1 layers 7 and 8 tend to group together (Figure 7.27). The clusters are clarified in the following hierarchical cluster analysis (Figure 7.28, Table 7.18a, Table 7.18b).

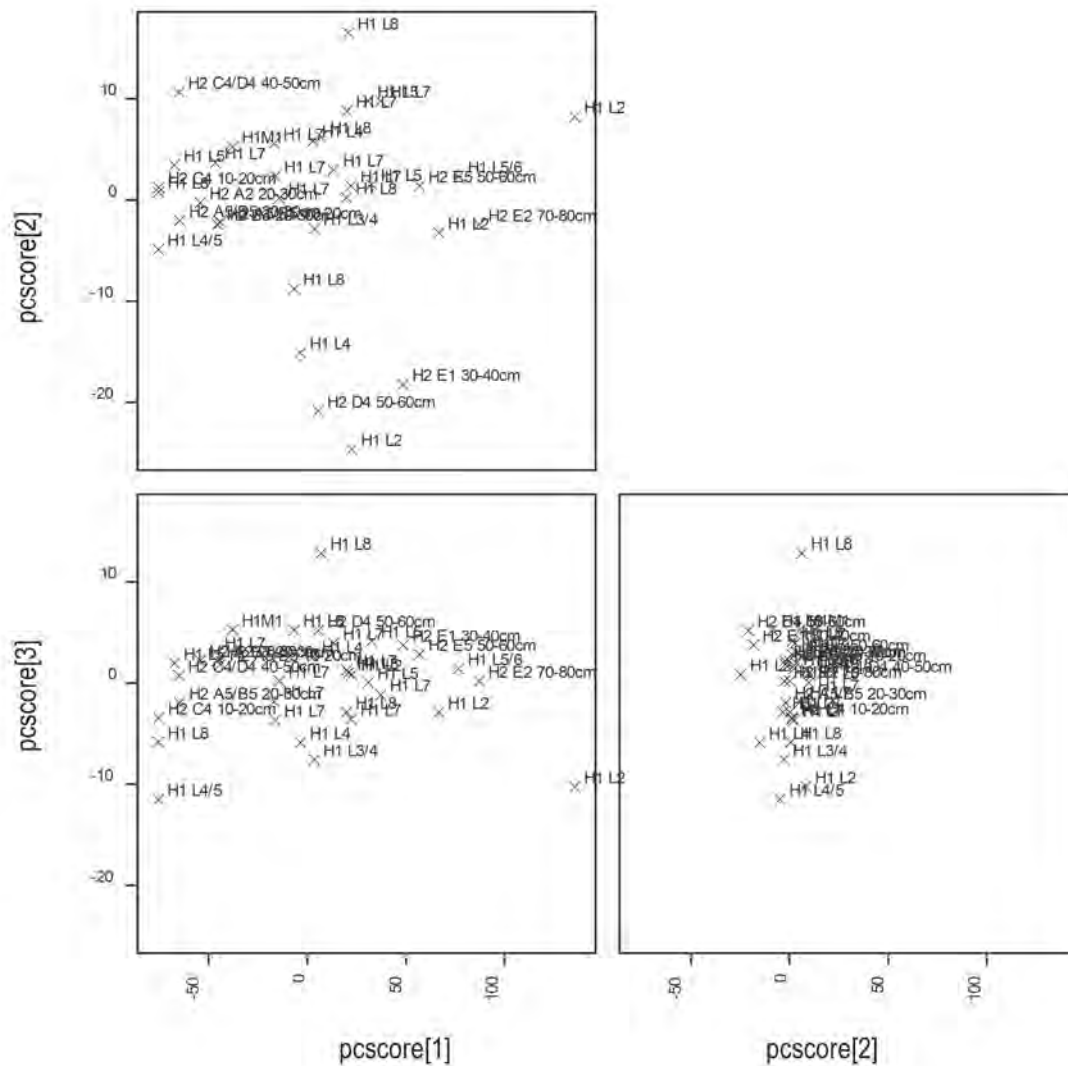


Figure 7.27. PCA plot of form A2a dimensional variables with layers/provenience labelled. First three dimensions. Key: H1 = 2009 Trench 1, H2 = 2009 Trench 2, L = Layer, M = Burial.

Source: C. Sarjeant.

Table 7.17. PCA loadings for Figure 7.27 of form A2a dimensional variables. First three dimensions. The bold values indicate the variables that presented the greatest variability in the PCA.

Variables	PC 1 (96.12%)	PC 2 (2.86%)	PC 3 (0.83%)
Angle of rim (degrees)	0.04199	<b>0.53170</b>	<b>0.84277</b>
Diameter (mm)	<b>0.98982</b>	0.09167	<b>-0.10562</b>
Length of rim (mm)	0.13508	<b>-0.83947</b>	0.52139
Thickness of body (mm)	<b>0.00273</b>	-0.05640	-0.02992
Thickness of rim (mm)	0.01554	0.03152	-0.07641

Source: Compiled by C. Sarjeant.

### Hierarchical cluster analysis

The dendrogram was cut at 0.90 (Figure 7.28) to divide the form A2a assemblage into groups. The number of samples within each layer/provenience in these groups is shown in Table 7.18a and Table 7.18b. The cluster analysis illustrates that there is no consistency in the dimensional variables of form A2a within any single layer.

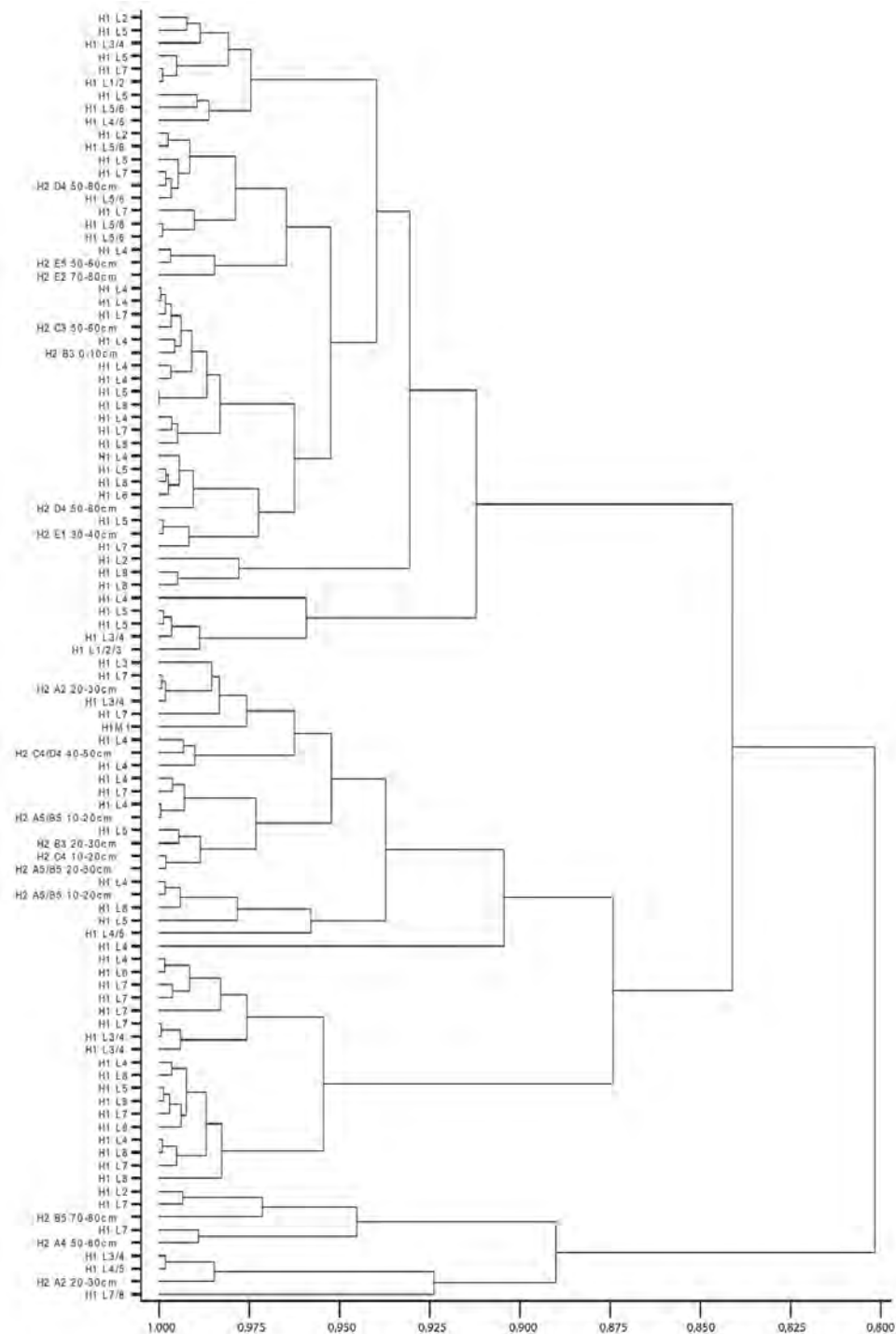


Figure 7.28. Dendrogram of average-linkage hierarchical cluster analysis of form A2a dimensional variables with layers/provenience labelled. Key H1 = 2009 Trench 1, H2 = 2009 Trench 2, L = Layer, M = Burial.

Source: C. Sarjeant.



Table 7.18a. Number of samples in the hierarchical cluster analysis dendrogram groupings by layer/provenience in Figure 7.28 of form A2a dimensional variables when cut at 0.90. Key: H1 = 2009 Trench 1, H2 = 2009 Trench 2, L = Layer, M = Burial: 2009 Trench 1.

Groups (cut at 0.90)	H1 L1/2	H1 L1/2/3	H1 L2	H1 L3	H1 L3/4	H1 L4	H1 L4/5	H1 L5	H1 L5/6	H1 L6	H1 L7	H1 L7/8	H1 L8	H1 M1
1	1	1	3	0	2	9	1	9	5	1	6	0	5	0
2	0	0	0	1	1	6	1	2	0	1	3	0	1	1
3	0	0	0	0	1	3	0	1	0	1	6	0	5	0
4	0	0	1	0	0	0	0	0	0	0	2	0	0	0
5	0	0	0	0	1	0	1	0	0	0	0	1	0	0

Source: Compiled by C. Sarjeant.

Table 7.18b. Number of samples in the hierarchical cluster analysis dendrogram groupings by layer/provenience in Figure 7.28 of form A2a dimensional variables when cut at 0.90. Key: H1 = 2009 Trench 1, H2 = 2009 Trench 2, L = Layer, M = Burial: 2009 Trench 2.

Groups (cut at 0.90)	H2 A2 20–30 cm	H2 A4 50– 60 cm	H2 A5/ B5 10–20 cm	H2 A5/B5 20–30 cm	H2 B3 0–10 cm	H2 B5 70–80 cm	H2 C3 50–60 cm	H2 C4 10–20 cm	H2 C4/ D4 40–50 cm	H2 D4 50–60 cm	H2 E1 30–40 cm	H2 E2 70–80 cm	H2 E5 50–60 cm
1	0	0	0	0	1	0	1	0	0	2	0	1	1
2	1	0	1	2	1	0	0	1	1	0	0	0	0
3	0	0	0	0	0	0	0	0	0	0	0	0	0
4	0	1	0	0	0	1	0	0	0	0	0	0	0
5	1	0	0	0	0	0	0	0	0	0	0	0	0

Source: Compiled by C. Sarjeant.

### Canonical variate analysis

The CVA shows that form A2a samples from Trench 1 layers 7 and 8 cluster together in terms of dimensional variables (Figure 7.29, Table 7.19), as displayed in the previous PCA (Figure 7.27, Table 7.17).

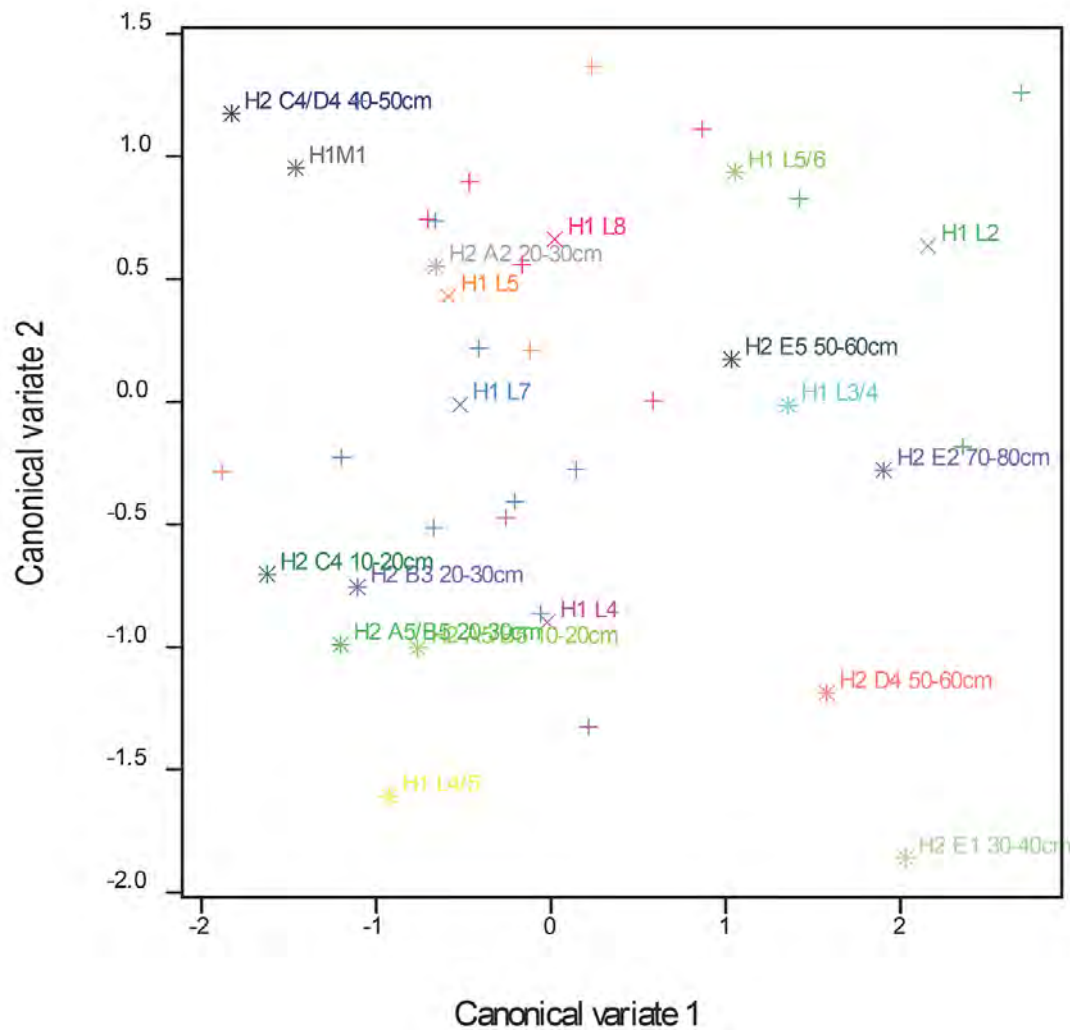


Figure 7.29. CVA plot of form A2a dimensional variables with layers/provenance labelled. First two dimensions. Key: H1 = 2009 Trench 1, H2 = 2009 Trench 2, L = Layer, M = Burial.

Source: C. Sarjeant.

Table 7.19. CVA loadings for Figure 7.29 of form A2a dimensional variables. First three dimensions.

Variables	1 (58.94%)	2 (24.03%)	3 (13.04%)
Angle of rim (degrees)	0.1069	-0.2396	-0.1641
Diameter (mm)	-0.0375	0.0703	0.049
Length of rim (mm)	0.2279	0.4279	-0.2971
Thickness of body (mm)	0.0499	-0.0553	0.0389
Thickness of rim (mm)	0.0118	0.011	0.0016

Source: Compiled by C. Sarjeant.

### Coefficient of variation

The CV values were mid-range for all of the dimensional variables. However, the angle of the rim was somewhat lower and thickness of the body somewhat higher, when compared to the other variables. A larger number of form A2a dimensional variables had low CV values in layer 5/6 of

Trench 1, as well as squares A5/B5 and D4 of Trench 2. The CV values of Trench 1 layers 4, 5, 5/6 and 6 were generally lower. These layers represent the mid-sequence when variability within the form A2a assemblage was low (Figure 7.30, Figure 7.31).

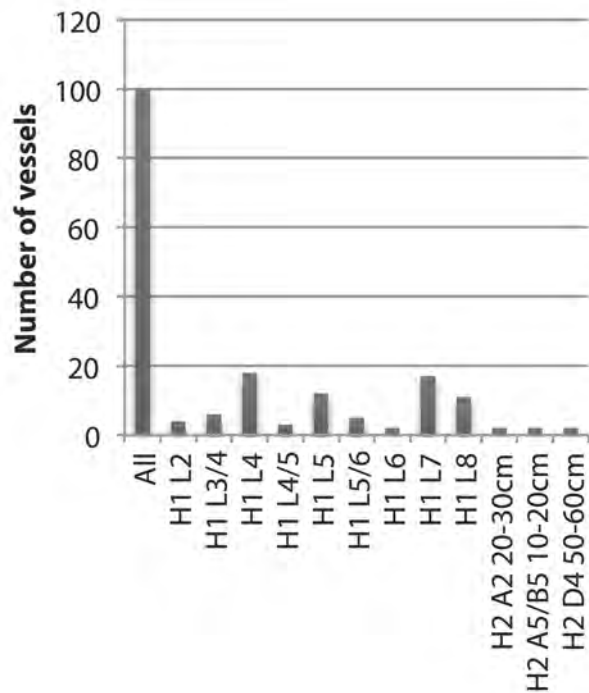


Figure 7.30. Number of form A2a samples of each layer/provenience in the study of standardisation. Key: H1 = 2009 Trench 1, H2 = 2009 Trench 2, L = Layer.

Source: C. Sarjeant.

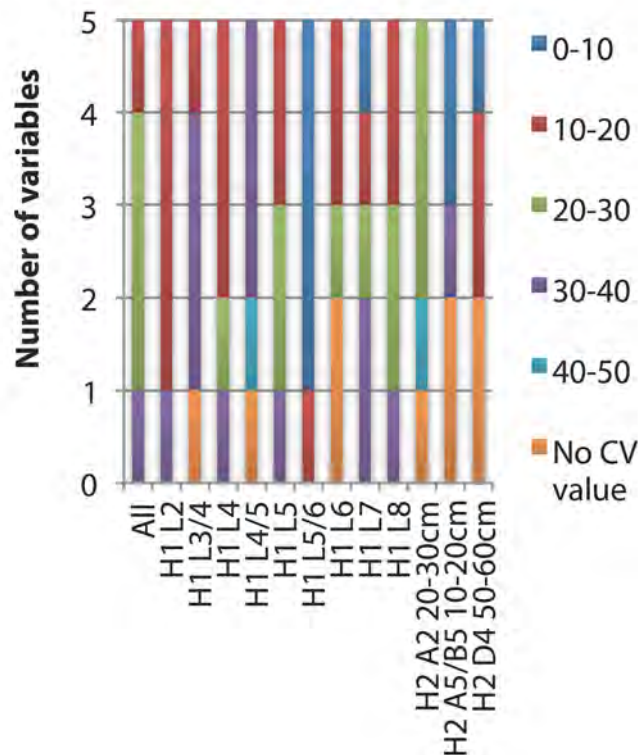


Figure 7.31. Number of variables with CV values 0–50% for each layer/provenience in the form A2a sample. 0–10% CV represents the lowest CV values, i.e. a higher level of standardisation, and 40–50% CV represents the highest CV values, i.e. a lower level of standardisation. Key: H1 = 2009 Trench 1, H2 = 2009 Trench 2, L = Layer.

Source: Compiled by C. Sarjeant.

### *Standardisation of decoration*

The form A2a vessels were predominantly roulette stamped around the shoulder. These band decorations were recorded by measuring the width of the band dimensions of the impressions within the decoration, and the mode and shape of the decoration. The varieties of roulette stamping, some of which are created by knotting cord around a rolling implement, are shown in Figure 7.32. The width of the band on each of the measured samples is shown in Figure 7.33. Most of the decorative bands were 20–30 mm wide, regardless of the mode and shape of the decoration. The decorative variables were analysed using the statistical method, CV.

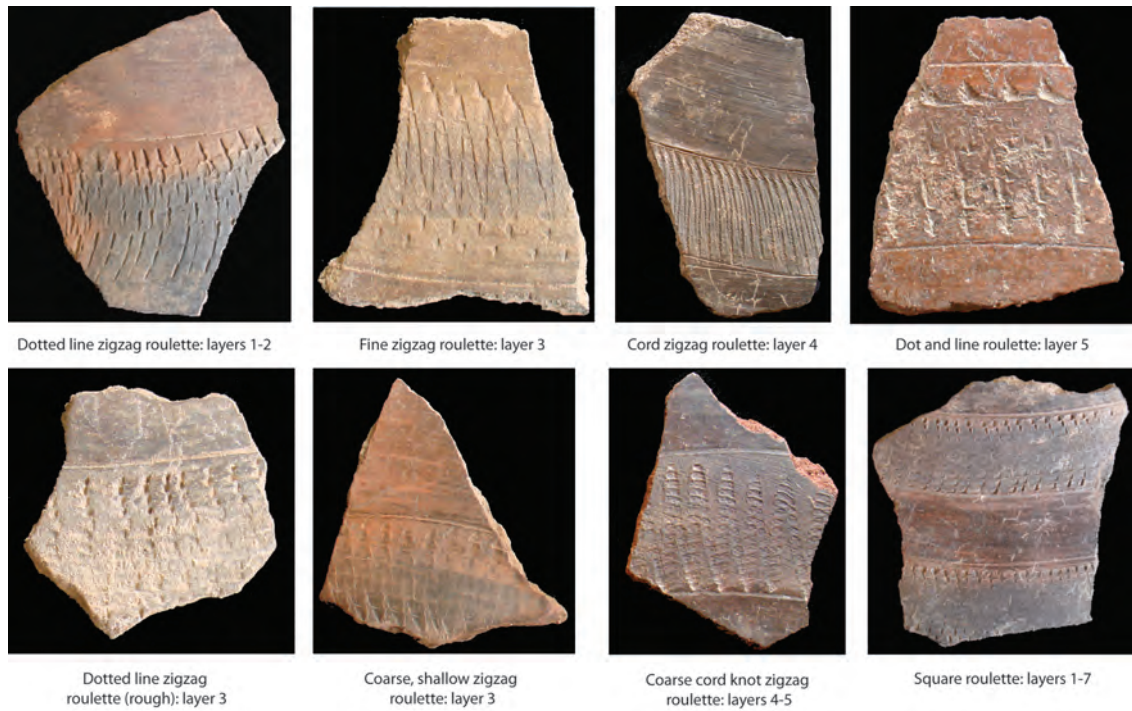


Figure 7.32. Roulette stamped decorations on form A2a vessels. All sherds are from Trench 1. Not to scale.

Source: Photos C. Sarjeant.

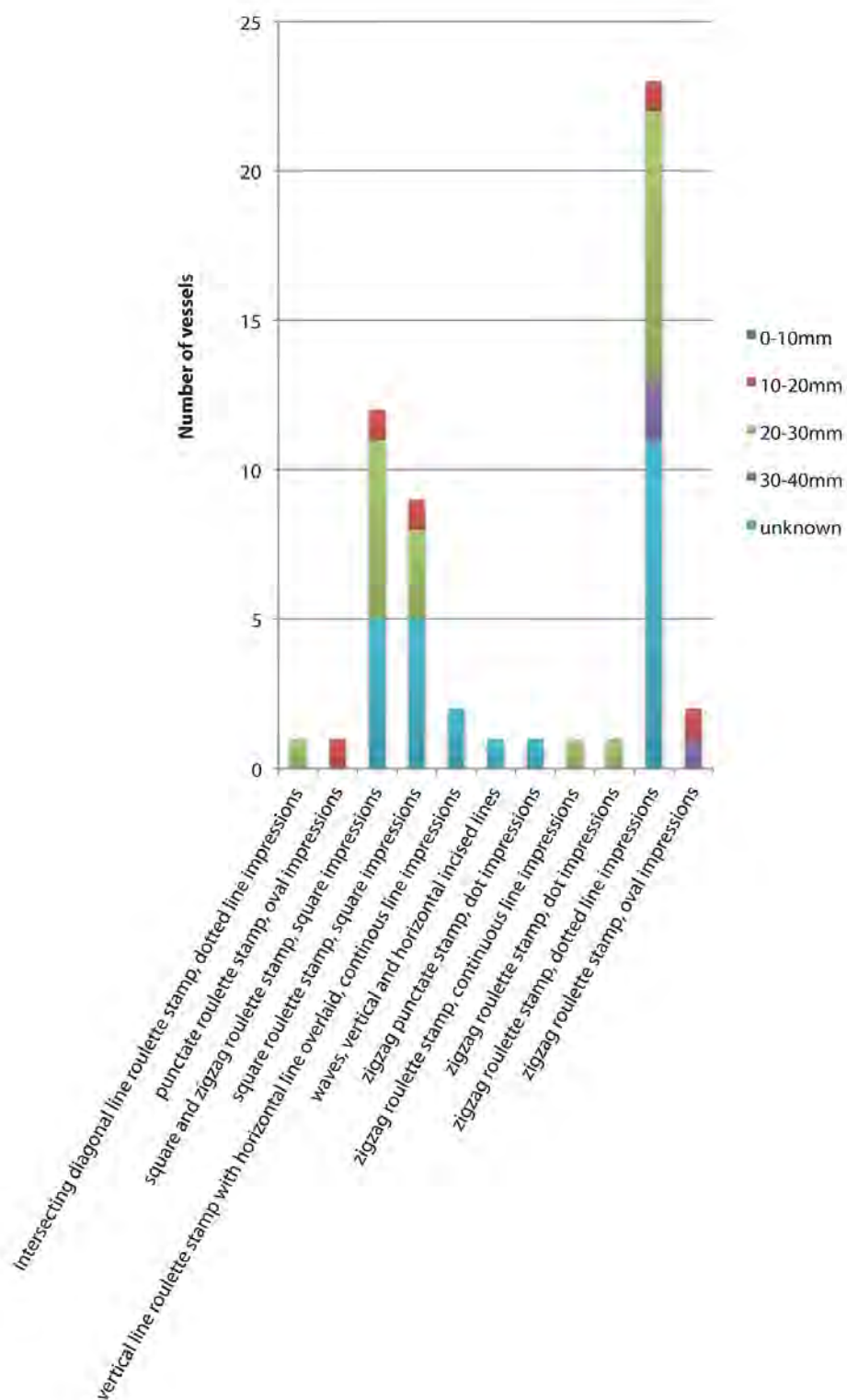


Figure 7.33. Number of form A2a sherds with each mode of decoration and the width (mm) of the decorative band. Total samples=54. Refer to Figure 7.32 for decoration images.

Source: C. Sarjeant.

### **Coefficient of variation**

The CV calculation for the decorative variables on the A2a vessels was conducted in a similar manner as for dimensional variables.

The decorative variables included:

- mode of decoration: continuous line, dot impression, oval impression, square impression, dotted line, incision
- shape of decoration: square roulette stamping, square and zigzag roulette stamping, zigzag roulette stamping, zigzag punctate stamping, intersecting diagonal line roulette stamping, wave and line incision, vertical line roulette stamping with horizontal line overlaid, punctate roulette stamping (some examples are shown in Figure 7.32)
- width of the decorative band
- size of the space between each horizontal decoration point
- size of the space between each vertical decoration point within the band
- number of vertical rows within the band when present.

Generally, decorative variables were calculated to mid to high CV values, although the width of the band variable had a lower CV value. The CV values indicated a high degree of variation within the decorations of A2a vessels. This implies the use of individual implements for applying these decorative bands. That is, each potter had their own implement with a unique pattern. Alternatively, highly perishable throwaway items were only used once or twice to decorate a vessel, before being discarded. The CV values were slightly lower for the square and zigzag roulette stamp decorated samples in comparison to the other modes and shapes of decoration on the form A2a vessels (Figure 7.34, Figure 7.35).

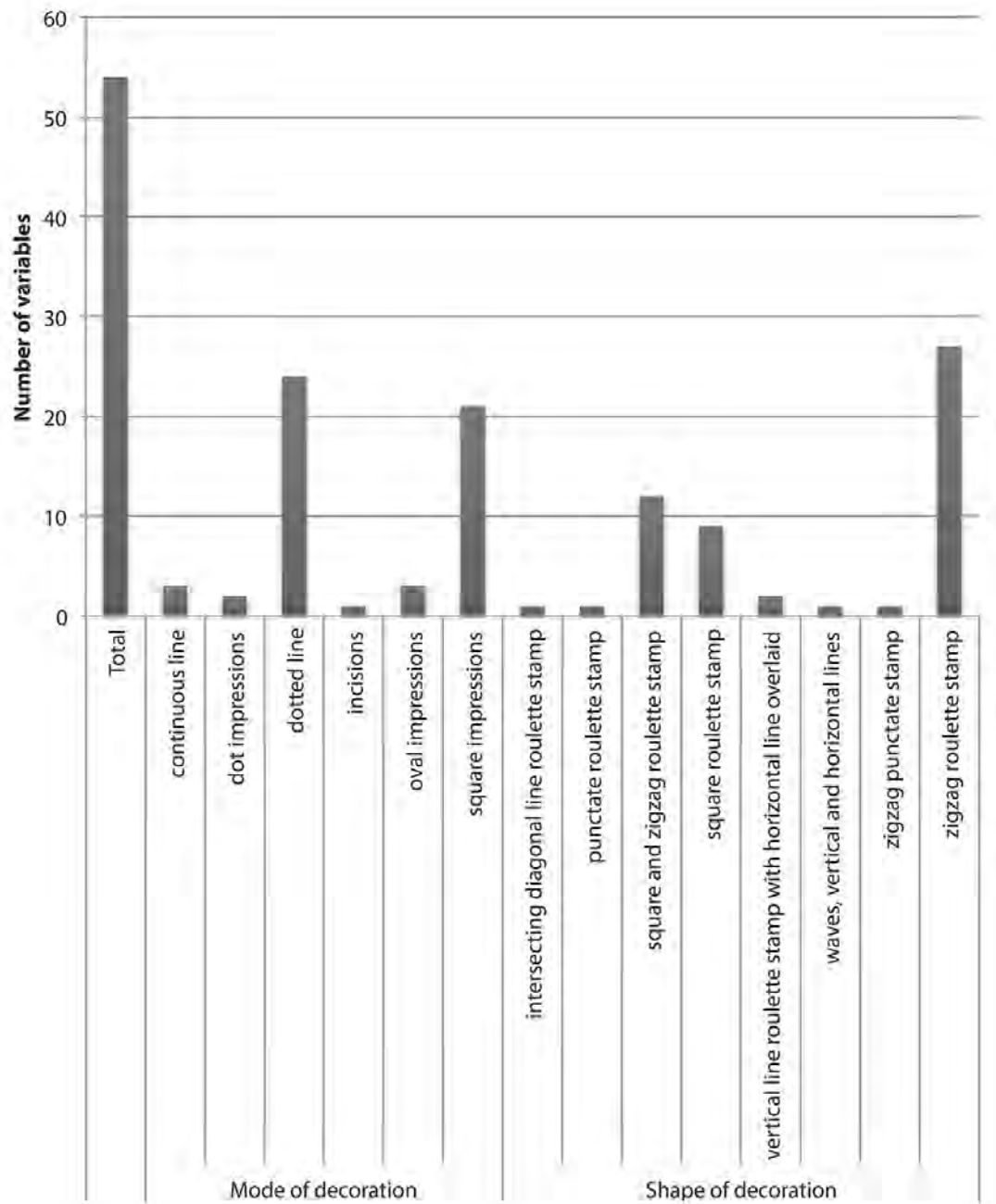


Figure 7.34. Number of form A2a samples with each mode or shape of decoration in the study of standardisation. One mode and one shape of decoration were identified for each sample. Total samples = 54. Refer to Figure 7.32 for decoration images.

Source: C. Sarjeant.



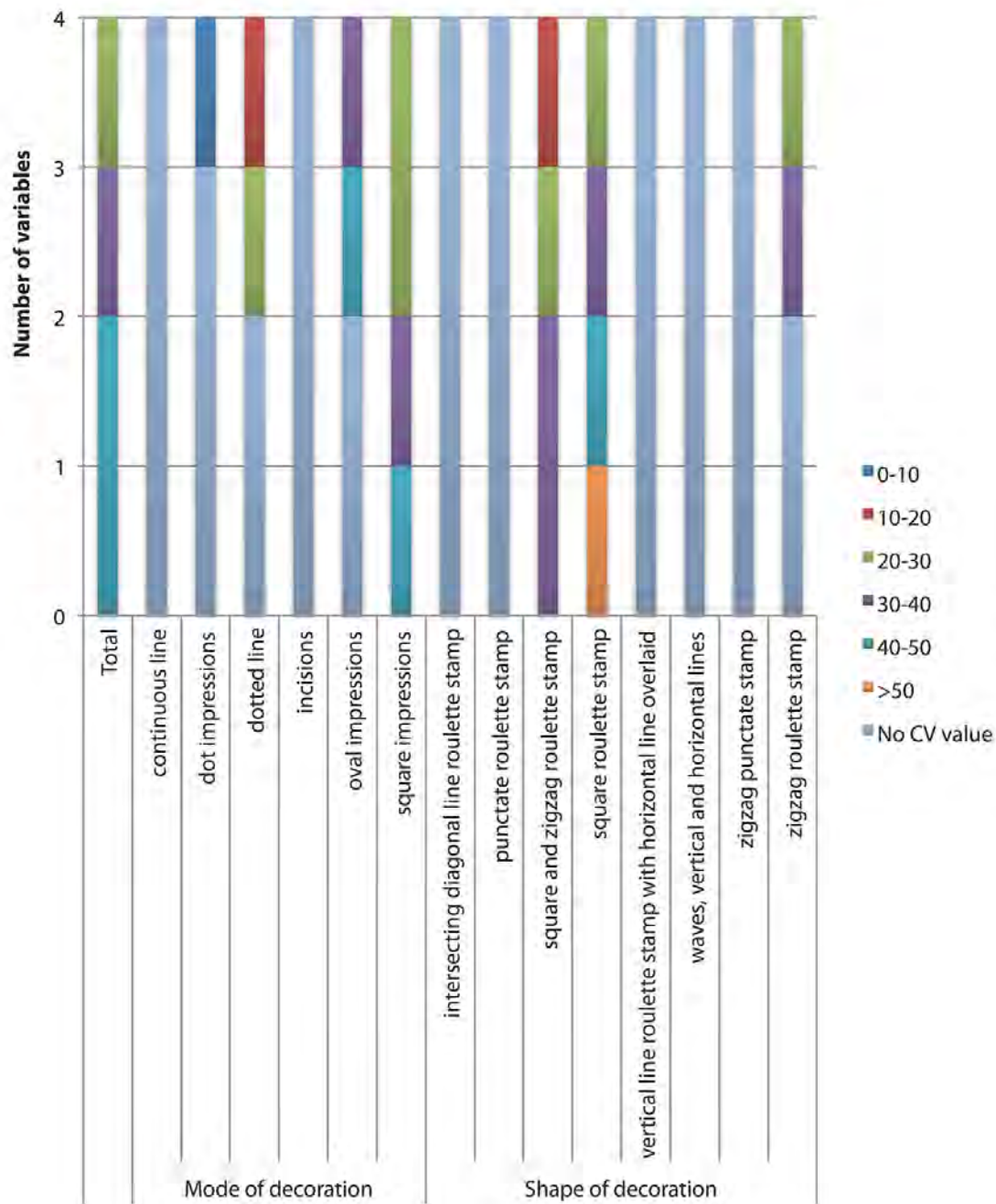


Figure 7.35. Number of variables with CV values 0–>50% for decorative mode or shape in the form A2a sample. 0–10% CV represents the lowest CV values, i.e. a higher level of standardisation, and 40–50% CV represents the highest CV values, i.e. a lower level of standardisation. One mode and one shape of decoration were identified for each sample. Total samples = 54. Refer to Figure 7.32 for decoration images.

Source: C. Sarjeant.

*Standardisation of fabrics*

The fabric analyses of temper and the clay matrix (Chapter 6) showed that there was consistency in the selection of sand tempers, TG A1-1, TG A1-2 and TG A1-5, for form A2a vessels. These temper groups contained sands of quartz and alkali feldspar; quartz, alkali feldspar and plagioclase feldspar; and quartz, alkali feldspar and amphibole, respectively. The clay matrix compositional data for the sampled form A2a rim and roulette decorated body sherds indicates homogeneity in the PCA plot, with the exception of one sherd from Trench 1 layer 5/6. The greatest variability was evident in the magnesium and sodium oxides variables (Figure 7.36, Table 7.20).

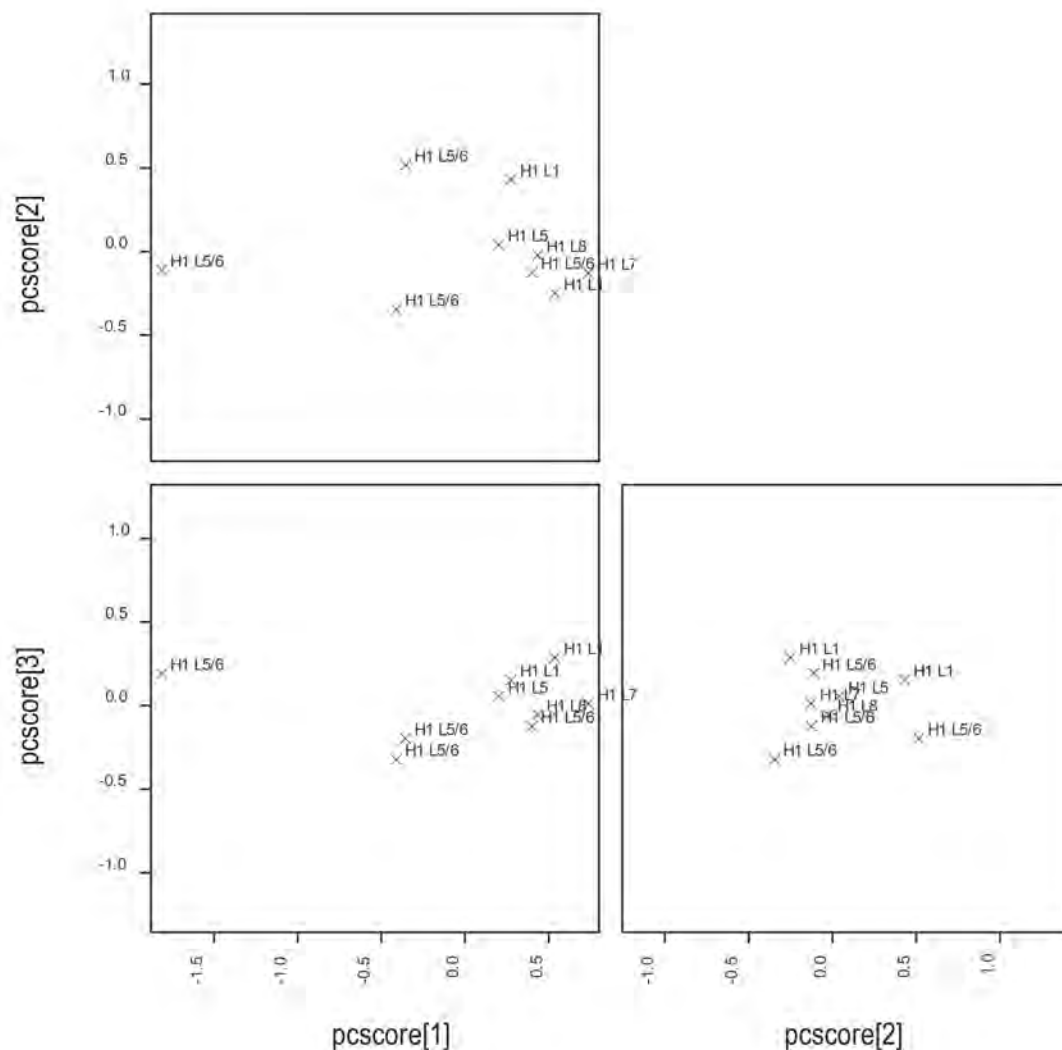


Figure 7.36. PCA plot of form A2a clay matrix composition with layers/provenance labelled. First three dimensions. Key: H1 = 2009 Trench 1, L = Layer.

Source: C. Sarjeant.

Table 7.20. PCA loadings for Figure 7.36 of form A2a clay matrix composition. First three dimensions. The bold values indicate the variables that presented the greatest variability in the PCA.

Variables	PC 1 (79.42%)	PC 2 (11.10%)	PC 3 (4.98%)
CaO	0.03276	0.27122	<b>0.42444</b>
FeO	0.05760	-0.18626	<b>-0.69495</b>
K <sub>2</sub> O	0.56883	<b>-0.59525</b>	0.01447
MgO	<b>-0.07147</b>	0.09223	-0.28644
Na <sub>2</sub> O	<b>0.81609</b>	0.40277	0.00919
SiO <sub>2</sub>	0.02244	0.42560	0.00956
TiO <sub>2</sub>	0.02039	<b>0.43077</b>	-0.50445

Source: Compiled by C. Sarjeant.

### *Summary of form A2a standardisation analysis*

The statistical analyses of form A2a vessels appear to have mid-range levels of standardisation, indicating there was variation in their manufacture. It is possible that many individuals who had knowledge of this widespread form manufactured this vessel locally at An Sơn (see Chapters 8 and 9). The basic morphology and fabrics were similar across the A2a form, but there was substantial variation in the measured dimensional and decorative variables, implying a variety of functions (inferred from the range in sizes) made by a number of individuals (inferred from the range of decorative modes and shapes).

### *Form B1a*

Form B1a is a simple, restricted bowl-shaped vessel with an inverted, thickened rim. The surface treatment is commonly cord-marked on the body (Figure 5.1). The morphological and fabric variables were assessed statistically. The measured variables include angle of the rim, diameter of the rim, thickness of the body, and thickness of the rim (Figure 7.1). Once again, the four previously described statistical methods (PCA, cluster analysis, CVA and CV) are applied to understand the variability and homogeneity in the morphology of the B1a form ceramics. The clay matrix compositional data were assessed using PCA.

### *Standardisation of morphology*

#### **Principal components analysis**

The PCA (Figure 7.37) of form B1a presents variability in the first principal component only, primarily in the angle of the rim and diameter (Table 7.21). There are few major outliers in the PCA plots, except for one sherd from Trench 1 layers 5 and 8 and two sherds from Trench 1 burial 2 (H1M2). The remaining sherds more or less cluster together (Figure 7.37). The clusters are clarified in the following hierarchical cluster analysis (Figure 7.38, Table 7.22).



very little evidence to suggest that B1a vessels from similar contexts had similar dimensions in the cluster analysis, except perhaps for those from Trench 1 layers 7/8 and 8, which cluster together in groups 2 and 3 (Table 7.22).

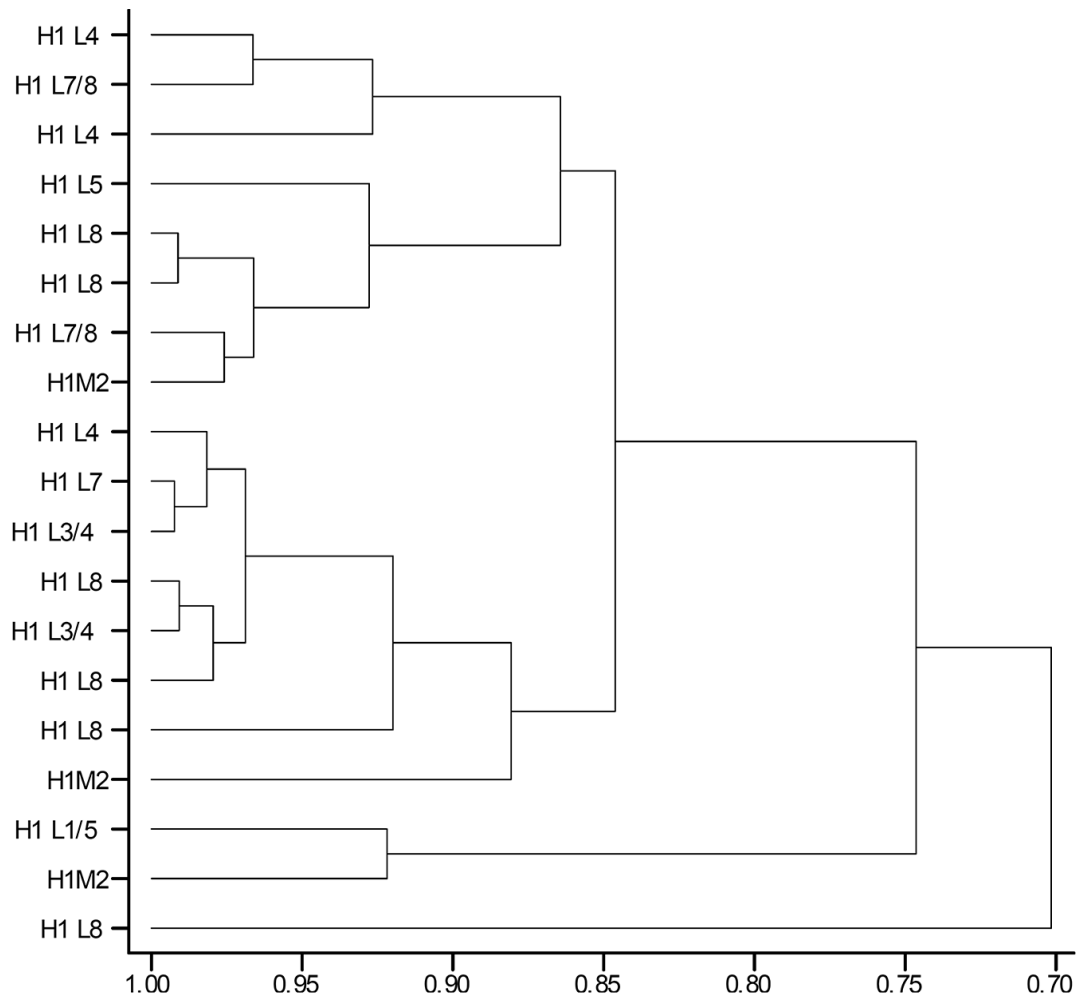


Figure 7.38. Dendrogram of average-linkage hierarchical cluster analysis of form B1a dimensional variables with layers/provenience labelled. Key: H1 = 2009 Trench 1, L = Layer, M = Burial.

Source: C. Sarjeant.

Table 7.22. Number of samples in the hierarchical cluster analysis dendrogram groupings by layer/provenience in Figure 7.38 of form B1a dimensional variables when cut at 0.90. Key: H1 = 2009 Trench 1, L = Layer M = Burial.

Groups (cut at 0.90)	H1 L1/5	H1 L3/4	H1 L4	H1 L5	H1 L7	H1 L7/8	H1 L8	H1M2
1	0	0	2	0	0	1	0	0
2	0	0	0	1	0	1	2	1
3	0	2	1	0	1	0	3	0
4	0	0	0	0	0	0	0	1
5	1	0	0	0	0	0	0	1
6	0	0	0	0	0	0	1	0

Source: Compiled by C. Sarjeant.

### Canonical variate analysis

The CVA shows that the form B1a sherds from Trench 1 burial 2 (H1M2) are homogeneous in dimensions, which are plotted alongside the sherds from Trench 1 layers 7/8 and 8. The sherds from the middle to upper layers present greater variation in the CVA (Figure 7.39, Table 7.23).

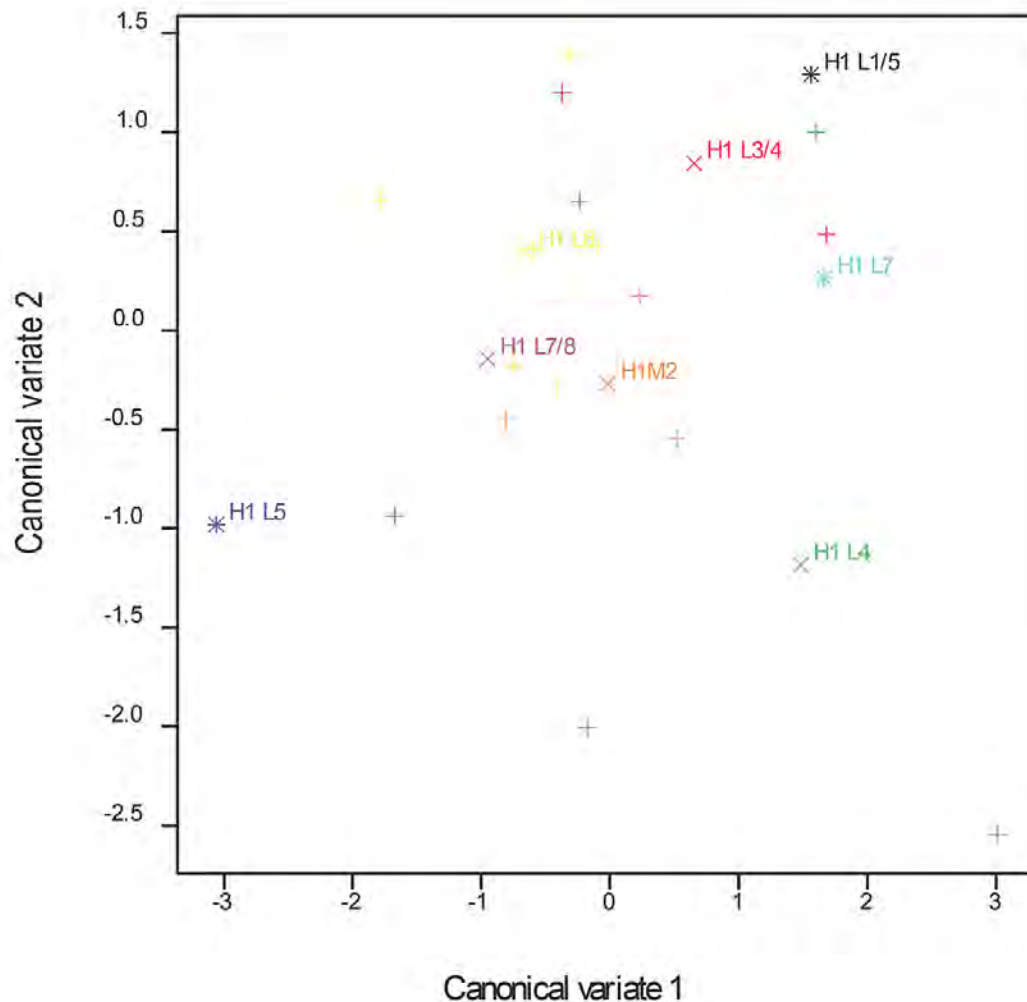


Figure 7.39. CVA plot of form B1a dimensional variables with layers/provenience labelled. First two dimensions. Key: H1 = 2009 Trench 1, L = Layer, M = Burial.

Source: C. Sarjeant.

Table 7.23. CVA loadings for Figure 7.39 of form B1a dimensional variables. First two dimensions.

Variables	1 (61.83%)	2 (22.34%)	3 (12.50%)
Angle of inverted aspect (degrees)	0.6068	-0.3412	-0.0056
Diameter (mm)	0.0658	0.0748	0.0725
Thickness of body (mm)	-0.824	-0.2066	0.516
Thickness of rim (mm)	0.0089	0.0038	0.0011

Source: Compiled by C. Sarjeant.

### Coefficient of variation

The angle of the rim was always calculated with a low CV value for form B1a, while the diameter and thickness of the body were often higher. There were a large number of variables with low CV values in the samples from Trench 1 burial 2 (H1M2) and Trench 1 layers 7/8 and 8, indicating less variability in form B1a in these contexts (Figure 7.40, Figure 7.41).

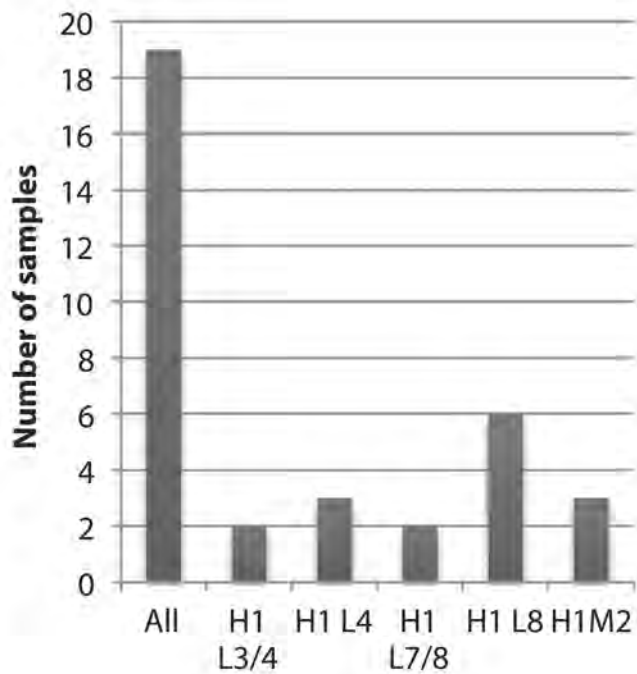


Figure 7.40. Number of form B1a samples of each layer/provenance in the study of standardisation. Key: H1 = 2009 Trench 1, L = Layer, M = Burial.

Source: C. Sarjeant.

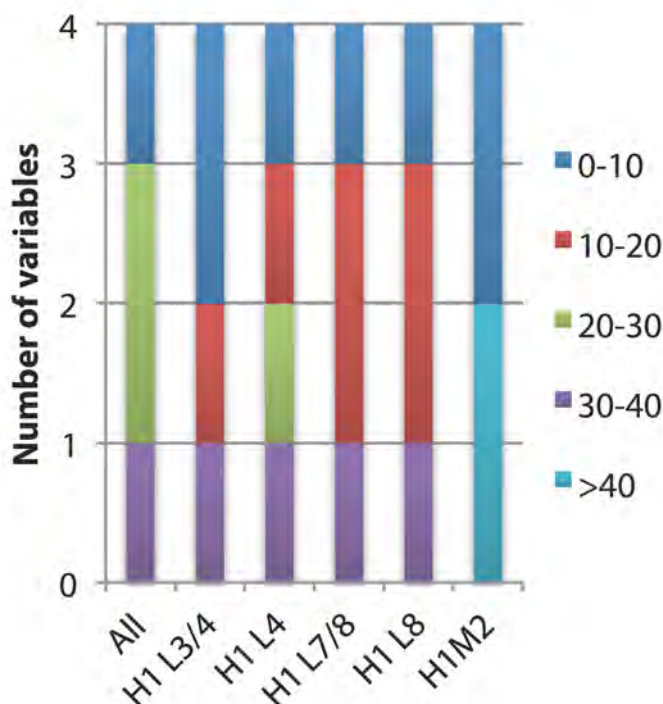


Figure 7.41. Number of variables with CV values 0–>40% for each layer/provenience in the form B1a sample. 0–10% CV represents the lowest CV values, i.e. a higher level of standardisation, and 30–40% CV represents the highest CV values, i.e. a lower level of standardisation. Key: H1 = 2009 Trench 1, L = Layer, M = Burial.

Source: C. Sarjeant.

#### *Standardisation of fabrics*

The B1a vessels were either tempered predominantly with fibre (TG B-1), with sand and trace amounts of fibre (TG A1-8), or a mix of quartz mineral sand with fibre (TG A1/B-2) (see Chapter 6, Part I). The PCA plot (Figure 7.42) of the clay matrix compositional data presents greatest variability in the iron and sodium oxide concentrations (Table 7.24). The second and third principal components also contributed to variability in the PCA, as observed in the sodium and silicon, and calcium and iron oxides (Table 7.24). The PCA shows there was no great similarity in the form B1a sherds in terms of the clay matrix composition (Figure 7.42). However, the CVA of all rim sherds (see Chapter 6, Part II) showed that the form B1a sherds cluster together, although they were outliers in comparison to the cluster of A2a, D1a and D1b forms (see Figure 6.38).



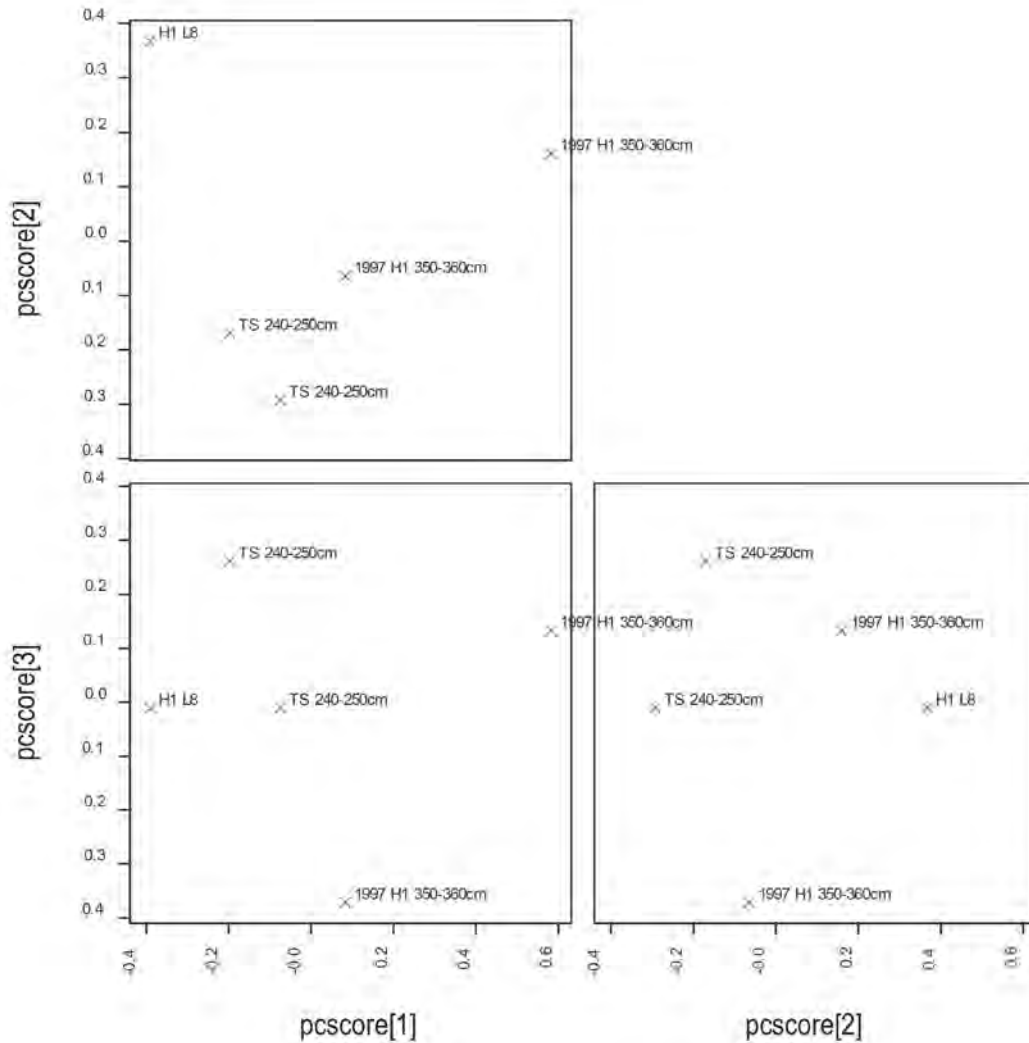


Figure 7.42. PCA plot of form B1a clay matrix composition with layers/provenance labelled. First three dimensions. Key: H1 = 2009 Trench 1, TS = 2009 Test Square, 1997 H1 = 1997 Trench 1, L = Layer.

Source: C. Sarjeant.

Table 7.24. PCA loadings for Figure 7.42 of form B1a clay matrix composition. First three dimensions. The bold values indicate the variables that presented the greatest variability in the PCA.

Variables	PC 1 (51.63%)	PC 2 (26.44%)	PC 3 (21.21%)
CaO	0.41008	-0.18843	<b>-0.84190</b>
FeO	<b>0.71755</b>	-0.18945	<b>0.35177</b>
K <sub>2</sub> O	0.01773	0.21492	0.03374
MgO	0.52722	0.42910	0.07097
Na <sub>2</sub> O	<b>-0.01729</b>	<b>0.79166</b>	-0.22769
SiO <sub>2</sub>	0.07207	<b>-0.25420</b>	-0.09496
TiO <sub>2</sub>	0.18217	0.08334	0.31690

Source: Compiled by C. Sarjeant.

*Summary of form B1a standardisation analysis*

The four statistical analyses presented a similar picture for the manufacture of B1a vessels with regard to dimensional variables. The B1a vessels from earlier in the sequence and from the burial context displayed some homogeneity, however these are not high levels of standardisation when considered against absolute CV measures. Variability in the production of form B1a in the middle to later part of the sequence may be attributed to a general decrease in this form over time; the form was made less frequently, therefore there was less structure or regularity in its manufacture. While there was consistency in the dimensions and morphology of B1a vessels, particularly in the lowest layers, there is little evidence of such consistency in temper and clay selection.

*Form C1b*

Form C1b is a simple, unrestricted dish-shaped vessel with a direct or inverted rim, and a defined angled shoulder. These vessels are commonly plain (Figure 5.1). The morphological and fabric variables were assessed statistically. The measured variables include angle of the rim, diameter of the rim, thickness of the body, and thickness of the rim (Figure 7.1). Four statistical methods (PCA, cluster analysis, CVA and CV) were applied to understand the variability and homogeneity in the morphology of the C1b form ceramics. The clay matrix compositional data were assessed using PCA.

*Standardisation of morphology***Principal components analysis**

The greatest variability in the following PCA plot (Figure 7.43) is a result of the angle of the rim and diameter (Table 7.25). There is a centralised cluster of most of the form C1b samples, with some outliers, primarily from Trench 1 layers 3, 4, 4/5, 5/6 and 6, i.e. mid-sequence at An Sơn. The samples from higher and lower layers of Trenches 1 and 2, and those from burial contexts, cluster together in the PCA plot (Figure 7.43). The clusters are clarified in the following hierarchical cluster analysis (Figure 7.44, Table 7.26).

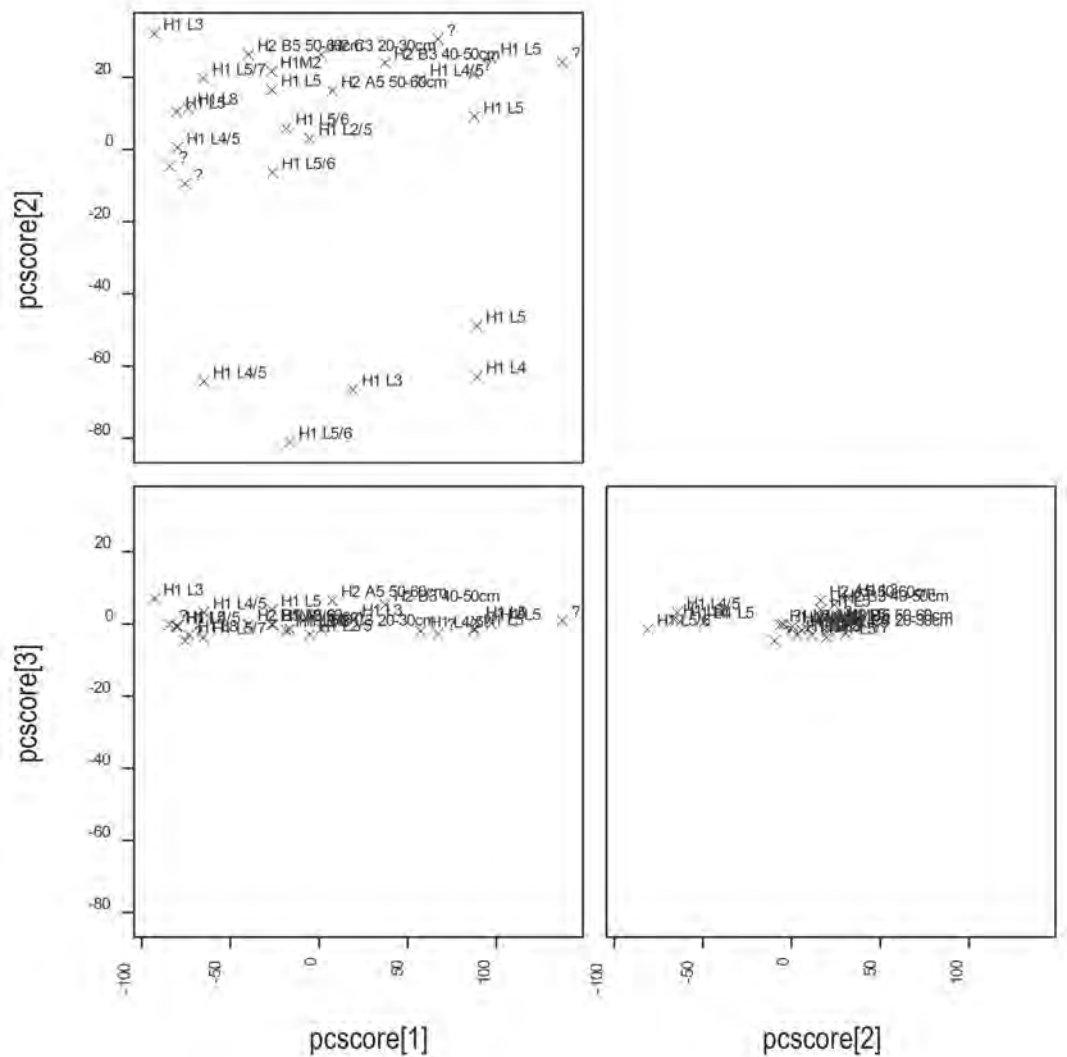


Figure 7.43. PCA plot of form C1b dimensional variables with layers/provenience labelled. First three dimensions. Key: H1 = 2009 Trench 1, H2 = 2009 Trench 2, L = Layer, M = Burial, ? = Unknown context.

Source: C. Sarjeant.

Table 7.25. PCA loadings for Figure 7.43 of form C1b dimensional variables. First three dimensions. The bold values indicate the variables that presented the greatest variability in the PCA.

Variables	PC 1 (80.37%)	PC 2 (19.44%)	PC 3 (0.15%)
Angle of rim (degrees)	-0.02178	<b>0.99952</b>	0.00169
Diameter (mm)	<b>0.99962</b>	0.02149	-0.00989
Thickness of body (mm)	0.01343	0.02232	<b>-0.02171</b>
Thickness of rim (mm)	0.01022	<b>-0.00099</b>	<b>0.99971</b>

Source: Compiled by C. Sarjeant.

### Hierarchical cluster analysis

The dendrogram was cut at 0.90 (Figure 7.44) to divide the form C1b assemblage into groups. The number of samples within each layer/provenience in these groups is shown in Table 7.26. The dendrogram displays very little evidence of form C1b samples grouping by context according to dimensional variables. This may be due to the small sample size within each context. However, many of the Trench 1 layer 5 vessels cluster close together in groups 2 to 5 (Table 7.26).

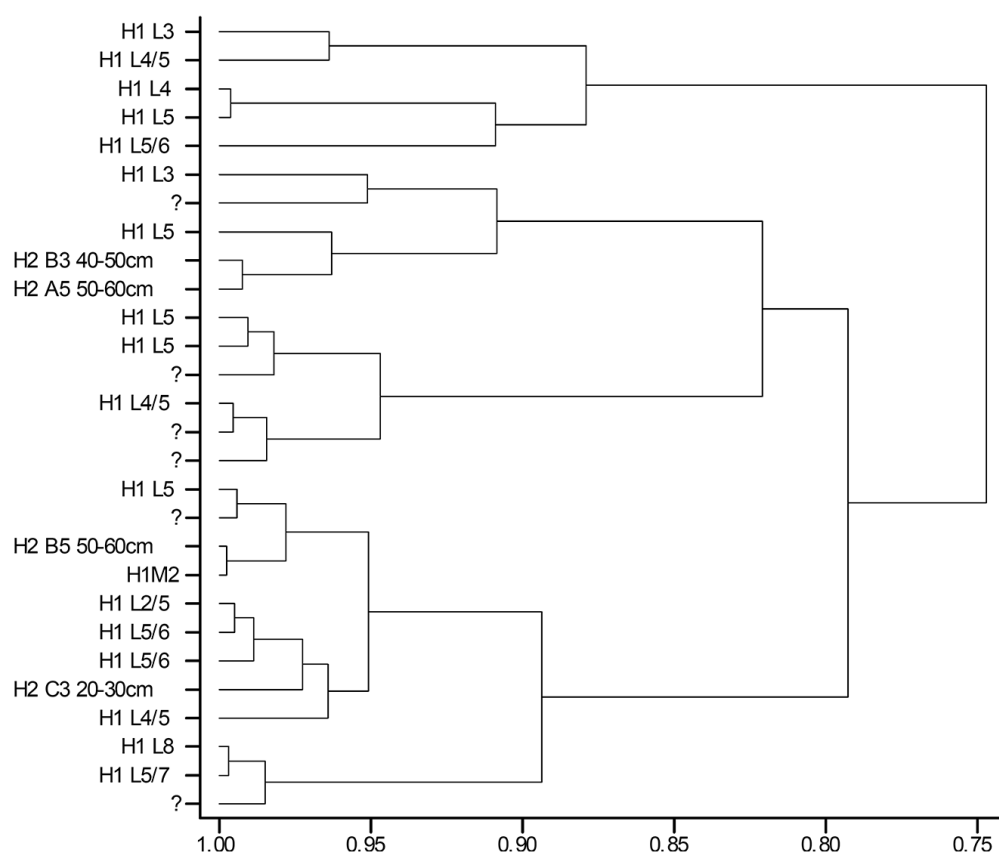


Figure 7.44. Dendrogram of average-linkage hierarchical cluster analysis of form C1b dimensional variables with layers/provenience labelled. Key: H1 = 2009 Trench 1, H2 = 2009 Trench 2, L = Layer, M = Burial, ? = Unknown context.

Source: C. Sarjeant.

Table 7.26. Number of samples in the hierarchical cluster analysis dendrogram groupings by layer/provenience in Figure 7.44 of form C1b dimensional variables when cut at 0.90. Key: H1 = 2009 Trench 1, H2 = 2009 Trench 2, L = Layer, M = Burial.

Groups (cut at 0.90)	H1 L2/5	H1 L3	H1 L4	H1 L4/5	H1 L5	H1 L5/6	H1 L5/7	H1 L8	H1M2	H2 A5 50– 60 cm	H2 B3 40– 50 cm	H2 B5 50– 60 cm	H2 C3 20– 30 cm	Unknown context
1	0	1	0	1	0	0	0	0	0	0	0	0	0	0
2	0	0	1	0	1	1	0	0	0	0	0	0	0	0
3	0	1	0	0	1	0	0	0	0	1	1	0	0	1
4	0	0	0	0	3	0	0	0	0	0	0	0	0	3
5	1	0	0	1	1	2	0	0	1	0	0	1	1	1
6	0	0	0	0	0	0	1	1	0	0	0	0	0	1

Source: Compiled by C. Sarjeant.

### Canonical variate analysis

The CVA plot shows overlap between the form C1b samples from Trench 1 layers 3, 4, 4/5, 5 and 5/6. The samples from Trench 2 and from Trench 1 layers 5/7 and 8 are outliers. The CVA indicates that there is some homogeneity within the form C1b samples mid-sequence (Fig 7.45, Table 7.27).

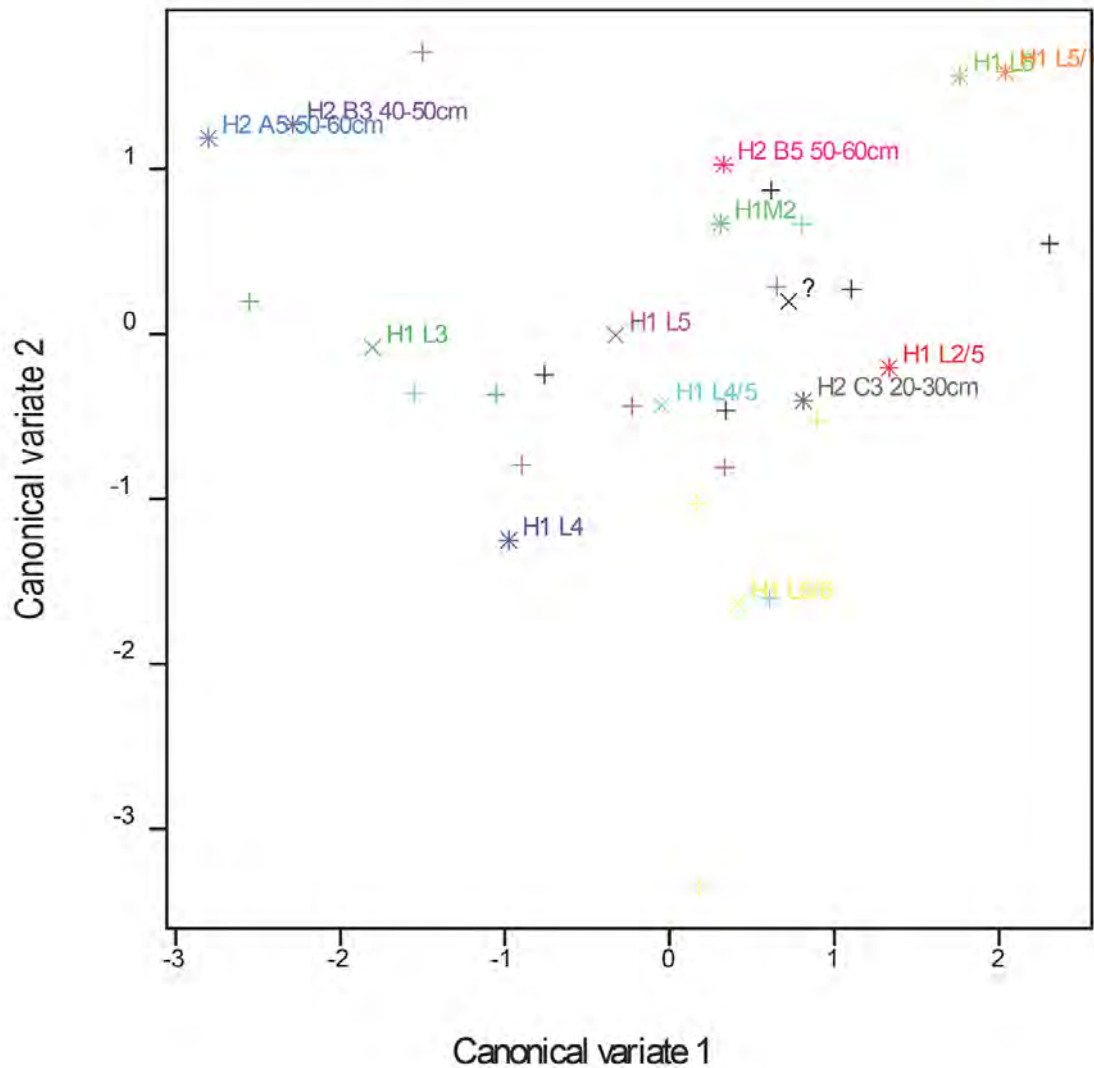


Figure 7.45. CVA plot of form C1b dimensional variables with layers/provenience labelled. First two dimensions. Key: H1 = 2009 Trench 1, H2 = 2009 Trench 2, L = Layer, M = Burial, ? = Unknown context.

Source: C. Sarjeant.

Table 7.27. CVA loadings for Figure 7.45 of form C1b dimensional variables. First two dimensions.

Variables	1 (54.10%)	2 (31.87%)	3 (8.14%)
Angle of rim (degrees)	-0.44349	0.03974	-0.0439
Diameter (mm)	0.0057	0.03271	0.00531
Thickness of body (mm)	0.00394	-0.52347	-0.00723
Thickness of rim (mm)	0.00084	0.00511	0.01243

Source: Compiled by C. Sarjeant.

### Coefficient of variation

The CV values of the form C1b dimensional variables were predominantly mid-range, however the angle of the rim and thickness of the body variable had high CV values. The sherds from Trench 1 layer 5/6 had lower CV values for the diameter, thickness of body and thickness of rim variable, suggesting greater homogeneity in the dimensions of C1b vessels from this layer (Figure 7.46, Figure 7.47).

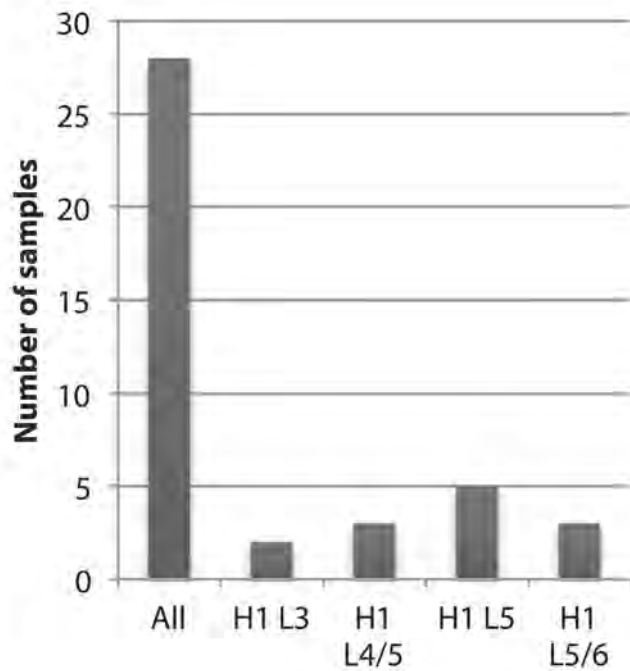


Figure 7.46. Number of form C1b samples of each layer/provenance in the study of standardisation. Key: H1 = 2009 Trench 1, L = Layer.

Source: C. Sarjeant.

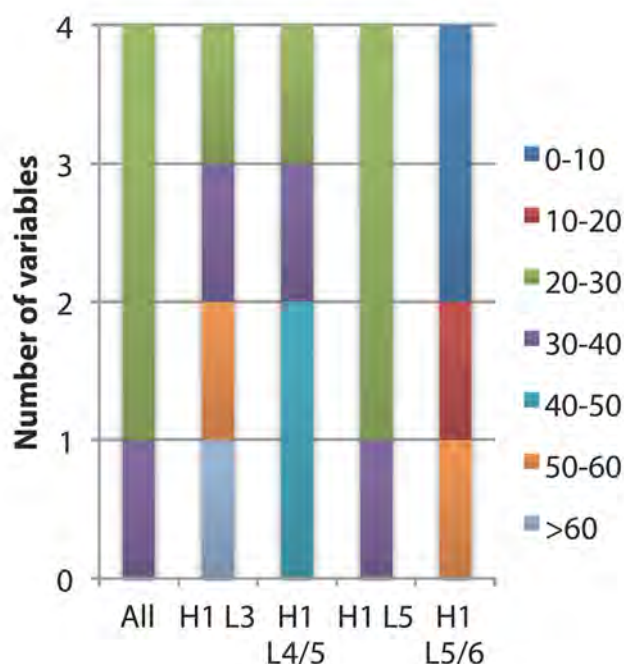


Figure 7.47. Number of variables with CV values 0–>60% for each layer/provenience in the form C1b sample. 0–10% CV represents the lowest CV values, i.e. a higher level of standardisation, and 50–60% CV represents the highest CV values, i.e. a lower level of standardisation. Key: H1 = 2009 Trench 1, L = Layer.

Source: C. Sarjeant.

### *Standardisation of fabrics*

The fabric analyses of temper and the clay matrix (see Chapter 6) showed that there was consistency in the selection of fibre tempers. Many of the fibre tempers also included iron and calcium phosphate sands, (TG B-1, TG B/C-1, TG B/C-2 and TG B/C-3) for C1b vessels. The PCA plot (Figure 7.48) of the clay matrix compositional data displays the greatest variability in calcium, iron and sodium oxides (Table 7.28). There were too few examples to identify any meaningful clustering in the PCA, however the small scale in this PCA plot suggests some compositional homogeneity (Figure 7.48). The PCA and CVA plots in Chapter 6, Part II (Figure 6.35, Figure 6.38) show that C1b vessels tended to cluster together, indicating homogeneity in the clay matrix compositional data.

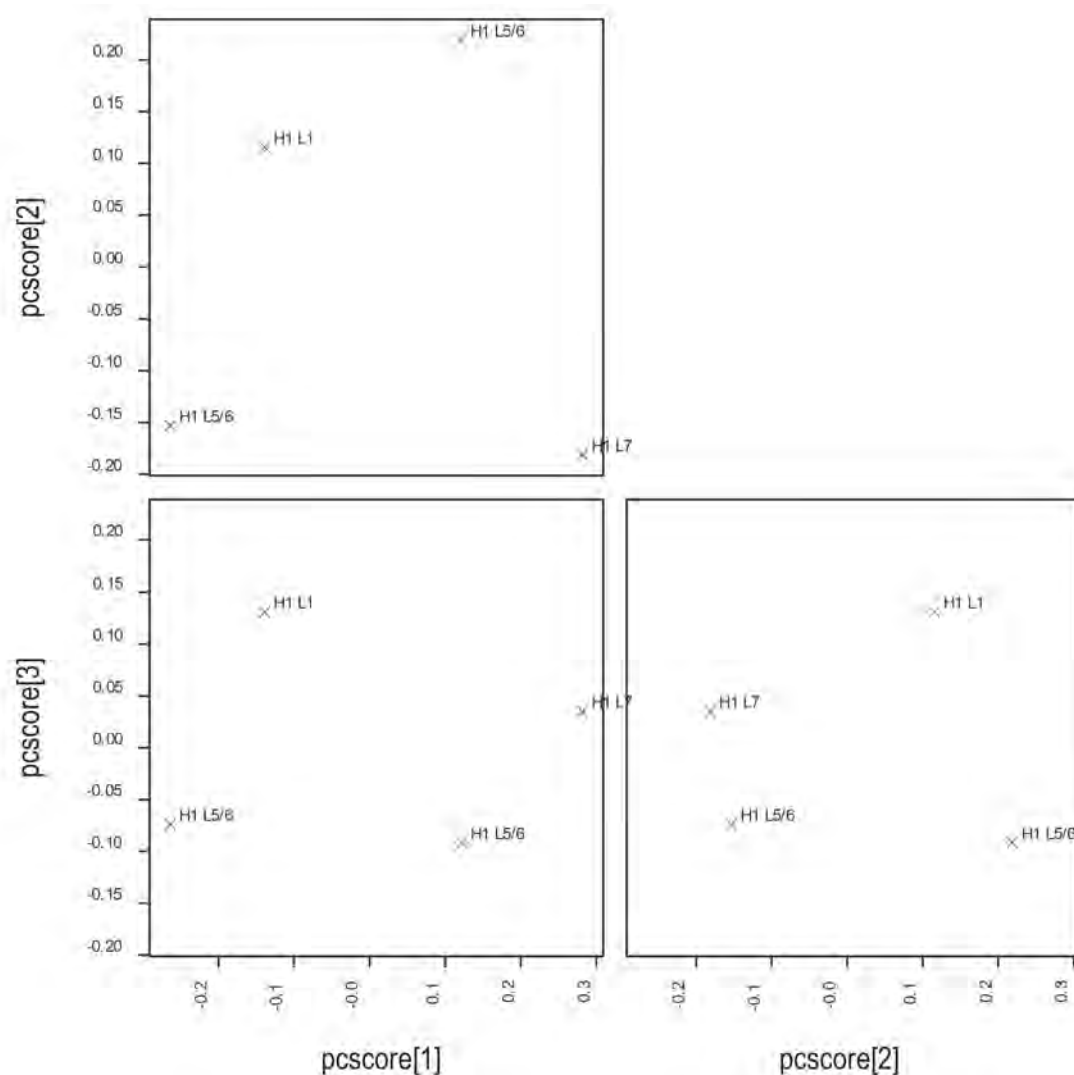


Figure 7.48. PCA plot of form C1b clay matrix composition with layers/provenance labelled. First three dimensions. Key: H1 = 2009 Trench 1, L = Layer.

Source: C. Sarjeant.

Table 7.28. PCA loadings for Figure 7.48 of form C1b clay matrix composition. First three dimensions. The bold values indicate the variables that presented the greatest variability in the PCA.

Variables	PC 1 (55.04%)	PC 2 (35.29%)	PC 3 (9.68%)
CaO	<b>0.40465</b>	<b>0.43414</b>	0.04846
FeO	<b>0.38303</b>	<b>-0.82541</b>	<b>-0.06191</b>
K <sub>2</sub> O	-0.05200	0.15216	0.17504
MgO	0.06815	-0.20169	<b>0.84590</b>
Na <sub>2</sub> O	<b>-0.78042</b>	-0.20388	0.00560
SiO <sub>2</sub>	0.18018	0.12462	0.25551
TiO <sub>2</sub>	-0.20169	0.09634	0.42698

Source: Compiled by C. Sarjeant.



*Summary of form C1b standardisation analysis*

The statistical analyses of dimensional variables indicates that C1b vessels were variable, but that homogeneity increased in this form during the middle of the sequence at An Sơn. This was perhaps a result of an increase in production of C1b vessels at this time. The PCA of An Sơn rims (see Chapter 6, Part II) show that C1b vessels tend to cluster together in terms of clay matrix composition, with both the selection of clay and temper homogeneous in the C1b samples analysed.

*Form D1a*

Form D1a is a simple, unrestricted bowl-shaped vessel with an everted, wavy rim and a defined internal ridge between the rim and body. These vessels are commonly paddle linear impressed or comb incised on the body, and impressions are also usually observed on the waves of the rim (Figure 5.1). The dimensional and fabric variables were assessed statistically. Measured variables include angle of the rim to the internal ridge, diameter of the rim, length of the rim to the internal ridge, height of a single wave, width of a single wave, thickness of the body, and thickness of the rim (Figure 7.1). Once again, the four previously described statistical methods (PCA, cluster analysis, CVA and CV) were applied to understand the variability and homogeneity in the morphology of the D1a form ceramics. The clay matrix compositional data were assessed using PCA.

*Standardisation of morphology***Principal components analysis**

The greatest variability in the following PCA plot (Figure 7.49) is a result of angle of the rim to the internal ridge and diameter variables (Table 7.29). According to these two variables, two main clusters are evident in the plots. The D1a vessels from burial contexts cluster together in one of these groups (Figure 7.49). The clusters are clarified in the following hierarchical cluster analysis (Figure 7.50, Table 7.30).



### Hierarchical cluster analysis

The dendrogram was cut at 0.90 (Figure 7.50) to divide the form D1a assemblage into groups. The number of samples within each layer/provenience in these groups is shown in Table 7.30. The dendrogram does not clarify any differences in the dimensional variables according to context, however most of the D1a vessels from burials contexts cluster together in groups 5 and 6 (Table 7.30).

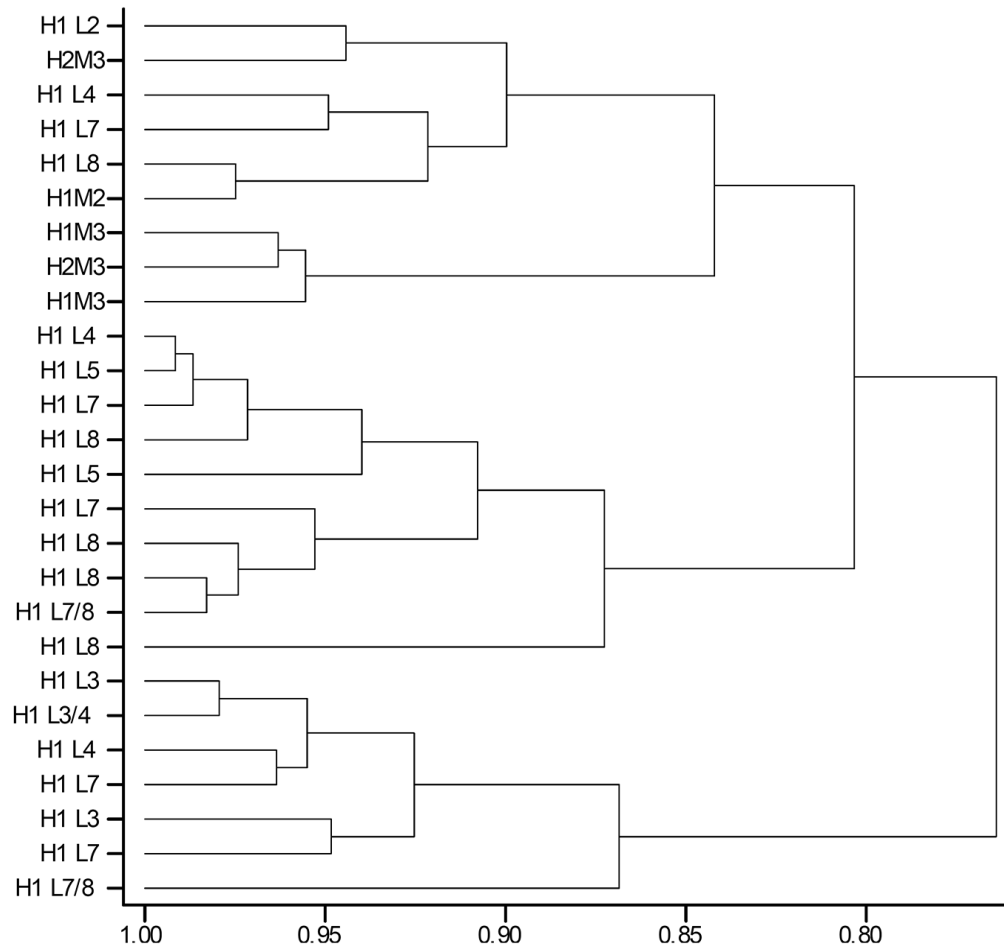


Figure 7.50. Dendrogram of average-linkage hierarchical cluster analysis of form D1a dimensional variables with layers/provenience labelled. Key: H1 = 2009 Trench 1, H2 = 2009 Trench 2, L = Layer, M = Burial.

Source: C. Sarjeant.

Table 7.30. Number of samples in the hierarchical cluster analysis dendrogram groupings by layer/provenience in Figure 7.50 of form D1a dimensional variables when cut at 0.90. Key: H1 = 2009 Trench 1, H2 = 2009 Trench 2, L = Layer, M = Burial.

Groups (cut at 0.90)	H1 L2	H1 L3	H1 L3/4	H1 L4	H1 L5	H1 L7	H1 L7/8	H1 L8	H1M2	H1M3	H2M3
1	1	0	0	1	0	1	0	1	1	0	1
2	0	0	0	0	0	0	0	0	0	2	1
3	0	0	0	1	2	2	1	3	0	0	0
4	0	0	0	0	0	0	0	1	0	0	0
5	0	2	1	1	0	2	0	0	0	0	0
6	0	0	0	0	0	0	1	0	0	0	0

Source: Compiled by C. Sarjeant.

### Canonical variate analysis

The CVA plot indicates that there is a difference in the dimensional variables between those D1a vessels from the mid to upper layers of Trench 1 layers 3, 4, 5 and 7; those from the lower layers, Trench 1 layers 7/8 and 8; and those from burial contexts. These groupings suggest some standardisation in the manufacture of contemporary D1a vessels (Figure 7.51, Table 7.31).

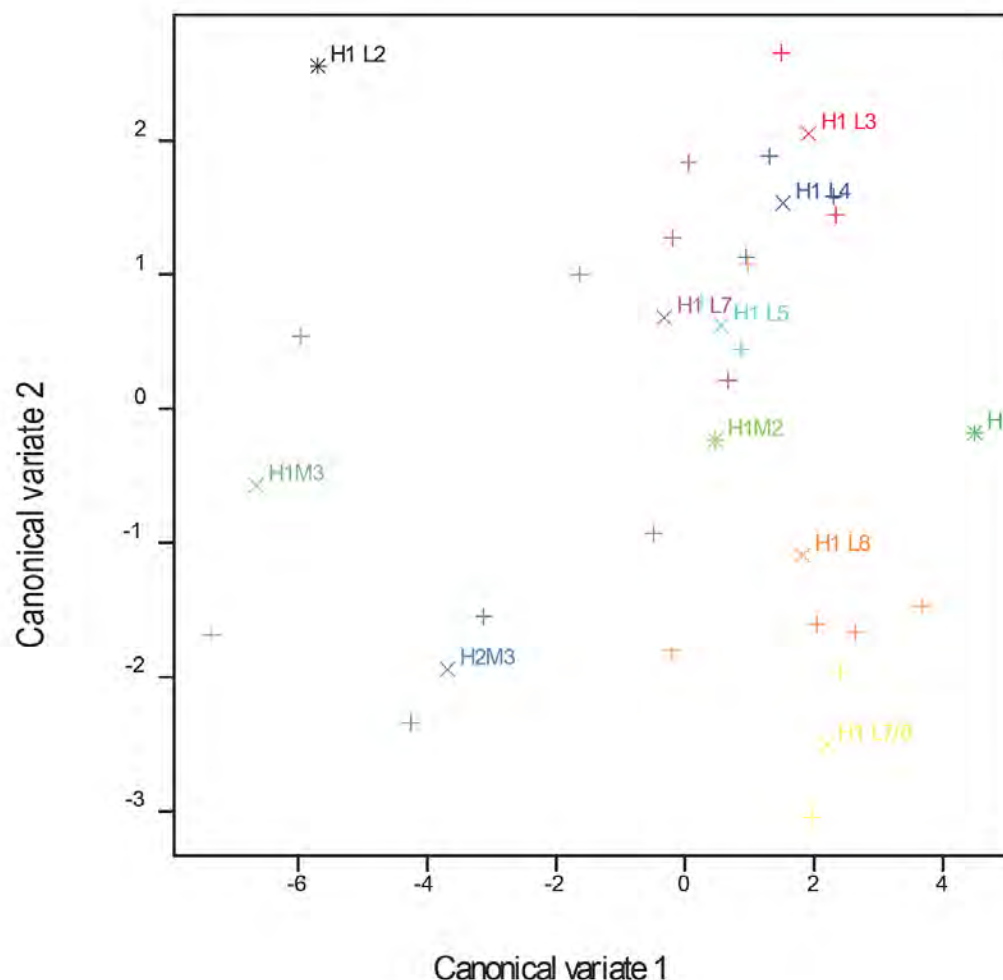


Figure 7.51. CVA plot of form D1a dimensional variables with layers/provenience labelled. First two dimensions. Key: H1 = 2009 Trench 1, H2 = 2009 Trench 2, L = Layer, M = Burial.

Source: C. Sarjeant.

Table 7.31. CVA loadings for Figure 7.51 of form D1a dimensional variables. First three dimensions.

Variables	1 (69.52)	2 (17.15)	3 (6.98)
Angle of rim to internal ridge (degrees)	-0.4212	-0.0167	0.1747
Diameter (mm)	0.0020	0.0072	0.0125
Length of lip to internal ridge (mm)	0.0330	-0.0647	0.0262
Height of single wave (mm)	-0.0901	0.4027	-0.2270
Width of single wave (mm)	-0.2851	-0.2317	-0.0383
Thickness of body (mm)	0.1382	-0.8569	0.2748
Thickness of rim (mm)	-0.2498	0.3615	0.2986

Source: Compiled by C. Sarjeant.

### Coefficient of variation

The CV values for form D1a were high for the angle of the rim to the internal ridge variable, while the values were lower for the variables of diameter and width of single wave at the rim. When separated into context groups the CV values decreased dramatically. This supports the previous claim for more homogeneity and the possibility of standardisation in methods for the manufacture of contemporaneous D1a vessels, yet this homogeneity was not constant over time. CV values were generally lowest in burial contexts (Figure 7.52, Figure 7.53), and it is possible that one person made these vessels for the specific purpose of mortuary offering.

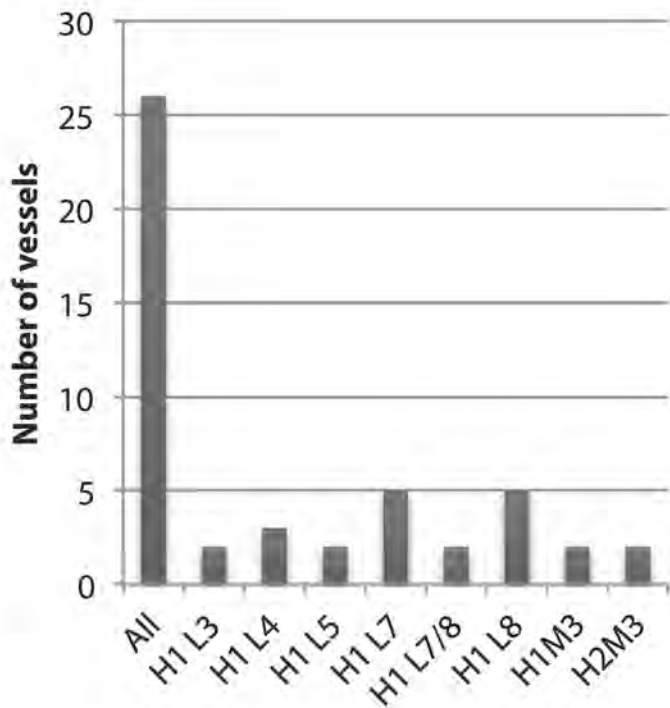


Figure 7.52. Number of form D1a samples of each layer/provenance in the study of standardisation. Key: H1 = 2009 Trench 1, H2 = 2009 Trench 2, L = Layer, M = Burial.

Source: C. Sarjeant.

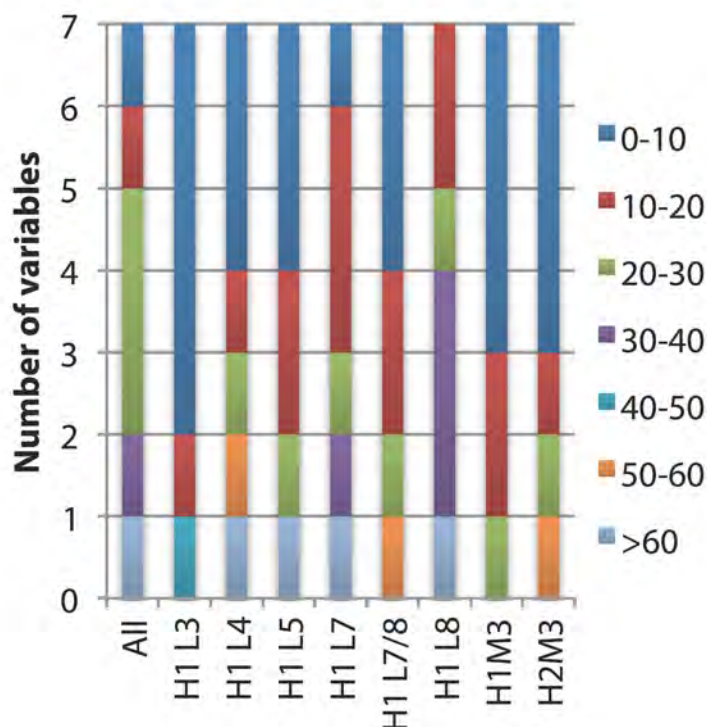


Figure 7.53. Number of variables with CV values 0–>60% for each layer/provenience in the form D1a sample. 0–10% CV represents the lowest CV values, i.e. a higher level of standardisation, and 50–60% CV represents the highest CV values, i.e. a lower level of standardisation. Key: H1 = 2009 Trench 1, H2 = 2009 Trench 2, L = Layer, M = Burial.

Source: C. Sarjeant.

#### *Standardisation of fabrics*

The fabric analyses of temper and the clay matrix (see Chapter 6, Part II) shows that there was consistency in the selection of sand temper, TG A1-1, TG A1-5, TG A1/A3-2 and TG A2-1, for D1a vessels. The sand inclusions were quartz and alkali feldspar, quartz, alkali feldspar and amphibole, quartz and impure iron oxide, and quartz, alkali feldspar, biotite and muscovite, respectively. The PCA plot (Figure 7.54) of the clay matrix compositional data displays the greatest variability in iron, potassium and magnesium oxides (Table 7.32). There were too few examples to identify any meaningful clustering, however the small scale in this PCA plot suggests some compositional homogeneity (Figure 7.54). The PCA, cluster analysis and CVA plots in Chapter 6, Part II (Figure 6.35, Figure 6.36, Figure 6.38) show that the D1a vessels tended to cluster together, indicating homogeneity in the clay matrix compositional data.

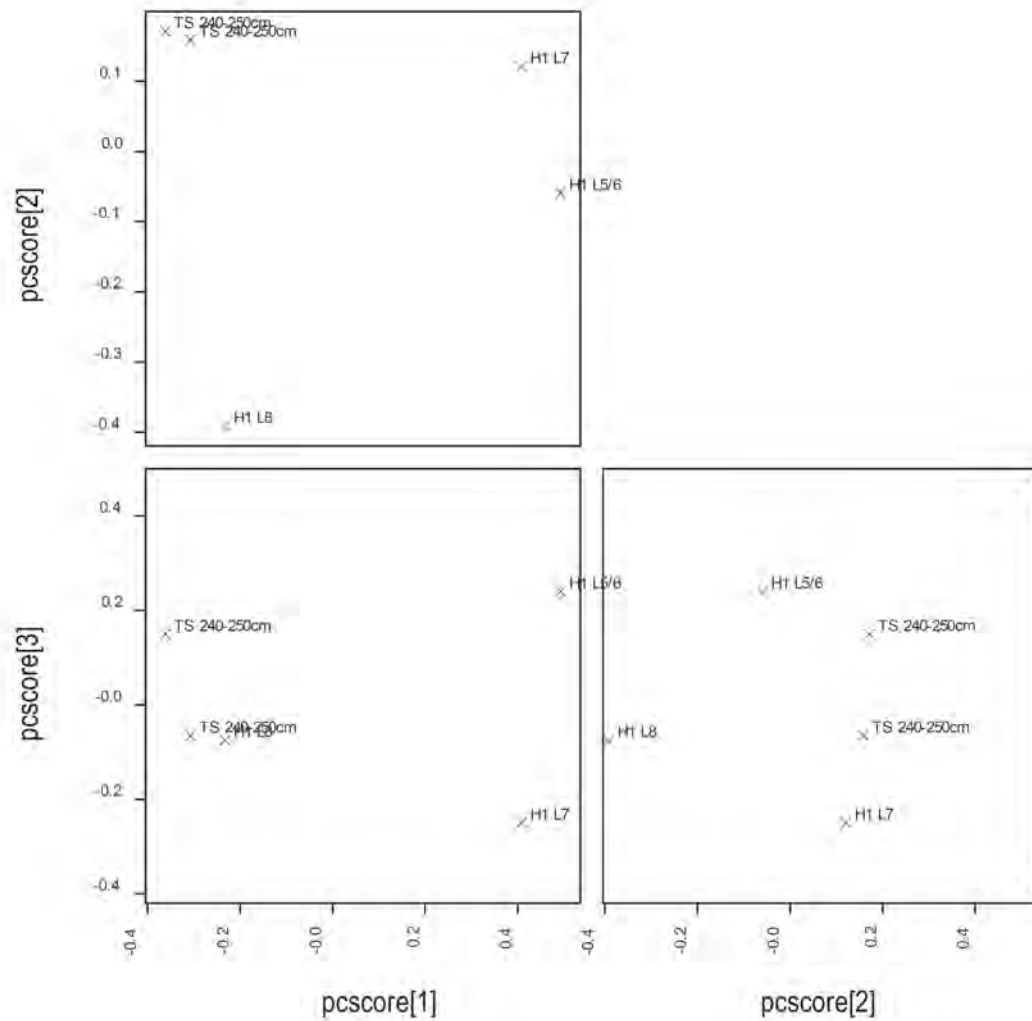


Figure 7.54. PCA plot of form D1a clay matrix composition with layers/provenience labelled. First three dimensions. Key: H1 = 2009 Trench 1, TS = 2009 Test Square, L = Layer.

Source: C. Sarjeant.

Table 7.32. PCA loadings for Figure 7.54 of form D1a clay matrix composition. First three dimensions. The bold values indicate the variables that presented the greatest variability in the PCA.

Variables	PC 1 (61.77%)	PC 2 (20.31%)	PC 3 (13.64%)
CaO	0.18272	<b>0.57642</b>	<b>0.43708</b>
FeO	<b>0.26039</b>	0.21028	0.08393
K <sub>2</sub> O	<b>-0.71545</b>	0.47208	-0.34902
MgO	<b>0.27919</b>	0.20306	<b>-0.45455</b>
Na <sub>2</sub> O	-0.48319	<b>-0.46425</b>	0.26081
SiO <sub>2</sub>	-0.27224	0.36574	<b>0.42689</b>
TiO <sub>2</sub>	-0.03751	0.10068	<b>-0.47246</b>

Source: Compiled by C. Sarjeant.

*Summary of form D1a standardisation analysis*

The standardisation study of the dimensional data indicates that there were two major groups within the D1a assemblage and that there was consistency in the dimensions of D1a vessels produced at the same time, i.e. those found in the same layer or context. This consistency extended to the selection of clay and temper.

*Summary of standardisation within A2a, B1a, C1b and D1a forms: Temporal trends*

The basic morphologies (Figure 5.1, Figure 7.1) of the forms A2a, B1a, C1b and D1a are homogeneous in appearance within each form group, at a superficial level. Through an examination of dimensional and fabric variables (and decorative variables in the case of A2a), this apparent homogeneity has been scrutinised. Variability within the form A2a and B1a rims increased later in the sequence, while there was homogeneity within the B1a rims earlier in the sequence. There was also homogeneity within the C1b and D1a rims. There were two distinct dimensional groups within the D1a form.

To summarise the level of variability and standardisation in forms A2a, B1a, C1b and D1a, each variable must be considered independently. The presented analysis showed that none of the forms were completely variable or standardised, although some forms exhibited some standardised variables at certain times during the sequence (Figure 7.55). All of the form A2a variables were more standardised in Trench 1 layers 5/6 and 7, mid to early sequence, than in the later layers. Similar form B1a variables were variable and standardised throughout the sequence, and the angle of the rim was consistently the least variable measured dimension. Form C1b was more standardised mid-sequence, in Trench 1 layer 5/6, compared to the earlier and later layers. The angle of the rim on form D1a was variable throughout the sequence, but less variation was evident in the upper layers (Trench 1 layers 5 to 3), as production of this form declined. When the temporal contexts are removed, it is evident that specific variables were more standardised in each form. The possible ritual/ceremonial sand tempered vessels, forms A2a and D1a (discussed in Chapter 5), were less variable in diameter, while the utilitarian fibre tempered vessels, forms B1a and C1b, were less variable in thickness of the body (Figure 7.56).



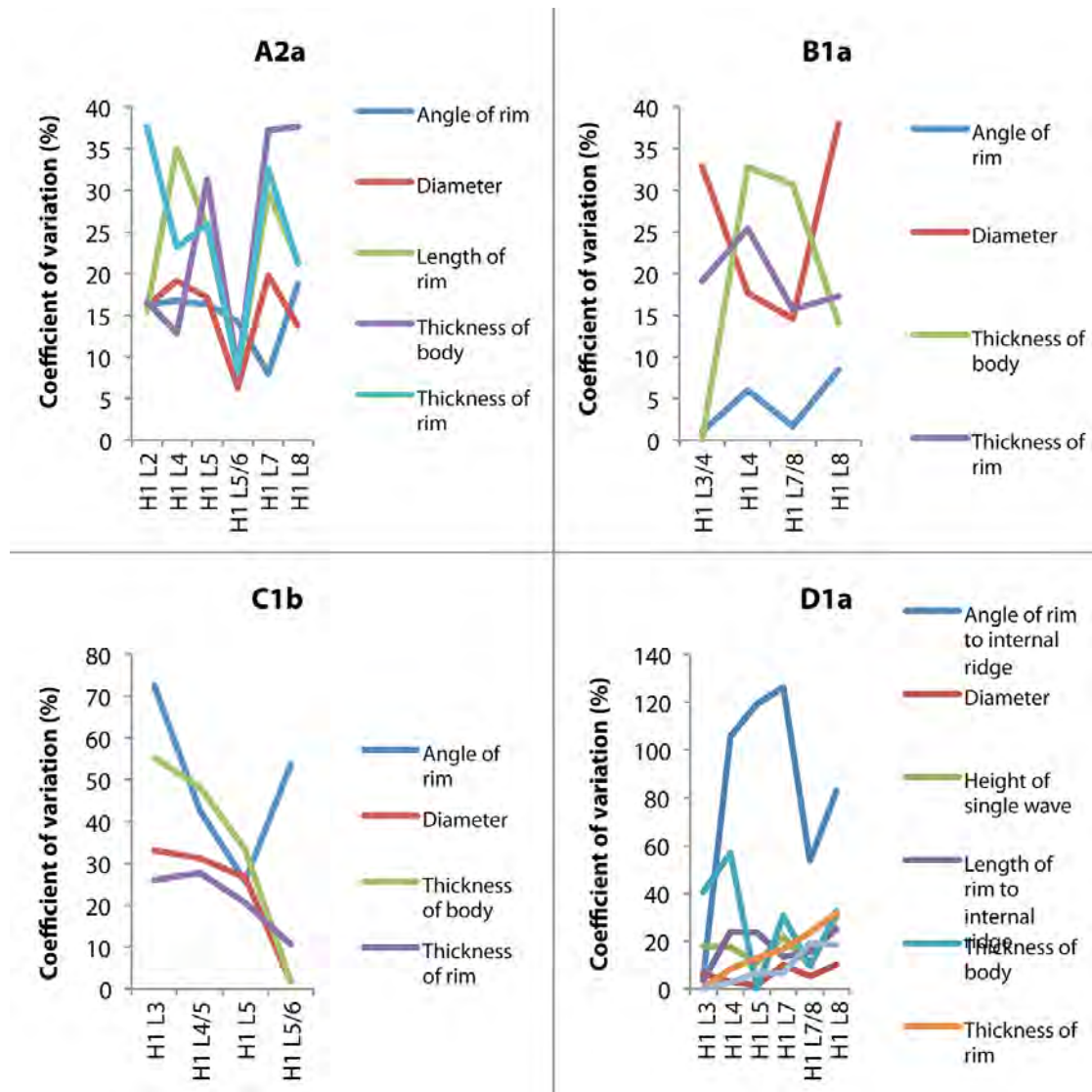


Figure 7.55. CV values (%) of each dimensional variable from represented layers of Trench 1 for each rim form. Refer to Figure 5.1 and Figure 7.1 for rim form images and measured variables. Key: H1 = Trench 1, L = Layer.

Source: C. Sarjeant.

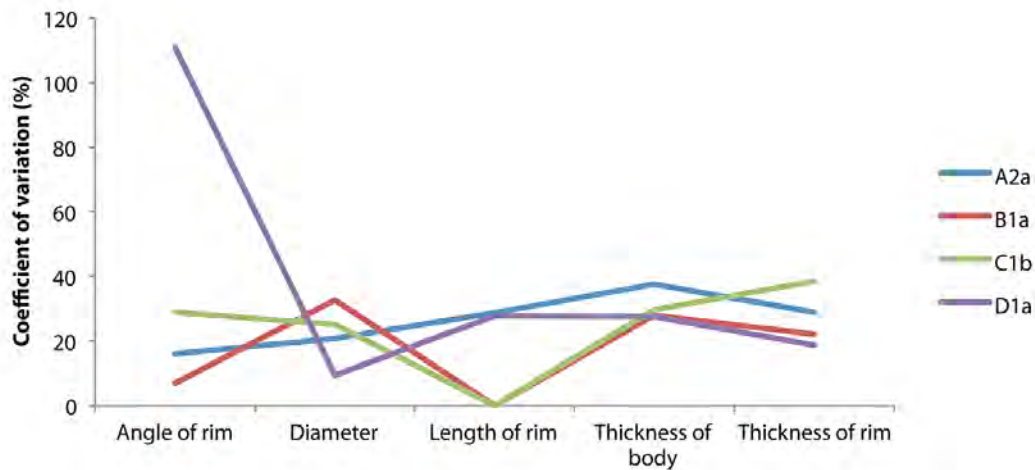


Figure 7.56. CV values (%) of each dimensional variable for each rim form. Note that forms B1a and C1b do not have length of rim variables, and are presented as '0' in the plot. Refer to Figure 5.1 and Figure 7.1 for rim form images and measured variables.

Source: C. Sarjeant.

### Summary: The degree of standardisation in the An Sôn ceramic assemblage

The analysis of the degree of standardisation allows for a greater understanding of the life history, or *chaîne opératoire* (Roux 2003b; Lemonnier 1983; Leroi-Gourhan 1964), of particular vessel forms, the structures in place to manufacture them, and the technical choices of the potters (Roux 2003b; Schiffer and Skibo 1997). With the exception for the coefficient of variation, the degree of standardisation was considered comparatively across the sample, between the different forms in this chapter. Other studies have determined CV values that represent standardised and variable assemblages. Eerkens and Bettinger (2001) identified a CV of 1.7% as the highest degree of standardisation and 57.7% the lowest degree. Research has shown that full-time specialists manufacture ceramic products with a CV between 5–10%, while products made by part-time artisans in small, household-level organisation have a CV of 15% (Foias and Bishop 1997; Blackman *et al.* 1993; Longacre *et al.* 1988). From this research, the An Sôn assemblage may be discussed as either standardised or variable in both relative and absolute ways.

The relative comparison between the rim forms was determined from the PCA, hierarchical cluster analysis and CVA. General trends have been identified within each vessel form group, where homogeneity was noted more often (standardised) or not (variable). The small sample size of some rim forms meant it was not always possible to come to a conclusion about the relative level of standardisation, and some forms displayed variable and homogeneous results in different statistical analyses. The analysis of the dimensional variables indicated that many of the A1 forms were rather standardised in comparison to each other, notably forms A1b, A1c, A1d, A1g, A1i and A1i-r, whereas A1a and A1e were not. The A2 forms were variable, while class B forms were comparatively standardised, as were the C2, D1b and D2a forms (Table 7.33). Refer to Figure 5.1 for rim form images.

The levels of standardisation for each rim form, as determined from the CV values, are presented here both as an average of the CV values (Figure 7.57) and the proportion of each dimensional variable within the total CV value (Figure 7.58). The averaged values show that only form A1g had a 5–10% CV, suggesting specialisation of this vessel form. Forms A1i-r and C2a had slightly higher averaged CV values than the other forms, suggesting some kind of household-based

organisation. The remaining forms had higher CV values in comparison to the forms mentioned above, indicating variability in the dimensional variables, with the highest CV value for form D2a. This is surprising since a great deal of homogeneity was observed in the D2a form in terms of dimensional and fabric variables (see Chapter 6, Part II). However, the averaged CV value for the D2a form has been affected by the small sample size, and the high CV values for the height and width of the serrated portions of the rim (Figure 7.57).

The proportion plot of CV values (Figure 7.58) showed that the angle of the rim was low for the majority of the A1 and A2 forms, B1b, B3a and D2a, and was very high for C2a, C2b, C3a, D1a, D1b and E1a. The proportion of CV values for the diameter was low for forms A1h, A2a, A2b, A2c, D1a, D1b and D2a, and very high for A1g and class B forms. The proportion of CV values for the length of the rim was low for forms A1d, A1g, A1h, D1a, D1b and D2a, and high for A1i-r. The proportion of CV values for the thickness of the body was low for forms A1f, A1i, D1a, D2a and E1a, and high for A1h and C2a. The proportion of CV values for the thickness of the rim was low for forms A1a, A1b, A1c, A1d, A1e, A1f, A1i-r, B2a, B3a, C2a, D1a, D1b and D2a, and high for A1g, C1b and E1a. The proportion of CV values for the height and width of a single wave were low for forms D1a and D1b, and very high for D2a.

The CV values of the stacked bar plot (Figure 7.59 and summarised in Table 7.34) clarify which variables for each form were within the range of potentially standardised (under 10%), manufactured under household production (around 15%), and non-standardised (over 57.7%). Based on the two plots of dimensional variables (Figure 7.58, Figure 7.59), it may be suggested that when those variables with very high CV values are excluded from the final interpretation, the forms that display a standardised level of production in more than one dimensional variable are forms A1g, A1i-r, D1b and D2a. One variable is standardised in forms A1h, A2c, B1a, B1b, C2a, D1a and E1a. A household level of production may be inferred for forms A1b, A1f, A1g, A1h, A1i, A1i-r, A2a, A2c, B1b, C2a, D1b and D2a (Table 7.34). Highly variable forms that do not present any kind of organisation in production are not included in the standardisation and household level columns of Table 7.34. These are forms A1a, A1c, A1d, A1e, A2b, B2a, B3a, C1a, C1b, C2b and C3a. Most of these forms had CV values between household level and the lowest level of standardisation (over 15 and less than 57.7%), i.e. they were not standardised.

It is commonly perceived that there was very little standardisation in pottery production during the neolithic occupation of mainland Southeast Asia (e.g. White and Pigott 1996) (see Chapter 10). While this may be true, very few studies have investigated the degree of standardisation in neolithic Southeast Asian ceramic assemblages. This chapter has discussed variability and standardisation between different forms and between different ceramic variables. While there were few definitive examples of standardised production for a specific form at An Sôn, developments in craft production were evident in the homogeneity of particular variables for some vessel forms. This homogeneity has arisen out of taught behaviours that are passed on for these particular variables of specific vessel forms, as a template for manufacture (see Chapter 10). This homogeneity extends beyond the dimensional variables to temper and clay selections of some forms, as shown when the study combined dimensional and fabric variables for the analysis of the B1a, C1b and D1a forms. Form A2a presented variable decorations, dimensions and fabrics. The longevity of many of the forms with standardised variables indicates a strong tradition in the teaching and manufacturing of particular vessels with specific methods, while the analysis of form B1a also suggests that there were modifications in these methods over time. These findings indicate that a common mental template was used by the An Sôn potters for certain vessel forms (discussed further in Chapter 10). The level of standardisation cannot be determined for the An Sôn assemblage as a single entity, since fluctuations in the homogeneity of a vessel form were evident in different variables and in different contexts over time.

Table 7.33. Relative level of standardisation for each rim form, based on all statistical methods presented in Chapter 7. Refer to Figure 5.1 and Figure 7.1 for rim form images and measured variables.

Standardised	Variable	Both variable/standardised dimensional variables	Unknown level
A1b	A1a	A1f	A1h
A1c	A1e	C1a	B3a
A1d	A2a	C1b	
A1g	A2b	C3a	
A1i	A2c	D1a	
A1i-r		E1a	
B1a			
B1b			
B2a			
C2a			
C2b			
D1b			
D2a			

Source: Compiled by C. Sarjeant.

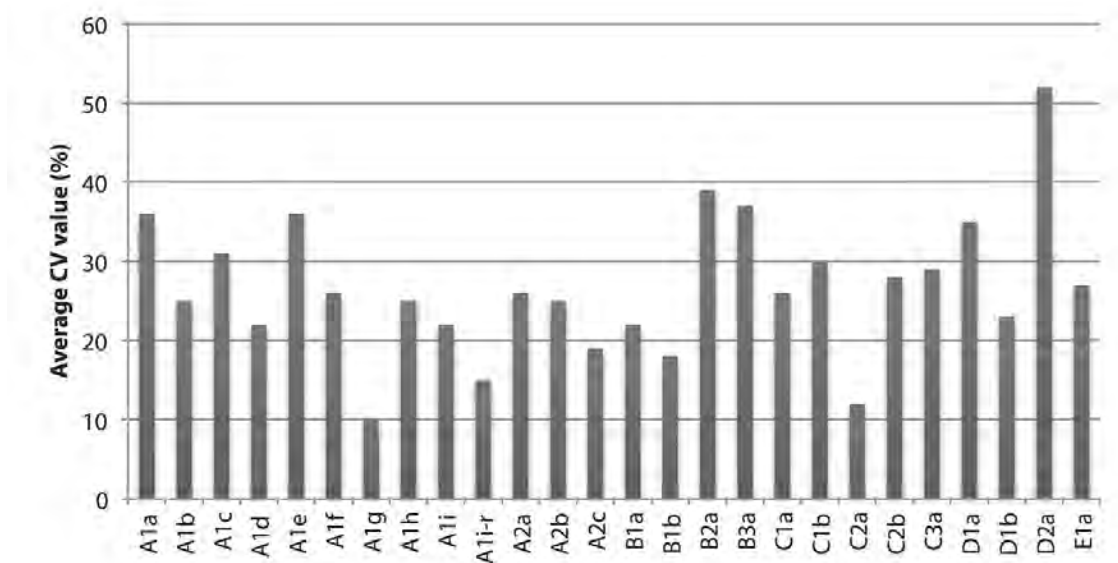


Figure 7.57. Average of CV values (%) for each rim form. Refer to Figure 5.1 for rim form images.

Source: C. Sarjeant.

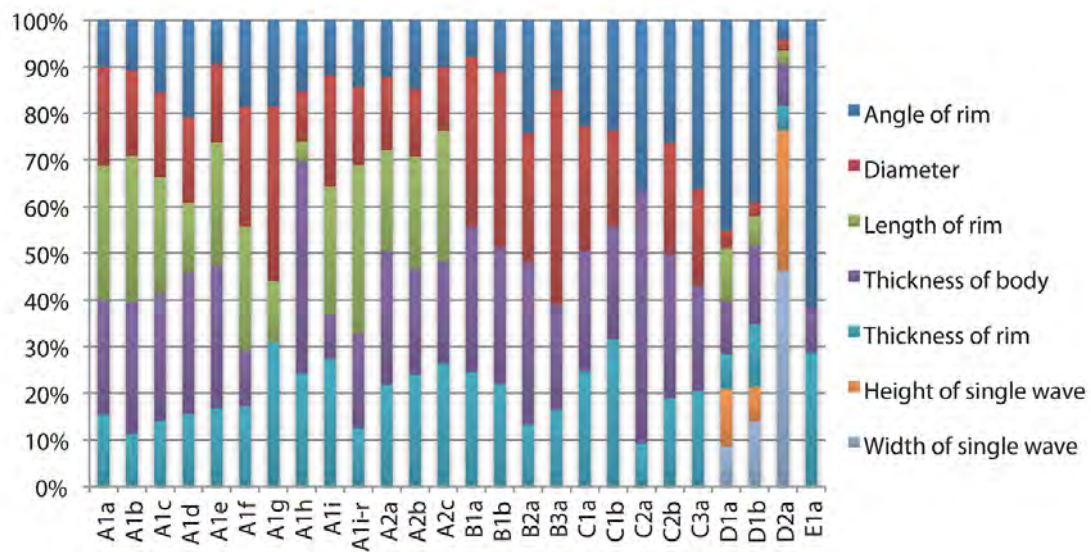


Figure 7.58. Proportion of CV values (%) for each variable within each rim form. Note that the length of the rim was not calculated for class B, C and E vessels and the height and width of single wave variables were only measured for class D. There was no thickness of body CV value calculated for A1g, no diameter CV value for C2a and E1a and no length of rim CV value for E1a. Refer to Figure 5.1 and Figure 7.1 for rim form images and measured variables.

Source: C. Sarjeant.



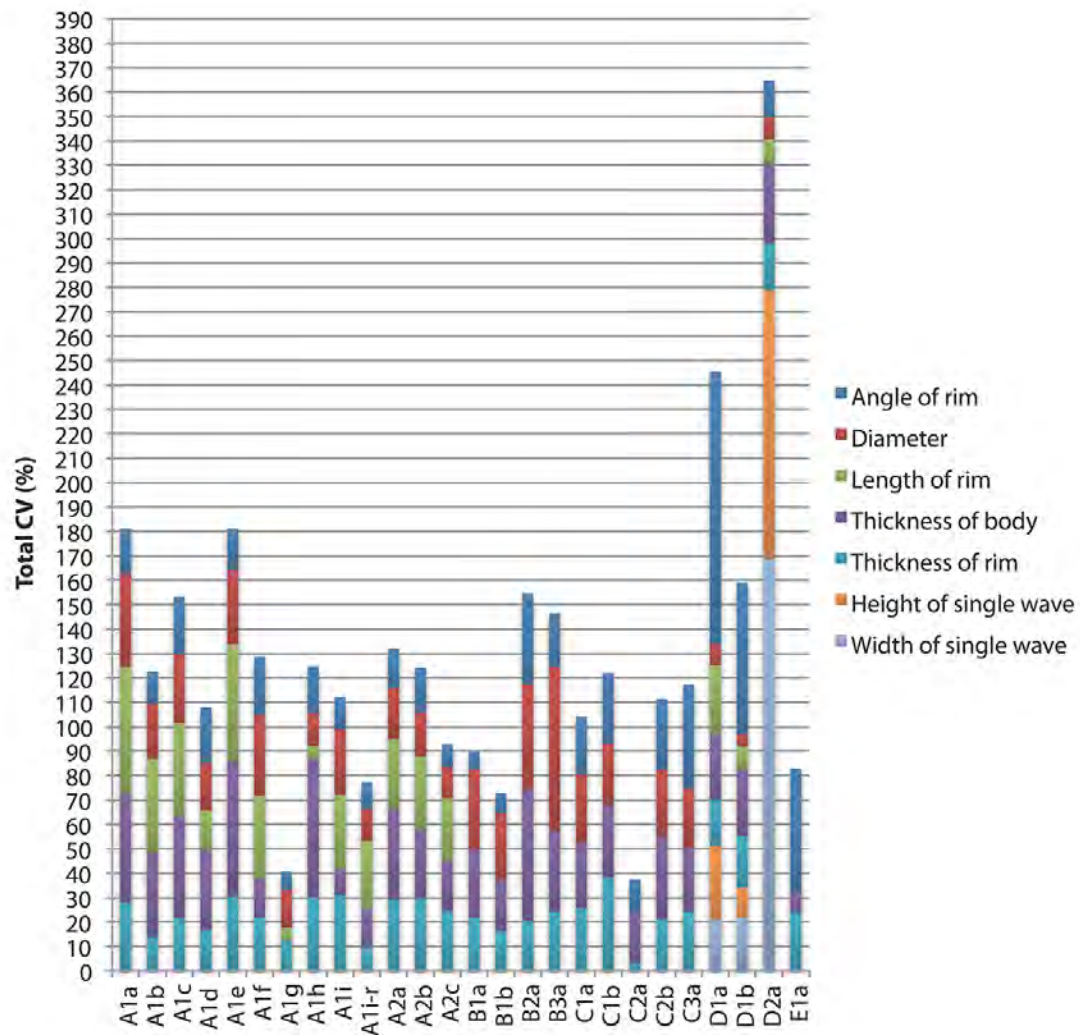


Figure 7.59. Total CV values (%) for each variable for each form. Note that the length of the rim was not calculated for class B, C and E vessels and the height and width of single wave variables were only measured for class D. There was no thickness of body CV value calculated for A1g, no diameter CV value for C2a and E1a and no length of rim CV value for E1a. Refer to Figure 5.1 and 7.1 for rim form images and measured variables.

Source: C. Sarjeant.

Table 7.34. The presence of dimensional variables with standardised level, household level and lowest level of standardisation in each rim form. Forms with values between ~15% and 57.7% not included in this table. Refer to Figure 5.1 and 7.1 for rim form images and measured variables.

Variables	Standardised level (<10%)	Household level (~15%)	Lowest level of standardisation (variable) (>57.7%)
<b>Angle of rim</b>	A1g A1i-r A2c B1a B1b	A1b A1i A2a C2a D2a	D1a D1b
<b>Diameter</b>	D1a D1b D2a	A1g A1h A1i-r A2c	B3a
<b>Length of rim</b>	A1g A1h D1b D2a	A1d	
<b>Thickness of body</b>	E1a	A1f A1i A1i-r	
<b>Thickness of rim</b>	A1i-r C2a	A1b A1g B1b	
<b>Height of single wave</b>		D1b	D2a
<b>Width of single wave</b>			D2a

Source: Compiled by C. Sarjeant.

This text taken from *Contextualising the Neolithic Occupation of Southern Vietnam: The Role of Ceramics and Potters at An Son*, by Carmen Sarjeant, published 2014 by ANU Press,  
The Australian National University, Canberra, Australia.